POSTER IMAGES

(sorted alphabetically by author's last name)

3rd Annual Health Equity Summit

FEBRUARY 29, 2024
8:00 AM - 3:00 PM
PURDUE MEMORIAL UNION NORTH/SOUTH BALLROOMS

Stone Soup – A Second Helping for Trauma Systems Development:
What to Make When Between a Rock and a Hard Place

Primary Ingredients

AAA Hoosier Motor Club
Air Evac Lifeteam
American Red Cross of Indiana
IN Congressman Dr. Larry Bucshon
Christopher Reeve Paralysis Foundation
Donna Edwards RN
Marcus Engel
Dr. Bill Fields
Wendy Hums RN
Indiana Emergency Nurses Association
Indiana Rural Health Association
Indiana State Department of Health
Indiana State Nurses Association
Thelma Kuska RN
Dr. Gregory Larkin
Colonel Sharon Lee RN
Tracie Pettit RN
Sigma Theta Tau
South Vermillion High School
Officer Curtis Stoeffel
Terre Haute Regional Hospital
Vermillion County Council
Vermillion County Emergency Management Agency
Vermillion County Health Department
Vermillion County Sheriff's Department
WCI–AHEC (West Central Indiana – Area Health Education)
Nicole Webb RN
Elizabeth Ramsey Wible
Greg Wible
Justin Wible
Tim Yocum, Vermillion County Commissioner

Seasonings

Add liberal quantities of
Love, Faith, Hope, Happiness, Belief, and Joy

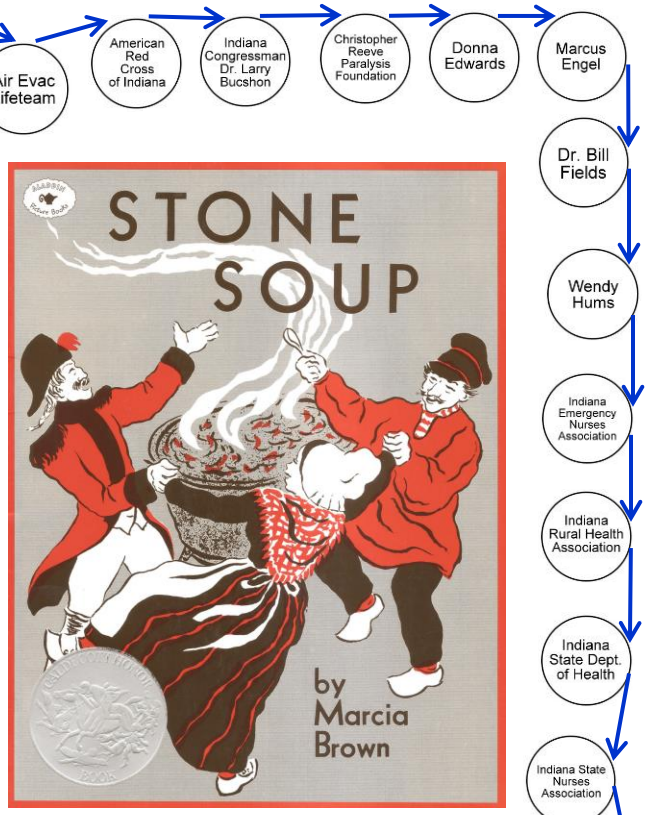

"Feed My sheep"
John 21:17

In the Soup?

Preparation Instructions

Talk, ask each other's stories, and tell YOUR story.

SHARE and CARE to get things done.

STIR WELL

Get close enough to show & tell - Proximity COUNTS.

Taste frequently to make adjustments and to know when to add more ingredients.

Finally, Connect the dots – be INclusive.

Enjoy!

"Make a Good Soup"
Marcia Brown

"Unifiers connect dots"
Eric Weiner,
Geography of Genius

Meredith Addison MSN, CEN, FAEN, RN
meredith.addison@yahoo.com

Addressing Hearing Health Equity in Indiana Using Precision Audiology

Joshua Alexander[1], Michael Heinz[1,2], Maureen Shader[1], Ananth Grama[3], Edward Bartlett[2,3], Jennifer Simpson[1]

[1] College of Health and Human Sciences, [2] College of Engineering, [3] College of Science

Abstract

Hearing health equity presents a significant challenge across Indiana, particularly affecting rural, minority, and economically disadvantaged populations. In Indiana, disparities in hearing aid usage are pronounced, with non-Hispanic white adults and those with higher socioeconomic status over twice as likely to use hearing aids compared to non-Hispanic Black, Hispanic, and lower-income or less-educated individuals. Hearing impairment is linked to several comorbidities, including depression, anxiety, poorer cognition, physical health, and increased falls, leading to 46% higher healthcare costs for those with untreated hearing loss. Notably, nearly 70% of rural residents with occupational noise exposure report hearing loss, emphasizing the need for targeted interventions, given that about 50% of hearing loss cases are preventable.

These disparities contribute to underemployment, limited access to healthcare, and lower quality of care. Additionally, the high costs of hearing aids, the stigma around hearing loss, and unequal access to quality care further challenge efforts to address hearing needs in minority and underrepresented communities. The underrepresentation of diverse populations in hearing research and clinical audiology (8% URMs) further exacerbates health disparities, limits the generalizability of research findings, and hinders effective interventions.

To combat these issues, the new Accessible Precision Audiology Research Center in Indianapolis, launched from the Life and Health Sciences Summit with support from Purdue's Office of Research and Provost's Office, will engage with a diverse group of Indiana residents. The center aims to raise awareness about the impact of untreated hearing loss and available management options through community outreach, standardized audiological evaluations, and free hearing screenings. By leveraging an open-source database and AI-powered analysis tools, the center seeks to advance precision audiology, enabling more personalized and effective hearing care solutions, thus fostering a deeper understanding of hearing health across the socioeconomic spectrum.

Hearing Loss is Correlated with Most Common Chronic Conditions

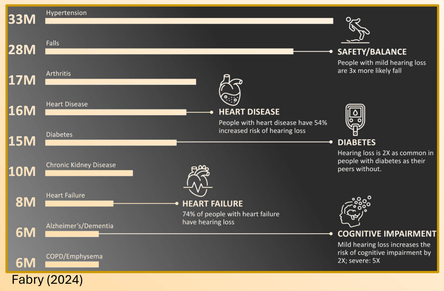

Fabry (2024)

16.8% of U.S. Adults (>40 million) and 12.5% of Hoosiers Have Hearing Loss

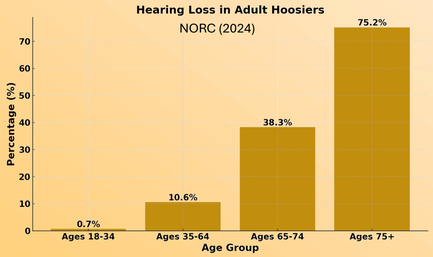

Untreated hearing loss is associated with 46% higher healthcare costs

This is attributed to factors such as more inpatient stays, a higher risk of 30-day hospital readmission, and greater utilization of healthcare services (Reed *et al*. 2019). The World Health Organization (2024) estimates that untreated hearing loss poses an **annual global cost of US $980 billion**.

Hearing Loss is Preventable

WHO estimates that around 50% of hearing loss cases could be prevented through improved public health measures that ensure early hearing assessment, prompt diagnosis, and appropriate medical management. Policies are also needed to reduce noise exposure, raise awareness about hearing loss risks, and inform legislation designed to safeguard hearing.

70% of Rural Hoosiers Exposed to Occupational Noise May Have Hearing Loss in at Least One Ear

Khan *et al.* (2017)

Most farm sounds (tractors, combines, grain dryers, chain saws, animals, and aerial spraying) are louder than the permissible noise levels in mines and factories. In addition, many of these individuals are exposed to ototoxic chemicals and pollutants.

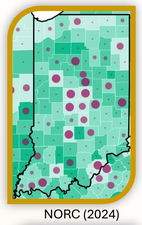

NORC (2024)

Audiology Services are Limited in Rural Counties which are Associated with Hearing Loss

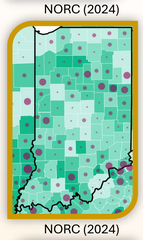

NORC (2024)

Economic Risk is Associated with Hearing Loss

Economic risk is an index comprised of poverty rate, # of industry dependencies, net migration, and labor force participation rate

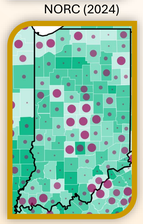

NORC (2024)

Education Level is Associated with Hearing Loss

Disparities in Hearing Aid Use (Adults >70 years)

Reed *et al.* (2023)

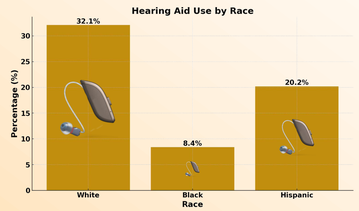

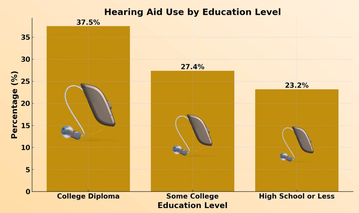

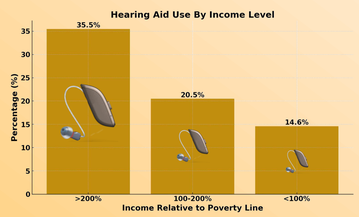

Precision Audiology

The Audiology Research Diagnostics Core (ARDC) in SLHS at Purdue West Lafayette leverages the university's international expertise in audiology and cross-species auditory neuroscience utilizing a standardized set of advanced in-lab and online audiological assessments. It consists of a full set of clinical audiology equipment in a double-walled sound booth. It is dedicated to advancing the field of auditory research by providing **1) standardized audiological assessments for all hearing-lab subjects on campus, 2) a targeted recruiting subject pool, and 3) a big-data repository to address questions requiring bigger data than any one lab can obtain.** It offers a range of services and projects aimed at developing precision audiology (diagnostics and interventions) by linking standardized assessments of clinical and research diagnostics that have been developed based on mechanistic insight from auditory neuroscience taking place in labs at Purdue and collaborating institutions.

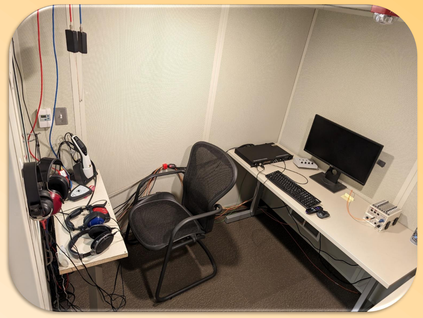

Accessible Audiology

16 TECH INNOVATION DISTRICT

The Purdue Center for Accessible Precision Audiology (PCAPA) in Indianapolis

Strategically located at the 16 Tech Innovation District near Purdue In Indianapolis, the PCAPA (funded by the Provost's Office and the Office of Research) is an extension of the ARDC. The center aims to become a hub for innovative research and community service in audiology. 16 Tech is a 50-acre community with cutting-edge facilities poised to become a cornerstone for faculty-led research, student education and training, and extensive community engagement. Located on the edge of the Artisan MarketPlace (AMP) in 16 Tech, PCAPA will provide direct access to a highly diverse (racial, socio-economic, etc.) population of community members. Being in 16 Tech provides access to innovative health initiatives being conducted by other universities and medical industries (e.g., Lilly).

Facility Features

- Clinical-grade data collection room with sound-attenuated booth (10'x12', double-walled)
- Front-facing intake/recruiting room with demos/videos
- Accessible and online data collection and analysis room
- Flexible space for offices and growth

Focus on Accessibility

With a heightened focus on engaging a more diverse community and extending outreach efforts statewide to address the critical issue of untreated hearing loss, the PCAPA will leverage major NIH grants to **1) inform diverse populations of Hoosiers about the many health and economic burdens associated with untreated hearing loss; 2) provide research-grade standardized audiological assessments for community members; and 3) develop an open-source data hub of standardized hearing measures with AI-enabled analysis tools/services to facilitate accessible precision audiology.**

Tools for Precision Assessment

Multiple-Measure Assessments Are Required to Improve the Sensitivity and Specificity of Hearing Diagnostics

(1) Standard assessments: wideband tympanometry for middle ear function, acoustic reflex testing, pure-tone and bone conduction audiometry across extended high frequencies, distortion product otoacoustic emissions to check cochlear health, and speech-in-noise test
(2) Online surveys and psychoacoustic measures
(3) Advanced assessments: additional types of otoacoustic emissions tests to separate cochlear sources, auditory brainstem responses to assess the auditory pathway, frequency-following responses for complex sound processing, and a broader range of evaluations for word recognition and speech perception in noise, as well as some cognitive assessments

Open-Source Hearing Assessment Platform

With support from a 5-year, multi-million-dollar grant (NIH SBIR 1R44DC021123-01, PI: Clavier), Purdue's collaboration with Creare, LLC aims to leverage **inexpensive** open-source technology to develop **accessible** audiological assessments (*i.e.*, not in a clinical sound booth). Synergizing Purdue's strengths in audiology/auditory neuroscience and **data analytics**, we aim to collect, curate, and analyze standardized audiological data at scale to support the development of **accessible precision audiology** with the ultimate goal being a **unique auditory profile** for each patient to facilitate **individualized counseling and treatments** and as a lens on their overall health profile.

Open-Source Hardware with firmware algorithms

The Tympan is a hardware platform with capabilities for audio processing and the production of calibrated audio output with various output devices.

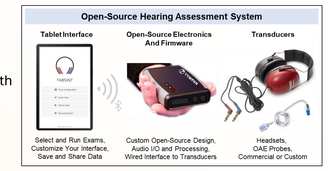

Open-Source Software with platform compatibility

TabSINT is a mobile app that allows researchers to generate test sequences and upload them to the cloud to distribute across a variety of locations for local testing on a mobile device.

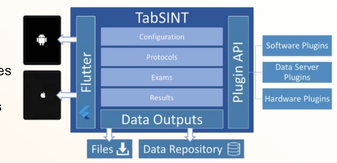

Open-Science Data Repository with standardized data schema

The datahub provides several data access mechanisms: (1) open API allowing search on index terms; (2) analytics workspaces for executing client code; (3) web services API for constructing analytics applications; and (4) techniques for processing data.

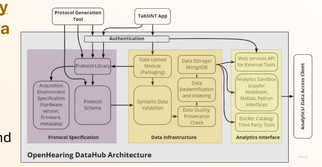

References

- Fabry, D. (2024). "AudiologyOnline 2024 Industry Roundtable," Course #39227. www.audiologyonline.com/audiology-ceus/course/2024-industry-roundtable-39227.
- Khan, K.M. et al. (2017). "Feasibility of a low-cost hearing screening in rural Indiana," BMC Public Health, 17(1).
- NORC at the University of Chicago (2024). "National Indicator Report on Hearing Loss 2024," Chicago, IL.
- Reed, N.S. et al. (2019). "Trends in health care costs and utilization associated with untreated hearing loss over 10 years," JAMA Otolaryngology – Head & Neck Surgery, 145(1), p. 27.
- Reed, N.S. et al. (2023). "Prevalence of hearing loss and hearing aid use among US Medicare beneficiaries aged 71 years and older," JAMA Network Open, 6(7).
- The World Health Organization (2024). "Deafness and hearing loss," www.who.int/news-room/fact-sheets/detail/deafness-and-hearing-loss.

Acknowledgments

Purdue's Office of Research and Provost's Office funded the PCAPA. Hari Bharadwaj, Andrew Sivaprakasam, Samantha Hauser, Madison McNeill, Elizbeth Jensen, and Isabella Huddleston have made invaluable contributions to the ARDC development.

Phonation Signal and Image Processing for Detecting and Classifying Dysphonia

***Pranjal Anand*[1], Rita Patel[2], Noah Parker[3], Benjamin Anthony[3], Preeti Sivasankar[4], Brett Meyers[5], Pavlos P Vlachos[1,5]**

[1] *School of Mechanical Engineering, Purdue University*
[2] *Dept. of Speech, Language and Hearing Sciences, Indiana University*
[3] *Dept. of Otolaryngology, IU Health*
[4] *Dept. of Speech, Language and Hearing Sciences, Purdue University*
[5] *Regenstrief Center for Healthcare Engineering, Purdue University*

OVERVIEW

Detecting voice – related pathologies early is challenging. Research on processing audio and high - speed video endoscopy (HSV) data reveal that recorded signals are difficult to classify. There is potential to detect dysphonia in its early stages, while it is still not very apparent to the human ear. We aim to use signal processing techniques to 1) Delineate pathophysiological features and 2) Classify different pathologies from audio and HSV data

THE VALUE OF VOICE

- Vocal communication could have a significant monetary value for many professionals. Despite the level of automation today, vocal communication is a fundamental part of society.
- Changes in muscle tension, subtle swelling, onset of tumors are not visually apparent, unlike the polyp in Fig 1[1]. These changes are reflected in the vibratory characteristics of vocal folds.
- We identified a need for better audio and video data analysis methods to rid the measurement chain of inter – recording variations and achieve better classification accuracy.

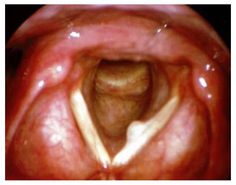

The right fold has a polyp. Such growths can also alter vocal fold vibrations, and a clear view from an endoscope, like this one, is enough for diagnosis.

Fig 1

HOW WE PHONATE

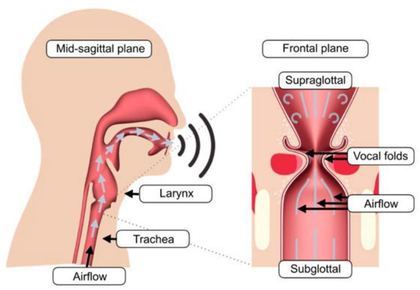

Thornton et al., 2019

Fig 2

Voice quality can hence be influenced by:-

➔Visually apparent growth like nodules or polyp
➔Change in muscle (vocal fold) strength

Videostroboscopy, the clinical standard today cannot capture true kinematics of vocal folds.
These methods are preferred by clinicians as they enable better qualitative assessment through color images and a live feed, as opposed to grayscale HSV images (Fig 3).

CHALLENGES TO VIDEO AND AUDIO DATA PROCESSING

- Signal processing methods and machine learning have been used to inform analysis of vocal fold vibrations. However, classification after applying quantitative assessment has not been successful to the point of making it a clinical standard.
- Glottal area waveform (GAW) and Phonovibrograms (PVG) help visualize vocal fold vibrations (Fig 4). We look to extract information about vibration irregularities from the visual data.
- Nyquist plots (Fig 5) generated by Hilbert transform have been used since 2005[3], but an attempt at quantification was made only in 2023[4].
- Data variability : The voice of a subject can change throughout the day, due to low hydration, or prolonged conversation, etc.
- The recording equipment can also lead to variability for large datasets.

To tackle these challenges, we look to discover fundamental properties of the signals. Our data analysis expertise has been useful in image processing for fluid mechanics experiments and medical imaging and will give some insight into overcoming the stated challenges.

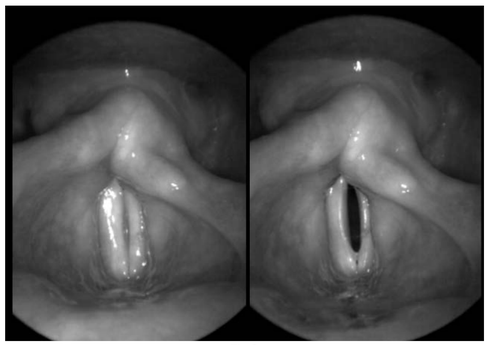

Fig 3

Closed and Open vocal folds as seen in HSV, steady phonation, at 4000 fps

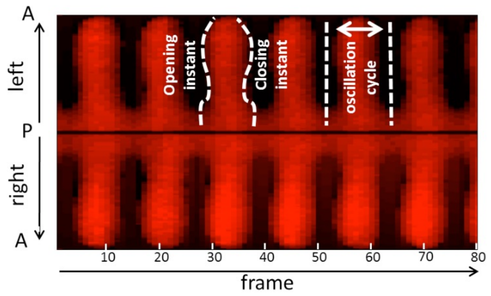

Fig 4

Phonovibrogram (PVG) from [5]., which enable visualizing displacements of each vocal fold, as opposed to the oscillations of the glottal area (black gap between folds in Fig 1) shown by the more widely-used Glottal Area waveforms (GAW).

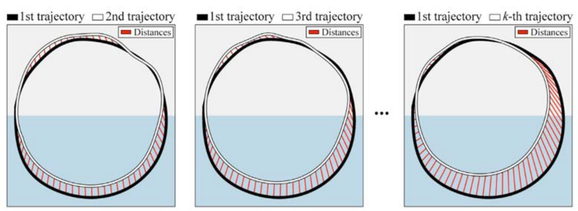

Fig 5(a)

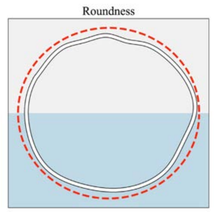

Fig 5(b)

Quantitative analysis of nyquist plot from GAW were used in [4] to inform vibration differences in pathological vocal folds. Within- trajectory variability (a) and consistency within a cycle (b) were calculated among other shape-based parameters.

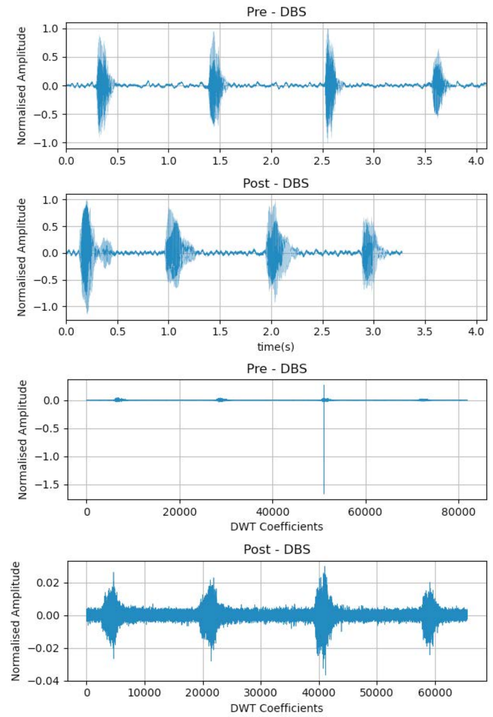

Fig 5

Waveform data of a patient saying 'hehe' , before and after Deep Brain Stimulation (DBS). DBS is a treatment for essential tremor – involuntary twitching of certain muscle groups.

Visually some differences can be noted, but signal processing methods can help us better. Here, a preliminary demonstration is shown with the discrete wavelet transform (DWT), which is used for denoising and compression. We look to also utilize the continuous wavelet transform (CWT) which can reveal discontinuities in both the time and frequency space of signals, and was used for analysing PVG in [5]

MOVING AHEAD

- Process simultaneous HSV and audio recordings for a patient with essential tremor (left), pre and post Deep Brain Stimulation, This is a specific application yet unexplored in literature.
- Scrutinize the data features (both audio and video) and look for features which can help in characterizing the changes after treatment.
- Ultimately, include normophonic control data and look towards classifying voice and video into pathological and non – pathological.

References
[1] https://www.amboss.com/us/knowledge/benign-laryngeal-lesions
[2] Thornton et al, **Impact of Subharmonic and Aperiodic Laryngeal Dynamics on the Phonatory Process Analyzed in Ex Vivo Rabbit Models**, MDPI Applied Sciences, 2019
[3] Yan et al., **Analysis of Vocal-fold Vibrations from High-Speed Laryngeal Images Using a Hilbert Transform-Based Methodology**, Journal of Voice, 2005
[4] Arias-Vergara et al., **Nyquist Plot Parametrization for Quantitative Analysis of Vibration of the Vocal Folds** , Journal of Voice, 2023
[5] Unger et al., **A Wavelet-Based Approach for a Continuous Analysis of Phonovibrograms**, Proceedings of 34th Annual International Conference of the IEEE EMBS

HPV 16 DNA AMPLIFICATION AND DETECTION FROM CELL LYSATES ON A PAPER SUBSTRATE WITH LATERAL FLOW READOUT

Luke P. Brennan[1,2] Francesca C. Hamacher[3] Ana Claure[1] Jacqueline C. Linnes[1,4] Natalia M. Rodriguez[1,4]

[1]Weldon School of Biomedical Engineering, Purdue University, West Lafayette, IN, USA
[2] Medical Scientist Training Program, Indiana University Medical School, Indianapolis, IN, USA
[3]Agricultural & Biological Engineering, Purdue University, West Lafayette, IN, USA
[4]Department of Public Health, Purdue University, Purdue University, West Lafayette, IN, USA

PURDUE UNIVERSITY
Weldon School of Biomedical Engineering

Background

- Cervical cancer is the 4th most common cancer in women globally, and is completely preventable with proper screening
- 20% of American woman are under-screened, and another 20% do not receive follow-up care
- Human papillomavirus (HPV) causes almost all cases of cervical cancer
- HPV DNA is a widely used analyte for clinical cervical cancer screening
- A rapid test that copies and detects HPV DNA could increase screening accessibility by facilitating same-visit results

SAPONIN AND ACHROMOPEPTIDASE CONSISTENTLY LYSE CELLS

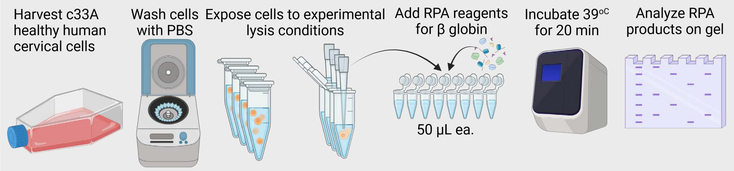

Cell lysis methods evaluated included 2.5% Saponin, 25U achromopeptidase (ACP) with heat inactivation, 10% Triton X100, 12µM Proteinase K with 56oC heat inactivation, 10% Tween20, 1µM Guanidinium Hydrochloride, and 25mM NaOH + 95oC. Probe sonication (3x 50% duty cycle for 10 seconds) and no lysis control served as positive and negative controls for cell lysis, and no DNA and 1E4 copies of c33A gDNA conditions served as Recombinase polymerase Amplification (RPA) control. Each method was assessed by conducting RPA on cell lysates and reading the intensity of the target band on a polyacrylamide gel.

Sample Adequacy Control (β-globin) Amplification Endpoint Intensity		No DNA control	Pure gDNA	No Lysis Control	Probe Sonication	2.5% Saponin	25U ACP
	Trial 1	-	+++	++	+		++
	Trial 2	-	+++	-	+++		++
	Trial 3	-	+++	+	+++	+	++
	Trial 4	-	++	++	+++	+	++
	Average	-	+++	+	+++	+	++

- No lysis control produced inconsistent, but noteworthy amplification results
- 2.5% Saponin and 25U ACP produced amplified target DNA the most consistently in <10 minutes in up to 20% cell lysate (n=2).

HPV 16 DETECTED AT 1000 COPIES PER REACTION

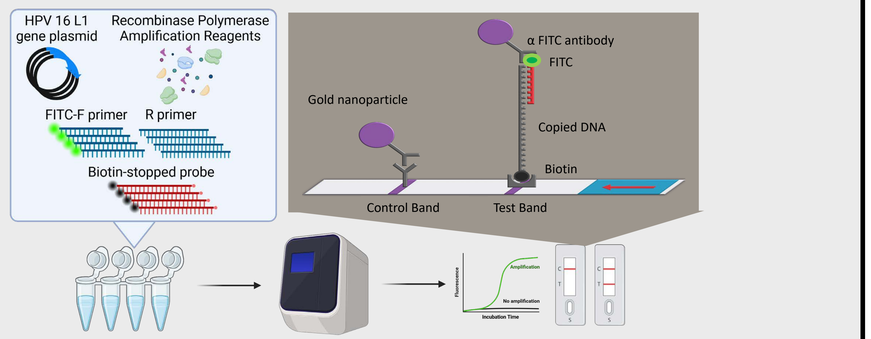

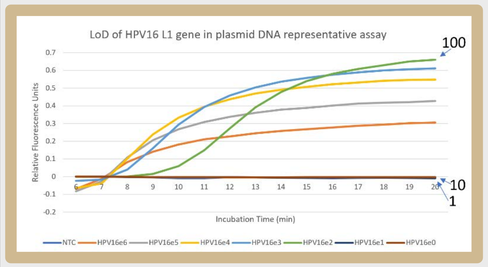

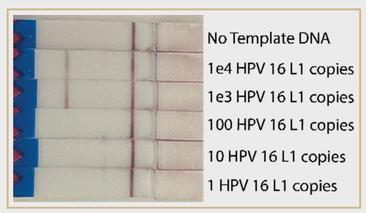

The HPV L1 gene was successfully amplified and detected to a limit of 100 copies/50 µL reaction with fluorescent detection and 1000 copies/50 µL on lateral flow strips (n=3 for each).

LIMIT OF DETECTION (LoD) OF 10,000 HPV L1 GENE COPIES/50 µL REACTION ON PAPER

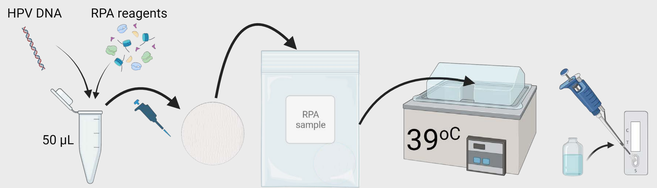

DNA from the HPV L1 gene inserted into the pUC57 plasmid was used as simulated HPV DNA. RPA reagents were purchased from TwistDx. After a 20-minute reaction, RPA product was eluted with 100 µL of Milli-Q water of which 2 µL was pipetted onto dipstick immunoassays from Milenia Biotec, Germany.

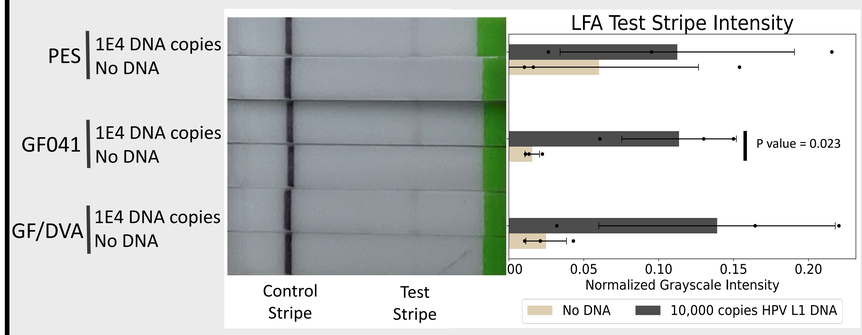

Previous literature[5,6] reported RPA was achieved on bound glass fiber ('GF041', GFCP203000, Millipore) and GF/DVA (Whatman). Another isothermal nucleic acid amplification assay worked best on Polyethersulfone ('PES', Milipore "GPWP04700"). RPA reactions amplified DNA in al paper types, with GF041 performing the most consistently; LoD = 1E4 (n=3).

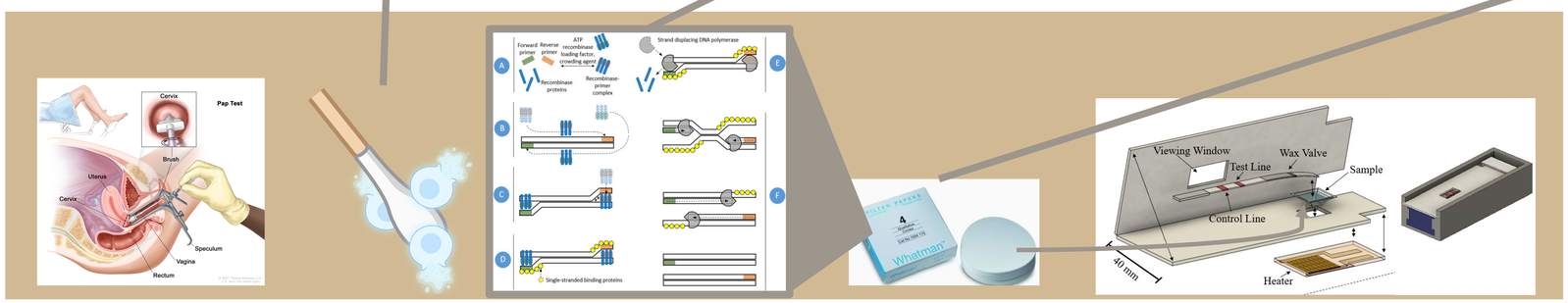

CONCLUSIONS

- Saponin and Achromopeptidase treatments demonstrated consistent cell lysis and DNA freeing with methods amenable to a rapid test platform using a resistive heater
- A 50 µL RPA reaction can copy HPV L1 DNA to a limit of detection of 1000 copies/50 µL reaction and read out on a lateral flow test.
- A 50 µL RPA reaction operates to LoD of 1E4 L1 gene copies on GF041.

ACKNOWLEDGEMENTS

This work was funded by the NCI grant number K01CA241073, PI: Rodriguez
Our thanks to the Indiana Cancer Consortium, and our community partners

REFERENCES

1. WHO, Cervical Cancer Factsheet, Accessed Oct 2023.
2. Vaginal Cancer Treatment (PDQ®): Patient Version. 2021 Dec 17.
3. Lobato et. al. *TrAC, Trends Anal. Chem.* 2018
4. Phillips E.A. et. al. *Lab Chip*, 2019, **19**, 3375-3386.
5. Rohrman et. al. *Lab Chip*, 2012, **12**, 3082-3088.
6. Linnes et. al. *Biomed Devices*, 2016, **18**, 1387-2176.

Linnes Lab Purdue
THQL Health TechQuity Lab

Geospatial distribution of COVID-19 related deaths among nursing home residents across the United States in each wave

Madeline Brown, MPH, CPH, Cody Mullen, PhD, & Randy Hubach, PhD, MPH

PURDUE UNIVERSITY | *Department of Public Health*

Introduction

Nursing home residents experienced a much higher rate of COVID-19 related deaths throughout the pandemic compared to the general population. In December 2020, the COVID-19 death rate for older adults in nursing homes was 9,200 per 100,000, while the rate for older adults not in nursing homes was 87 per 100,000. This study aimed to investigate how the rate of COVID-19 related deaths were geospatially distributed and which areas of the United States had significantly higher or lower rates.

Methods

CMS COVID 2020-2023 and Provider Information

▼

Facilities with COVID-19 data

▼

Merged by Provider Number

▼

Wave Determination

▼

Optimized Hot Spot Analysis

The COVID-19 dataset was updated on a weekly basis and collection began May 24, 2020. The number of COVID-19 related deaths per facility were cumulative for each week. Based on rates of COVID-19, the three waves included cumulative data up to these respective dates: June 27, 2021, April 10, 2022, and April 10, 2023. Analysis was run for each wave in ArcGIS Pro 3.1 and the final table was exported to evaluate the characteristics of nursing homes that returned with significant hot and cold spots.

References: Behavioral Risk Factor Surveillance System Survey Questionnaire. Atlanta, Georgia: U.S. Department of Health and Human Services, Centers for Disease Control and Prevention, 2019, 2020.

Results

Figure 1: Hot and Cold Spots Across the U.S.

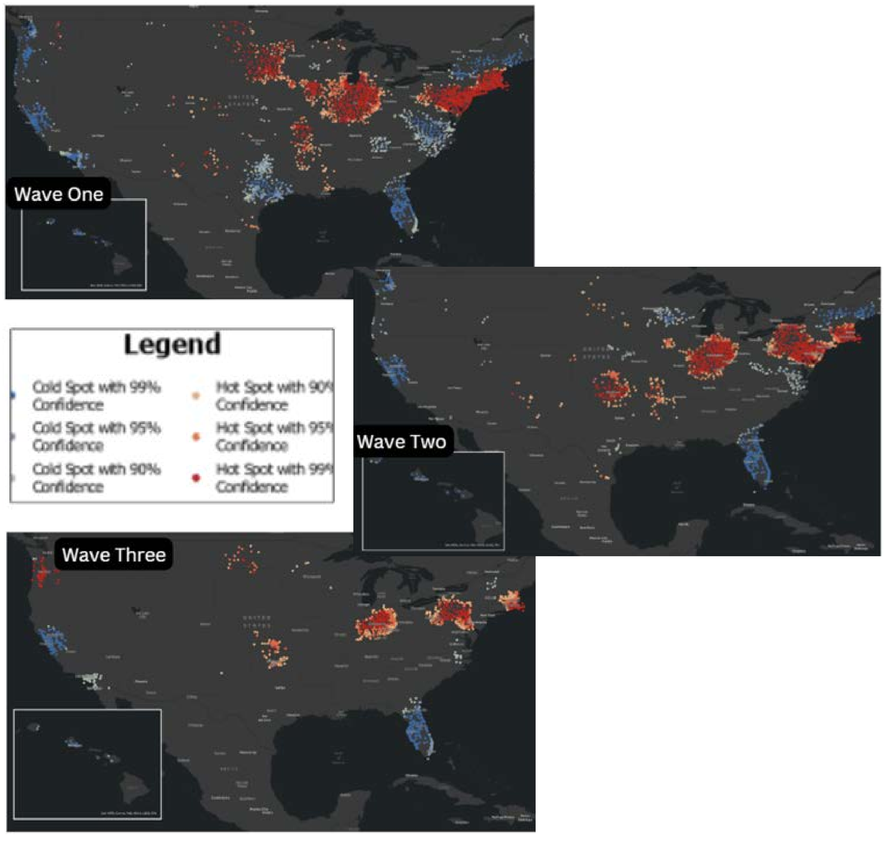

Wave 1 Results: Regions with clear hot spot clusters of COVID-19 death rate included the Midwest, parts of Northeastern United States, and Arkansas. Cold spot clusters included Florida, North Carolina, and Georgia. Hawaii and California had cold spot clusters throughout each wave.

Wave 2 and 3 Results: Hot and cold spot clusters became more concentrated, the cold spot in Georgia disappeared, and a new hot spot appeared in Washington and Oklahoma. However, the hot spots in Oklahoma significantly decreased in Wave 3.

Table 1: Facility Characteristics in Hot and Cold Spots

Variable		Cold Spot	Hot Spot
Quality Rating			
	1	2.05%	4.04%
	2	9.34%	11.59%
	3	18.5%	20.77%
	4	28.9%	28.13%
	5	38.4%	32.72%
Provider Type			
	Medicare	3.92%	3.37%
	Medicare and Medicaid	94.71%	94.71%
Ownership Type			
	For profit	69.86%	67.40%
	Government	3.86%	4.81%
	Nonprofit	24.91%	25.88%

Significance

This study aimed to investigate whether further research was needed on the geographic locations as significant predictors of COVID-19 mortality. As the pandemic continued, significant changes occurred across the states. This study shows that more research needs to be done about the policies implemented or state-level regulations that increased or decreased the risk of COVID-19 deaths in nursing homes.

Limitations and Concerns

One concern of this study is that nursing home facilities did not undergo routine examination and regulatory activities by CMS, which could have resulted in errors of the reported data. Additionally, hot spot spatial analysis does not account for population density or community COVID-19 rates, which have been shown to be significant predictors of long-term care facility COVID-19 rates for cases and deaths.

Evaluation of a Social Justice Institute for Higher Education Faculty and Staff

Jennifer M. Jabson Tree, PhD, MPH, Purdue University; Katherine Buchman, MPH, Purdue University; Dorian McCoy, PhD, University of Tennessee-Knoxville; Stefanie Benjamin, PhD, University of Tennessee-Knoxville

Study Objectives:

- Social Justice Institute (SJI) was implemented and evaluated to address faculty and staff self-efficacy for engaging equity and inclusion activities in one college of education, health, and human sciences.
- Evaluation Questions:
  - What were the associations between attending the program and self-efficacy for engaging equity and inclusion activities?
  - How did program participants rate the quality of the program daily content and setting?

Background

- Public health, like other disciplines often included in colleges of education, health, and human sciences, is rooted in social justice and committed to advancing equity in health, education and professional development for faculty, staff, and students.
- Colleges often struggle to make changes that advance and prioritize equity, inclusion, and justice across policies, practices, procedures, and departments.
- Colleges of education, health, and human sciences are not immune to being influenced by systems of oppression including racism, heterosexism, sexism, ageism, antisemitism, cissexism, ableism, classism, religious discrimination and more. Institutions, social systems, and individuals' behavior are produced, reinforced, organized, and reproduced by systems of oppression[1].
- Faculty and staff self-efficacy to engage equity and inclusion activities is required to support equity and inclusion in college's policies, practices, and procedures.
- Self-efficacy to engage in equity and inclusion activities may improve with in-depth, experiential education about systems of oppression theory and practice in equity and inclusion activities[2].
- SJI is a curriculum designed to increase the self-efficacy of university faculty and staff to develop departments, policies, practices, and curricula which produce health services professionals who are able to address health equity in their work and combat systems of oppression as they appear in their college.

Positionality of SJI instructors:

- The first instructor is an associate professor and identifies as White-Latina, cisgender, queer, female, first-generation college graduate in her forties. It was critical for her to consider how her white privilege and position in the institution may influence participants' engagement with the curriculum.
- The second instructor is a tenured faculty/administrator and identifies as a Black male. It was critical for him to consider how his position as a director (college-level administrator) might influence participants' engagement during the institute.
- The third author is an associate professor and identifies as a White, Jewish, cisgender woman in her thirties. It was critical for her to decenter her whiteness and to soften her approach toward racial dialogues.



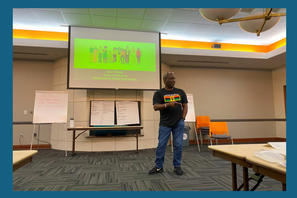


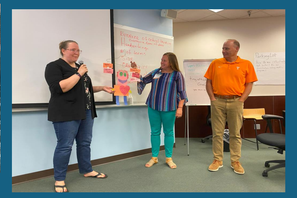

Methods

- Full-time faculty, staff, or administrators in the college of education, health, and human sciences were eligible for inclusion.
- The SJI was conducted as a 7-day, 56-hour immersive training at a large southeastern university.
- Participants completed a pre- and post-quantitative survey of their self-efficacy relative to their ability to engage in equity and inclusion activities in their respective departments/units, as well as their evaluation and impression of the SJI.

Measures

Self-efficacy: Self-efficacy survey questions were developed from Bandura's [2,3] theory of human agency. Examples of questions are below:

- How much can you do to make your department/unit see diversity, equity, and inclusion as valuable?
- How much can you do to get your department/unit to engage in diversity, equity, and inclusion activities?
- How much can you do to get your department/unit to engage in diversity, equity, and inclusion activities (e.g., syllabi reviews, incorporating diversity and equity content into courses, evaluating the department/unit climate for inclusion, etc.)?

SJI Content Quality and Process: Additional items on the post-SJI survey solicited participant perceptions of the quality of each day's content and presentation. Example of questions are below:

- Please rate the quality of the curriculum and experiential learning activities concerning systems of oppression, privilege, and power (Day 1).
- Please rate the quality of the curriculum and experiential learning activities concerning race, racism, ethnocentrism, nativism, and whiteness (Day 3).

Analysis

- Summary and descriptive statistics were calculated to describe participant's self-efficacy ratings and ratings of daily content quality, space quality, and learning.
- Pre-and-post self-efficacy means were calculated for the full scale and for paired individual items.
- Paired t-tests were calculated on individual scale items and on full-scale scores to assess for change in self-efficacy before and after SJI participation.

Results

Table 1. Participant Demographics

Total Participants	14	13
Nonbinary/ genderqueer	1	1
Cisgender Female	11	11
Cisgender Male	2	1
Black/ African American	2	1
Latiné	0	2
White	12	10
Faculty	9	7
Staff	3	5
Extension	0	1
Graduate Student	2	0

Fear Sphere– SJI 2023

Individual Self Efficacy Items

Table 2. Total self-efficacy to engage in equity and inclusion activities

Year 1					Year 2				
	Mean (SD)	Range	t-test	p		Mean (SD)	Range	t-test	p
Pre SJI Self-Efficacy	5.84 (0.76)	3.76, 7.0	-2.11	0.1	Pre SJI Self-Efficacy	5.83 (0.37)	4.98, 6.67	-1.51	0.2
Post SJI Self-Efficacy	6.49 (1.19)	4, 8.12			Post SJI Self-Efficacy	6.46 (0.48)	5.33, 7.58		

Table 3. Social Justice Institute Topics and Activities by Day

			Year 1		Year 2	
Topic	Didactic Learning	Experiential Learning Activities	Mean	SD	Mean	SD
Day 1: Introductions and Foundations	Introduce systems of oppression, set expectations, introductions, objectives	If the shoe fits; micro-lab; power shuffle; action planning;	4.5	0.52	4.86	0.36
Day 2: Sex, Gender, Sexism, and Cis Sexism	Lecture and discussion regarding definitions and influence of sexism, gender and gender identity, transgender experiences, cis-sexism in higher education	Gender case studies; image analysis; performing gender; take a stand; walk like a man/sit like a lady; action planning	4.75	0.45	4.86	0.36
Day 3: Race, Racism, Whiteness	Lecture and discussion regarding definitions and influence of racism, whiteness, and race in higher education	Theatre of the oppressed (simultaneous dramaturgy); Safe the Last Word; Action planning	3.75	0.97	4.71	0.61
Day 4: Heterosexism, Sexual Orientation	Lecture and discussion regarding definitions and influence of heterosexism, homophobia, and sexual orientation in higher education	Coming Out Stars and Discussion; Heterosexual questionnaire; LGBTQ case studies; action planning	4.58	0.51	4.79	0.58
Day 5: Disability and Ableism	Lecture and discussion regarding definitions and influence of disability, ableism, in higher education	Image theatre; Stereotypes, violence, and institutions; photovoice of accessibility issues; Normative body in STEM; action planning	3.83	0.83	4.64	0.63
Day 6: Classism (half day) & Religious Discrimination (half day)	Lecture and discussion regarding definitions and influence of class and religious discrimination, in higher education	Make a mobile activity (inequitable resources); class background inventory; unconstitutional practices activity; action planning	4.08	0.67	4.64	0.63
Day 7: Allyship, Reconciliation, Coalition Building	Lecture and discussion regarding definitions and action points for allyship, reconciliation, and coalition building, in higher education	Being an ally case studies; colleagues say the darndest things activity; Hot Moments on the Search Committee theatre; action planning	4.08	0.9	4.71	0.61

EQUITY INCLUSION + JUSTICE AGENT CEHHS 2021

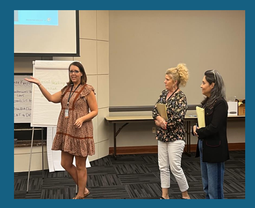




Conclusions

Evaluation:

Our program showed positive associations of between SJI participation and self-efficacy to engage in equity and inclusion activities. We also found that participants enjoyed the substantive program content and the quality of the space. Based on our findings we contend the SJI is one means for advancing and increasing self efficacy for engaging equity and inclusion activities in a college of education, health, and human sciences.

Scalability:

The positive associations between SJI and self-efficacy in equity and inclusion activities highlights the promise of such programs in colleges of education, health, and human sciences. Within the U.S., there continues to be extreme pushback against equity and inclusion as a pedagogical approaches and frameworks for understanding injustices and inequities in health and society.

Public Health Implications:

The SJI is a tool that can be used in any college producing health and human science professionals. Engaging faculty and staff in programmatic efforts such as SJI may be a promising strategy for ensuring that colleges of education, health, and human sciences are accurately educating the next generations of health and human sciences professionals in equity and inclusion topics that are vital to their professions and the work they will do.

References:

1. Johnson, A. (2017). Privilege, Power, and Difference (3rd ed.). McGraw-Hill Professional.
Kellar, S. P., & Kelvin, E., A. (2013). Munro's statistical methods for health care research (6th ed.). Wolters Kluwer.
2. Bandura, A. (1977). Self-efficacy: Toward a unifying theory of behavioral change. Psychological Review, 84(2), 191–215.
3. Bandura. A. (2006). Toward a psychology of human agency. Perspectives on Psychological Science, 1(2), 164–180.

Acknowledgements: Funding provided by the College of Education, Health, and Human Sciences at University of Tennessee, Knoxville

Impaired visual experience-dependent oscillations and underlying interareal circuit in the visual cortex of Fmr1 KO mice

Xi Cheng[1,2], Sanghamitra Nareddula[1,2], Hao-Cheng Gao[3], Yueyi Chen[4], Tiange Xiao[4], Paige A. Edens[1]
Adam J. Kimbrough[4], Fang Huang[3], Alexander A. Chubykin[1,2]
1. Department of Biological Sciences, Purdue University, West Lafayette, IN 2. Purdue Institute for Integrative Neuroscience (PIIN), Purdue University, West Lafayette, IN
3. Weldon School of Biomedical Engineering, Purdue University, West Lafayette, IN 4. Department of Basic Medical Sciences, College of Veterinary Medicine, Purdue University, West Lafayette, IN

Introduction

Fragile X syndrome (FXS) is the most common form of inheritable autism spectrum disorder, which is often characterized by intellectual disability and visual learning deficits. Previous studies have described attenuated encoding of familiar stimuli in V1 by theta oscillations, disrupted excitatory to inhibitory (E/I) balance, impaired short-term plasticity, and altered functional connectivity in Fmr1 KO (FX) mice, the model of FXS. The reciprocal projections connecting the primary visual cortex (V1) and higher visual areas, including both the ventral and dorsal pathways, have been implicated in regulating cognitive processes such as prediction, attention, and visual learning. However, how the inter-areal connectivity is affected in FXS is poorly understood.

Reciprocal inter-areal circuits in visual pathway — Feedforward — Feedback

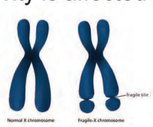

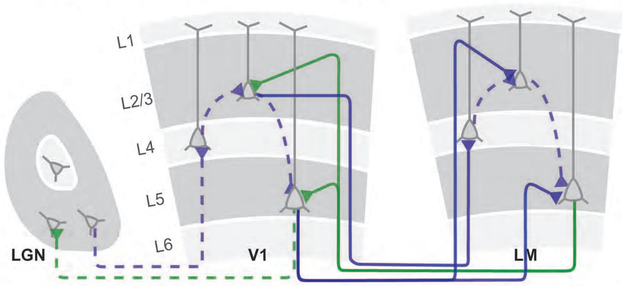

Method

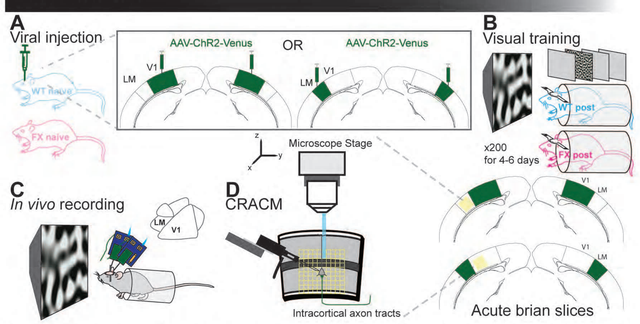

Figure 1.WT and FX mice were recorded *in vivo* and injected with AAV1-ChR2-Venus into V1 or LM to study feedforward or feedback projections. (A) Viral injections were done into V1 and LM. **(B)** About half of the mice underwent pink noise (0.12 cpd 0.75 HZ) visual training for 4-6 days and were designated as post-visual experience groups. **(C)** We conducted *in vivo* simultaneous silicon probe recording in some of the mice. **(D)** Some mice were sacrificed and acute brain slices were obtained for the CRACM experiment. PCs from cortical L2 to 5 in LM or V1 were recorded by whole-cell patch-clamp.

Cell traces of patched neurons

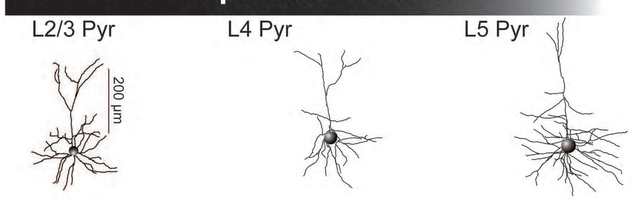

Attenuated visual experience evoked oscillations

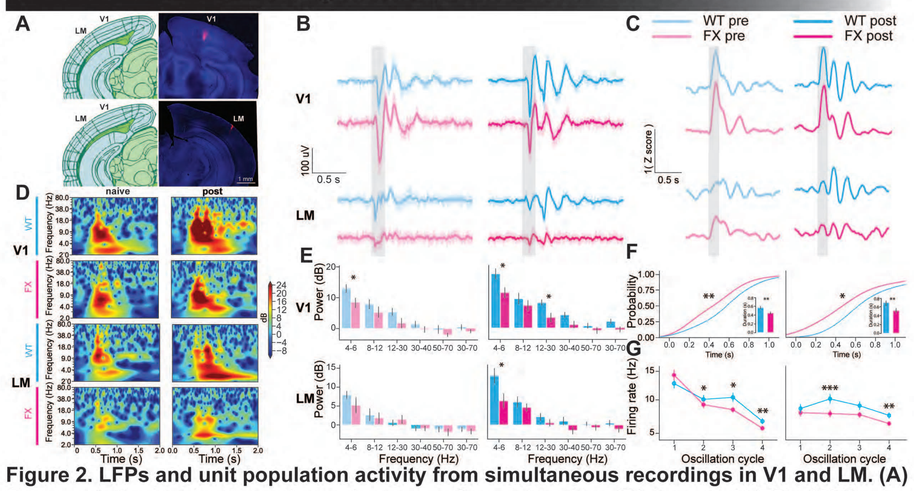

Figure 2. LFPs and unit population activity from simultaneous recordings in V1 and LM. (A) Representative histology showing probe traces of recording sites. **(B)** Averaged VEPs. **(C)** Baseline normalized population averaged z-score firing rates of single units. **(D)** Heatmaps showing time-frequency spectrograms of trial averaged VEPs. **(E)** Quantified power across various frequency bands for trial averaged VEPs. **(F)** CDF of the duration of identified local maxima of averaged z-score firing rates of units post-visual experience. **(G)** Maximum firing rates at 4 oscillation cycle windows averaged across units shown post- experience.

Mapping experience-dependent V1->LM FF circuits

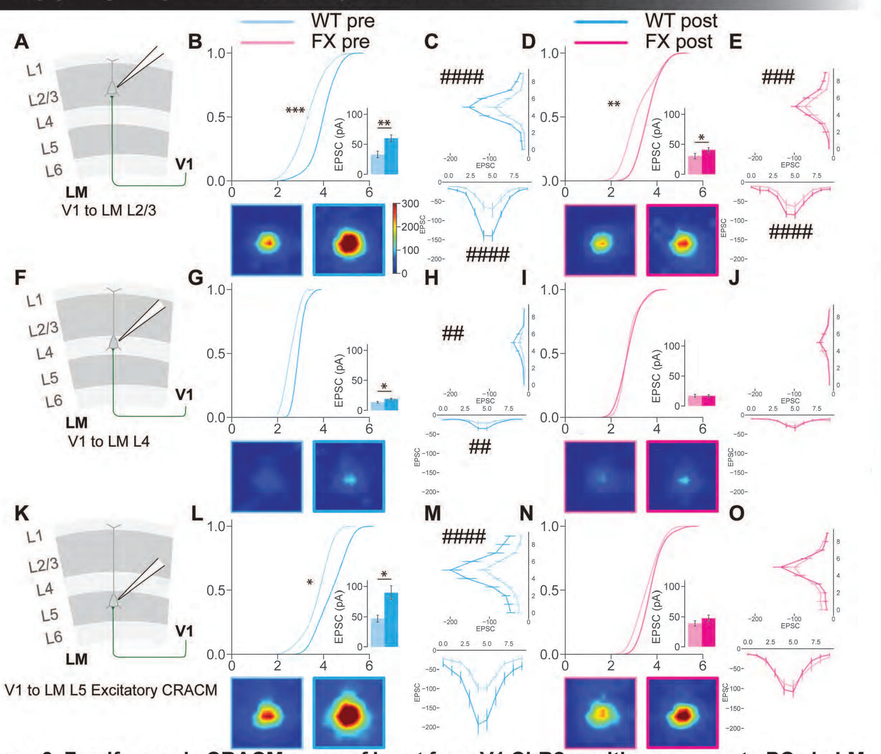

Figure 3. Feedforward sCRACM maps of input from V1 ChR2 positive neurons to PCs in LM. (A) Illustration of V1 to LM L2/3 PC projections. **(B)** The cumulative distributions (top) of the averaged EPSC$_{CRACM}$ plotted in ln scale in sCRACM map from LM L2/3 PCs in WT mice. Bar graphs of averaged EPSC$_{CRACM}$ amplitudes ± SEM (inset). The average sCRACM maps across each grid were plotted below the corresponding cumulative. **(C)** Averaged EPSC$_{CRACM}$ amplitudes ± SEM by grid position in the vertical from V1 L2/3 PCs in WT mice (top). Averaged EPSC$_{CRACM}$ amplitudes ± SEM by grid position in the tangential direction (bottom). **(F, G, H, K, L, M)** same as (A, B, C) but for L4, and L5. **(D, E, I, J, N, O)** same as (B, C, G, H, L, M) but for FX mice.

Mapping experience-dependent LM->V1 FB circuits

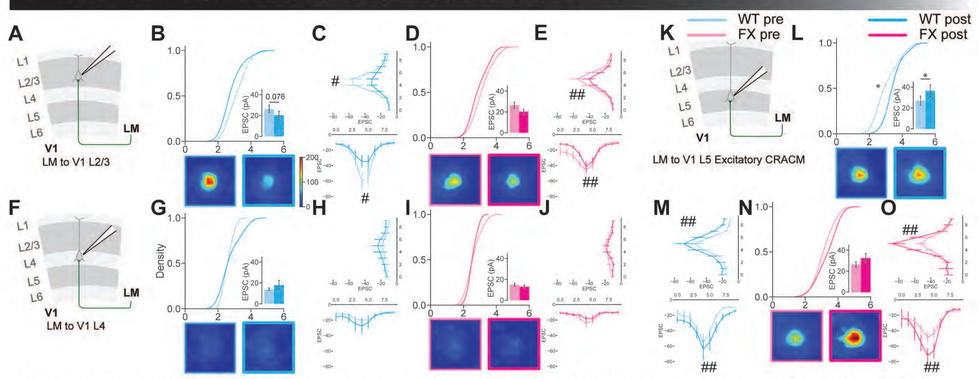

Figure 4. Feedback sCRACM maps of input from LM ChR2 positive neurons to PCs in V1. (A) Illustration of V1 to LM L2/3 PC projections. **(B)** The cumulative distributions (top) of the averaged EPSC-$_{CRACM}$ plotted in ln scale in sCRACM map from LM L2/3 PCs in WT mice. Bar graphs of averaged EPSC$_{CRACM}$ amplitudes ± SEM (inset). The average sCRACM maps across each grid were plotted below the corresponding cumulative. **(C)** Same as Figure 3C but for FB pathway. **(F, G, H, K, L, M)** same as (A, B, C) but for L4, and L5. **(D, E, I, J, N, O)** same as (B, C, G, H, L, M) but for FX mice.

iDisco & lightsheet: c-fos labeling of V1 and LM

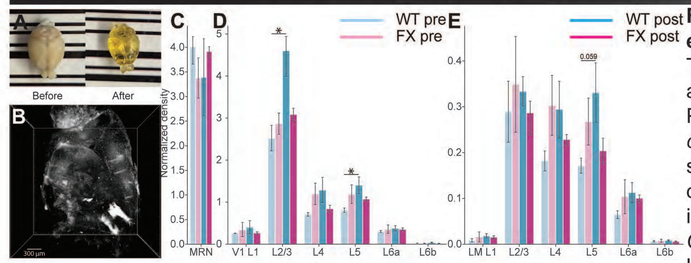

Figure 5. Normalized *c-fos* expression in V1 and LM. (A) The whole mouse brain before and after iDISCO clearing. **(B)** Projection of a whole-mount *c-fos* immunolabeling in the sagittal direction. **(C)** *C-fos+* cell number in MRN normalized to overall number **(D)** *C-fos+* cell number in V1 and LM normalized to it in MRN.

SMLM thick tissue imaging of dendritic spines in V1 L5 PCs

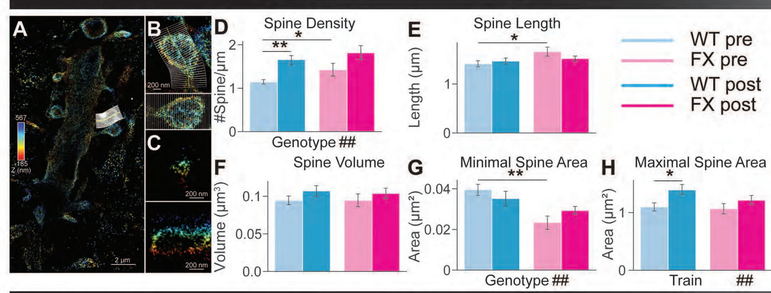

Figure 6. Spine morphology of V1 L5 PC dendrites. (A-C) An image showing dendrites from L5 PC by **4Pi Superresolution Microscopy**. **(D-H)** Barplots of different spine measurements.

Discussion and Acknowledgements

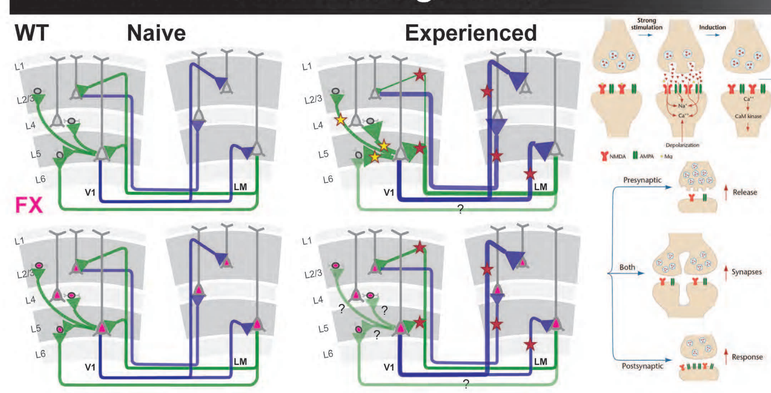

Thank my advisor, colleagues, and collaborators for the directions and support during my experiment. Thanks for the financial support from the National Institutes of Health.

National Institutes of Health

Interventions for Parents to Increase HPV Vaccine Uptake: An Integrative Review of Randomized Controlled Trials

Yeseol Cho BSN, RN, Soojung Jo, Ph.D, RN
School of Nursing, College of Health and Human Sciences, Purdue University, West Lafayette, IN

PURDUE UNIVERSITY
School of Nursing

OVERVIEW

This review synthesizes nine randomized controlled trials targeting parents to increase HPV vaccine uptake in adolescents aged 9 to 17.
In seven studies, particularly with interventions such as in-person education and mobile health showed significant effects.
We suggest further research on tailored strategies for wider application and optimal post-test timeframe.

Introduction

Efforts to prevent and control HPV infections are crucial for public health, requiring increased awareness, safe behaviors, and utilization of preventive measures. Understanding the extent to which parental interventions can influence vaccine decision-making is key to designing effective strategies to elevate adolescents' HPV vaccination rates.

Objectives

This systematic review aims to synthesize findings from randomized controlled trials (RCTs) that targeted parents to increase **HPV vaccine uptake** in their children.

Methods

A systematic search was conducted in PubMed and CINAHL based on the keywords: HPV vaccine, parents, intervention, and vaccine uptake. The inclusion criteria are RCTs published between 2014 and 2023, focusing on parents of HPV vaccine-eligible children (boys and girls aged 9 to 17) who had not initiated or completed the vaccine series. Articles were screened in their title, abstract, and full text.

*** Article screening flow chart (PRISMA)**

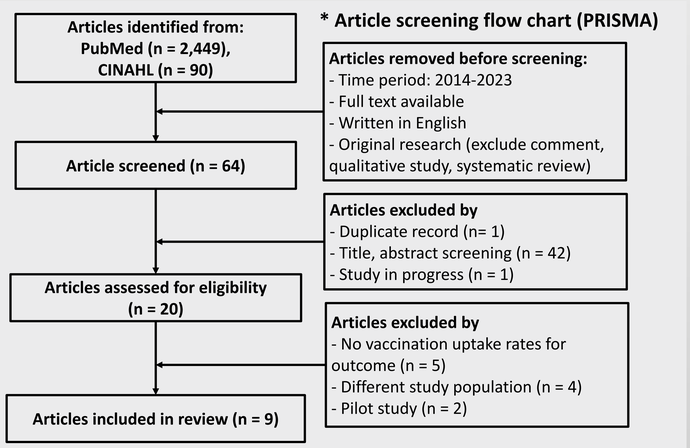

Results

A total of nine studies were included. The primary outcomes of the studies were the initiation or completion of HPV vaccination in adolescents. Seven studies were from the US, one from Israel, and one from Australia. Among them, **seven studies showed statistically significant effects in improving HPV vaccine initiation or completion**. Four studies utilized **in-person education on HPV vaccine and cervical cancer**, using brochures or presentations. Two studies **utilized mobile health to provide information on the HPV vaccine** and one study utilized **SMS reminders**. Among them, three studies conducted post-tests twice (at 6 months, 7 months, and 1-4 months), while four studies conducted post-tests once. Two studies found no significant difference in outcomes. One utilized Facebook campaigns (Israel), and the other utilized web-based tailored education (US).

Interventions included in the study

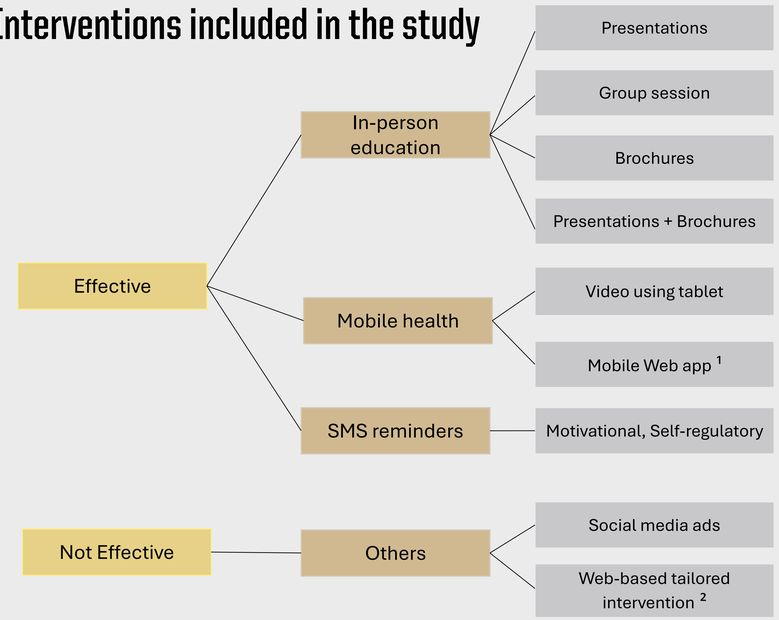

[1] Vacteens.org: mobile app (digital) platform
[2] CHICOS (Combatting HPV Infection and Cancers)

KEY FINDINGS

In-person education and mobile health interventions to parents are significantly increase HPV vaccine uptake in adolescents.

Discussion & Conclusion

This study provides insights into effective intervention strategies among parents to increase HPV vaccine uptake in their adolescents. Based on the results, we recommend further investigation for each type of intervention proven effective. Additionally, future studies should explore how these interventions could be widely applied to different populations or settings. We also suggest evaluating the optimal timeframe for the post-test.

Keywords: HPV vaccine, parents, intervention, adolescents, vaccine uptake

Contact
Yeseol Cho cho567@purdue.edu
Soojung Jo soojungj@purdue.edu

Deep transfer learning identifies novel markers for benign prostate at high risk for oncogenesis

Justin L. Couetil, Ziyu Liu, Ahmed Alomari, Jie Zhang, Kun Huang, Travis Johnson
IU School of Medicine Depts. of Genetics, Biostatistics, and Pathology

INDIANA CTSI Clinical and Translational Sciences Institute
IMPROVING HEALTH THROUGH RESEARCH
INDIANA UNIVERSITY SCHOOL OF MEDICINE
indianactsi.org

Motivation

- The transition of normal tissue to cancer is ill-defined, making basic research on carcinogenesis difficult.
- Pathologists do not have a good method to predict prostate cancer development.
- Existing screening tools (e.g., PSA) have low predictive values.

Methods

- Diagnostic Evidence Gauge of Spatial-transcriptomics (DEGAS) is a deep transfer learning framework that identifies links between spatial transcriptomics (ST) and patient outcomes using large longitudinal studies with bulk transcriptomics.
- We map this learned information onto ST to understand what cells/cell states are associated with poor outcomes.
- DEGAS provides clinically-driven hypothesis generation.

DEGAS workflow

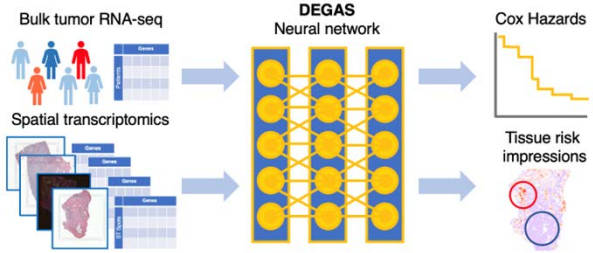

https://github.com/tsteelejohnson91/DEGAS

Funding: CTSI-TL1 UL1TR002529, NIH-NIGMS 1RO1GM148970, NIH-NCI 1R21CA264339, ACS 19-144-32. MMRF Research Foundation

Results

DEGAS highlights morphologically benign epithelial tissue as being associated with poor outcomes. These transcriptomic signatures are enriched for neoplasia and wound healing.

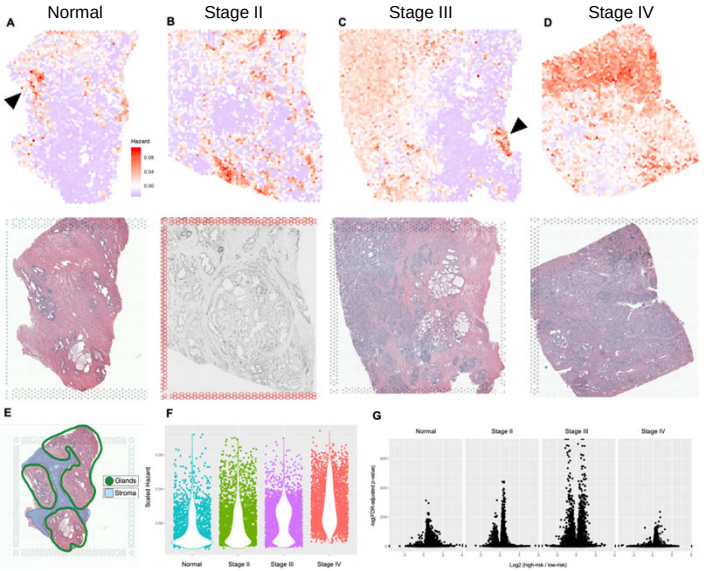

DEGAS hazards correlate with overall RNA expression, but some normal markers are lost in the highest risk glands.

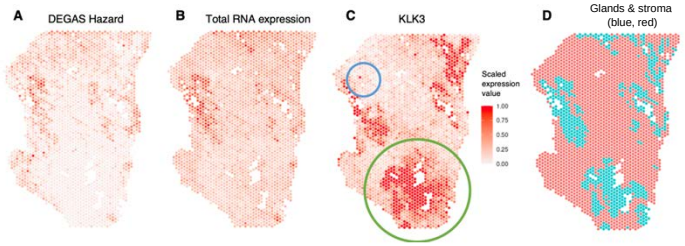

MSMB is consistently correlated with low-risk tissue

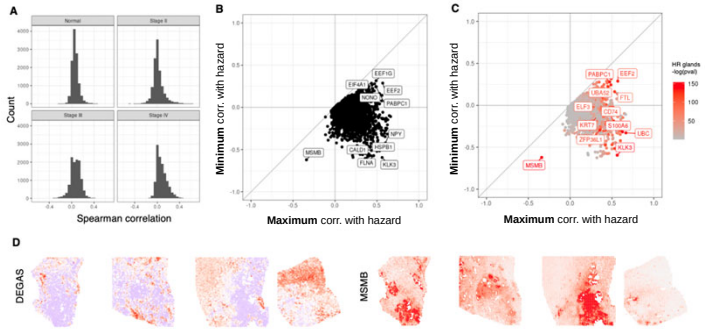

We identify similar results in a disparate prostate ST dataset: High-risk morphologically benign epithelial tissue with four distinct groups of increasing DEGAS hazard

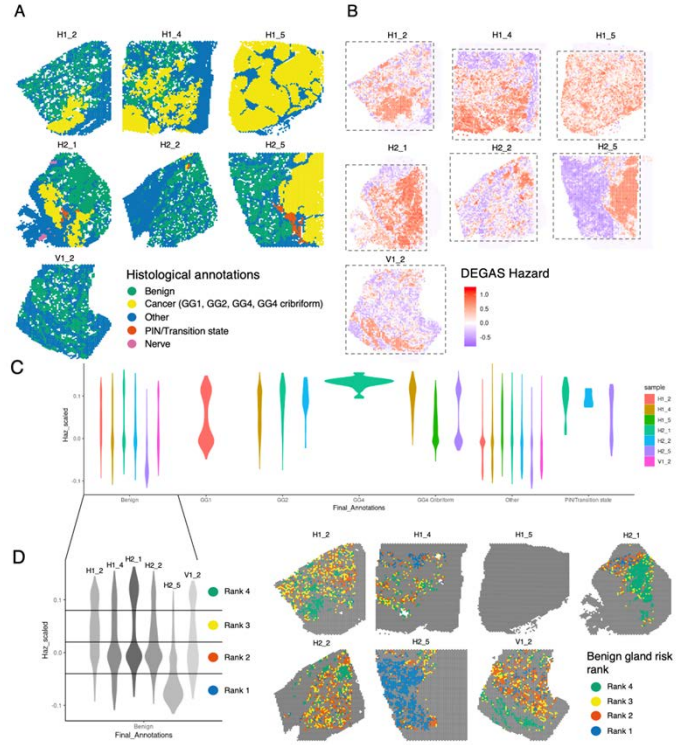

Cell-type specific differential expression is associated with DEGAS hazard and highlights MSMB & oncogenes

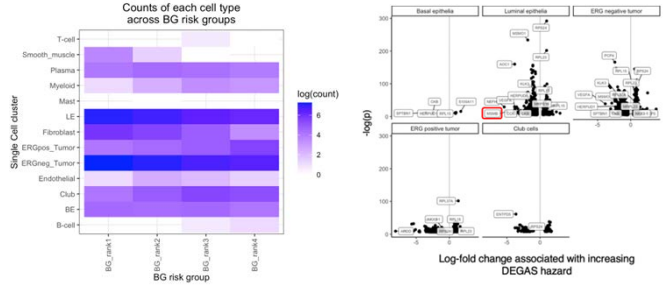

Conclusions

- There are transcriptional changes in benign epithelia that suggest de-differentiation and carcinogenesis.
- We are developing a gene panel and building a retrospective cohort to study the associations between these genes and prostate cancer incidence

EXPANDING THERAPEUTIC POTENTIAL: ENGINEERED IL-27 VARIANTS WITH PROLONGED HALF-LIFE FOR ENHANCED ANTI-TUMOR EFFICACY

ABSTRACT

Interleukin-27 (IL-27) presents a promising avenue in the quest to slow down tumor progression and induce regression across various cancer models. However, the clinical translation of cytokine-based therapeutics is hindered by their inherently short half-lives, typically ranging from 1 to 5 hours. Numerous strategies, including PEGylation and lipidation, have been devised to address this limitation. Yet, most of these strategies involve post-production modifications, escalating production costs and complicating purification processes while potentially triggering immunogenic responses.

In this project, our focus centers on the expression of proteins fused with a Pro-Ala-Ser (PAS) domain, which can be genetically encoded, offering a promising avenue for extending protein stability. To this end, we have designed an IL-27 variant featuring a PAS200 domain (addition of a 200 repetitions of amino acid Pro-Ala-Ser sequence to the N-terminus) aimed at prolonging the protein's half-life, alongside a non-PASylated version serving as a control. The primary objective of this phase of the project was to devise efficient expression and purification strategies for both IL-27 variants.

During the course of this study, we successfully developed methods for the expression and purification of these protein variants. Notably, while IL-27 was expressed in Escherichia coli (E. coli), its expression was unattainable in mammalian cells. Conversely, the PAS200 IL-27 variant could only be expressed in mammalian cells, failing to express in E. coli. To ensure consistency in testing conditions, we elected to express the PASylated IL-27 in Expi 293FGnTI cells, a mammalian cell line which lack N-acetylglucosaminyltransferase I (GnTI) activity and therefore lack complex N-glycans. This makes the PAS 200 IL27 variant akin to the non-glycosylated IL-27 expressed in E. coli.

Our expression and purification strategy revolved around affinity and size exclusion chromatography techniques. Subsequent animal studies are planned to elucidate the activity and stability of these variants further, thus paving the way for a comprehensive understanding of their therapeutic potential.

INTRODUCTION

Interleukin-27 (IL-27), belonging to the Interleukin-12 (IL-12) cytokine family, emerges as a prospective therapeutic agent for impeding tumor growth and fostering tumor regression[1]. The field of Osteoimmune activity delves into interdisciplinary investigations exploring the nexus between the immune and skeletal systems, elucidating shared components such as ligands, receptors, signaling molecules, and transcription factors. Bones are fertile ground for tumor cell proliferation, owing to the conducive bone matrix growth factor environment. Tumor cells exploit the equilibrium between osteoclasts (bone resorption) and osteoblasts (bone formation) to bolster tumor expansion and precipitate skeletal-related events (SRE), including severe pain and fractures[2].

Current research surrounding IL-27 as a treatment modality targets diseases straddling the immune and skeletal systems, such as Prostate cancer, a form of tumor bone metastases that not only interfaces with the immune microenvironment but also interacts with bone cells, rendering them viable targets for therapeutics like IL-27. Improving IL-27's efficacy in cancer treatment by activating the immune system and affecting bone cells is crucial. However, its short half-life of 1 to 5 hours presents a significant challenge for clinical use. While PEGylation and lipidation have been investigated to prolong IL-27's lifespan, they often require costly post-production modifications, complicate purification, and may trigger immune reactions[3].

As an alternative avenue to enhance the circulation time of IL-27, PASylation emerges as a viable strategy. By introducing a Pro-Ala-Ser domain at the N-terminus of IL-27, the hydrodynamic radius of the protein can be increased, thereby mitigating renal filtration and potentially amplifying its efficacy. This approach holds promise not only for IL-27 but also for several other secreted factors commonly employed in PEGylated clinical settings, such as granulocyte colony-stimulating factor (GCSF) and interferon alpha-2 (IFNa2)[4].

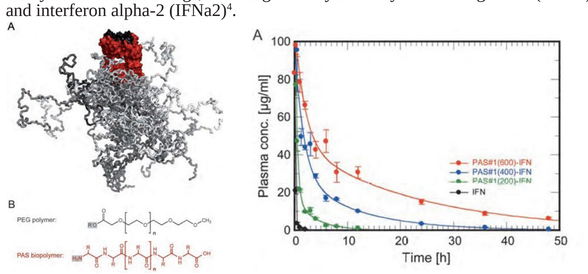

Fig 1 (L) illustrates the concept of PASylation through a modelled structure of the PASylated Fab fragment of an antibody[5]. Fig 2 (R) illustrates the impact of PASylation on a proteins PK[5].

Moreover, it may serve as a more efficient alternative to cytokines currently undergoing gene delivery in various clinical trials and applications, including IL-12. The initiation of our project entailed the incorporation of a ~200 amino acid (aa) PAS domain at the N-terminus of IL-27. Considering the size of our protein, this domain length was deemed suitable, necessitating only one domain to validate our hypothesis[6]. Notably, previous endeavors with N-terminus Flex27 fusions, such as the Nanolux IL-27 fusion, have yielded functional proteins, underscoring the feasibility of this approach. The significance of PASylation is further emphasized by the hydrophobic nature of specific proteins, exemplified by IFN, exhibiting meager solubility due to the abundance of hydrophobic residues on its surface. In contrast, PAS polypeptide chains exhibit high solubility, facilitated by their propensity to form numerous hydrogen bonds with water molecules. Considering the physiological filtration thresholds in the glomeruli, proteins with molecular weights below 15 kDa are freely filtered, while those between 45 to 60 kDa face restricted filtration[5]. To pursue our objectives, a histidine (His) tag was incorporated for purification, facilitating streamlined isolation processes. This comprehensive approach holds promise for advancing the therapeutic potential of I -27 and other related cytokines, laying the groundwork for enhanced clinical outcomes in cancer treatment and beyond.

METHODS

Frozen cell pellets (1L) were resuspended in 20ml buffer (50mM NaP, 300mM NaCl, EDTA-free protease inhibitor) supplemented with 6M GuHCl. Sonication (59sec bursts, 30sec cool down, 45% amplitude) for 5 minutes ensured complete lysis. Subsequent centrifugation (10k xg, 30min) yielded the clarified lysate. Metal-affinity chromatography employed 100uL Biorad IMAC resin pre-equilibrated with Buffer A (50mM NaP, 300mM NaCl, 8M Urea, 2mM DTT). Lysate incubation and gravity flow-through collection captured bound protein. Elution utilized 1000uL Buffer B (high imidazole). Urea removal involved buffer exchange via Amicon Ultra centrifugal filters to achieve 1.2ml in 1XPBS. Protein presence and purity were confirmed by SDS-PAGE and Western blot using an anti-IL27 antibody. This protocol facilitates efficient IL27 purification for further analysis.

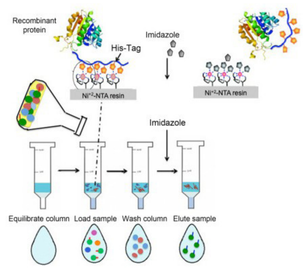

Fig 3 illustrates the gravity filteration mechanism employed for the first-stage purification of IL-27 expressed in *E.coli.* The equilibriation, sample application, wash and elution stages have been highlighted[7].

Cell culture and expression of pasylated IL-27 in mammalian cells were executed employing the Expi293 GnTI cell system in conjunction with a commercial kit sourced from ThermoFisher Scientific. Adherence to ThermoFisher protocols for the Expi293 GnTI system governed cell growth and procedural steps. Following expression, supernatant retrieval was accomplished through centrifugation at 300xg for 30 minutes, succeeded by filtration utilizing a 0.22µm filter. Subsequently, a Protease cocktail devoid of EDTA was introduced to the filtered supernatant at a recommended ratio of 1 tablet per 10ml. Purification procedures entailed Ni NTA affinity chromatography, employing Buffer A (50mM NAPO4, 300mM NACL, 20mM Imidazole, pH 7.4, 0.5% CHAPS) and Buffer B (50mM NAPO4, 300mM NACL, 500mM Imidazole, pH 7.4, 0.5% CHAPS). Gel filtration followed, utilizing 20mM MOPS and 1% CHAPS. For visualization, sample preparation involved mixing 20µL of sample with 5µL of 5X SDS loading buffer, followed by heating at 95°C for 10 minutes. These treated samples were then loaded onto 10-well TGX BioRad gels and subjected to SDS-PAGE at 120V for 60-63 minutes or 200V for 30 minutes using a BioRad Transfer machine. Primary anti-IL27 antibodies were applied at dilutions ranging from 1:1000 to 1:50000, succeeded by secondary donkey anti-mouse antibodies at a dilution of 1:10000.

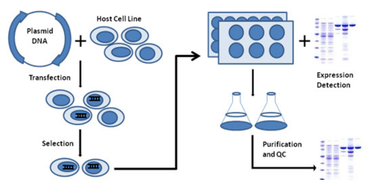

Fig 4 illustrates the expression and purification stages followed in the protocol for the PAS200 IL-27 expression in mamillian Expi293 GnTi cells[8].

RESULTS & DISCUSSION

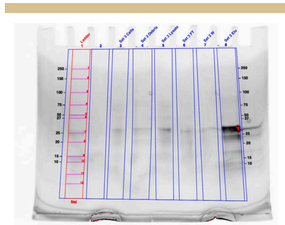

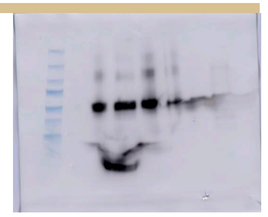

Fig 5 (L) and Fig 6 (R) depict the SDS-Gel and Western Blot conducted for the IL-27 purification. Presence of the protein on the Gel is depcited but the blot is unclear due to the nature of HRP binding.

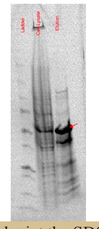

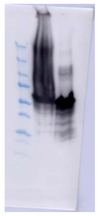

Fig 7 (L) and Fig 8 (R) depict the SDS-Gel and Western Blot conducted for the IL-27 purification. Presence of the protein on the Gel (red arrow) is well established and the blot shows a clearer protein binding from the elution stage

The benchtop experimentation for the purification of IL-27 yielded promising outcomes. Utilizing 8M Urea and 6M GuHCl proved effective for the purification process. However, subsequent dialysis of the fractions using either 1x PBS or 0.5x PBS was essential for protein refolding. The buffer set examination demonstrated that purifying the protein with 6M GuHCl and 8M Urea led to denaturation, suggesting improper folding within bacterial hosts and potential hindrance in binding to the resin via His tag. Due to precipitation challenges in SDS-PAGE caused by GuHCl and Urea, obtaining clear relative data for cell fractions, debris, lysate, flow-through, and wash fractions proved difficult. Despite this limitation, the recovered relative protein amount notably increased to approximately 11.04mg compared to alternative methods employing different buffer compositions. These findings underscore the efficacy of the proposed purification approach in enhancing protein yield despite initial folding challenges.

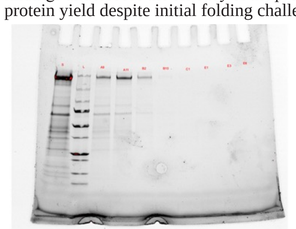

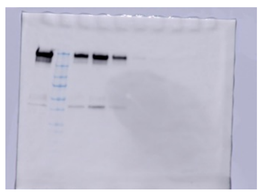

Fig 9 (L) and Fig 10 (R) depict the SDS-Gel and Western Blot conducted for the PAS-200 IL-27 purification. Presence of thick, dark abnds indicate the protein being sucessfully expressed and purified

The expression of PAS200 IL-27 in *E. coli* cells posed challenges, leading us to resort to mammalian cell expression using a commercial kit. Purification optimizations mirrored those employed with E. coli cells, with the exception of employing a different detergent while adhering to similar principles. Our results revealed a low protein yield, albeit sufficient for further analyses. Utilizing PierceTM BCA Protein Assay Kits, we determined a protein concentration of 600 g/ml, indicating successful expression and purification. This concentration aligns well with our expectations, signifying the effectiveness of the mammalian cell expression system and the purification strategy employed.

CONCLUSION

In conclusion, our findings underscore the successful purification of the protein, albeit with ongoing efforts to optimize purity and yield. To this end, Size Exclusion Chromatography (SEC) utilizing a buffer comprising 1xPBS, 2mM DTT, and 0.1% Triton X-100 for both IL-27 and PAS200 IL-27 samples will be employed. SEC, capitalizing on molecular size disparity, promises effective separation of target proteins from contaminants and aggregates. Through meticulous application of this technique alongside specified buffer conditions, we anticipate obtaining a final sample of unparalleled purity and maximal yield. This purified specimen will subsequently undergo rigorous assessment for its potential therapeutic utility.

TRANSLATIONAL IMPACT

PASylation of interleukin-27 (IL-27) marks a transformative step in cancer therapy, addressing the challenge of short cytokine half-lives. By genetically encoding a Pro-Ala-Ser domain at IL-27's N-terminus, PASylation extends its circulation time, enhancing therapeutic efficacy. This innovation not only benefits IL-27 but also holds promise for other cytokines like GCSF and IFNa2. Streamlining production with a histidine tag further facilitates clinical scalability. PASylation's impact spans beyond cancer, offering potential solutions for autoimmune disorders, infections, and inflammatory conditions reliant on cytokine therapies. By overcoming clearance limitations, PASylation introduces durable treatment options, bolstering patient outcomes across diverse medical domains. In essence, PASylation of cytokines represents a pivotal translational advancement, fostering interventions with profound implications for human health and the future of cytokine-based therapy.

CITATIONS

1. Yoshimoto, T., Chiba, Y., Furusawa, J., Xu, M., Tsunoda, R., Higuchi, K., & Mizoguchi, I. (2015). Potential Clinical Application of interleukin-27 as an antitumor agent. Cancer Science, 106(9), 1103–1110. https://doi.org/10.1111/cas.12731

2. Okamoto, K., & Takayanagi, H. (2018). Osteoimmunology. Cold Spring Harbor Perspectives in Medicine, 9(1). https://doi.org/10.1101/cshperspect.a031245

3. Kumar, S., Mulia, G. E., & Figueiredo, M. L. (2023). Cabozantinib and IL-27 combinatorial therapy for bone-metastatic prostate cancer. Frontiers in Molecular Biosciences, 10. https://doi.org/10.3389/fmolb.2023.1259336

4. Powers, N. E., Swartzwelter, B., Marchetti, C., de Graaf, D. M., Lerchner, A., Schlapschy, M., Datar, R., Binder, U., Edwards, C. K., Skerra, A., & Dinarello, C. A. (2019). Pasylation of IL-1 receptor antagonist (IL-1RA) retains IL-1 blockade and extends its duration in mouse urate crystal-induced peritonitis. Journal of Biological Chemistry, 295(3), 868–882. https://doi.org/10.1074/jbc.ra119.010340

5. Schlapschy, M., Binder, U., Borger, C., Theobald, I., Wachinger, K., Kisling, S., Haller, D., & Skerra, A. (2013). Pasylation: A biological alternative to pegylation for extending the plasma half-life of pharmaceutically active proteins. Protein Engineering Design and Selection, 26(8), 489–501. https://doi.org/10.1093/protein/gzt023

6. Nguyen, K. G., Vrabel, M. R., Mantooth, S. M., Hopkins, J. J., Wagner, E. S., Gabaldon, T. A., & Zaharoff, D. A. (2020). Localized interleukin-12 for cancer immunotherapy. Frontiers in Immunology, 11. https://doi.org/10.3389/fimmu.2020.575597

7. Velarde-Salcedo, A. J., De León-Rodríguez, A., Calva-Cruz, O. J., Balderas-Hernández, V. E., De Anda Torres, S., & Barba-de la Rosa, A. P. (2023). Extraction of bioactive compounds from rubus idaeus waste by maceration and supercritical fluids extraction: The recovery of high added-value compounds. International Journal of Food Science & Technology, 58(11), 5838–5854. https://doi.org/10.1111/ijfs.16687

8. Dumont, J., Euwart, D., Mei, B., Estes, S., & Kshirsagar, R. (2015). Human Cell Lines for biopharmaceutical manufacturing: History, status, and future perspectives. Critical Reviews in Biotechnology, 36(6), 1110–1122. https://doi.org/10.3109/07388551.2015.1084266

ACKNOWLEDGEMENTS

We would like to express our sincere gratitude to the Protein Engineering Partners Initiative (PEPI) award and the Purdue Institute of Inflammation, Immunology, and Infectious Disease (PI4D) for their generous support and the invaluable opportunity to utilize the resources of the Molecular Evolution, Protein Engineering, and Production (MEPEP) facility. Their contributions have been instrumental in advancing our research efforts, enabling us to explore new avenues in protein engineering and molecular evolution. We are truly appreciative of their ongoing commitment to fostering scientific innovation and collaboration.

AUTHORS

Dewan, A. ; Ibrahium, O.M.H; Zami, A.; Figueiredo, M, Ostafe, R

PURDUE UNIVERSITY
Purdue Institute of Inflammation, Immunology and Infectious Disease

Identifying the Sexual Health Needs of Formerly Incarcerated Men

Stigar, L.V., Smith, A., Donnelly, E., Bencie, N., & Hubach, R.D.
Purdue University; University of Louisville

OBJECTIVE

The purpose of this study was to evaluate Pre-Exposure Prophylaxis (PrEP) interest, knowledge, and utilization among recently incarcerated men. Furthermore, this study aims to identify barriers to PrEP education and access, related sexual health needs, and competing needs during re-entry, such as housing and employment, for study participants.

INTRODUCTION

Background:

- HIV prevalence is 3-5 times higher in the criminal justice system compared to the general population.
- Low knowledge of PrEP and perceived HIV risks are associated with low levels of PrEP utilization.

Current Study:

- Evaluated PrEP interest, knowledge, and utilization among recently incarcerated men from Ohio and Indiana.

METHODOLOGY

The study utilized semi-structured individual interviews that aimed to acquire insight into barriers and facilitators to PrEP knowledge and utilization. The interviews were transcribed and subjected to thematic coding analysis, revealing several overarching themes.

Final sample consisted of 28 participants with an average age of 32.86 years and average incarceration period of 69 months.

Of the 28 participants n=24 were not prescribed PrEP and n=4 were prescribed PrEP at time of data collection.

RESULTS

Perceptions of HIV Risk

- "because I am not a highly active promiscuous male"

Barriers of PrEP Adoption

- (...)this is really even the first time I've ever even considered or thought about it [accessing PrEP]. Aside from the commercial that I kind of just rubbed off, brushed off(…)"

What Men Want in Programming

- **Pre-Release:**
  - "(...)And it is like, and bringing the awareness up(…) just getting into the system and actually like advertising for it. Like it could be as simple as just like flyers or brochures cause people just don't know what they don't know in there. Cause there is a lot of people in there that don't have the capacity to read or comprehend for themselves. So I guess that could be hard. But if, I guess if if you made it seem like it is easy to access and like you, you're willing to reach out and answer questions and maybe have like a seminar or something, like you could probably spark some potential interest that way as well, that actually might work."
- **Post-Release**
  - "(...)I would definitely I would definitely probably wait till the end. (...) When everybody, 'cause while you're in prison, you're making all these plans and all these plans to do when you get home (...), but when you get a month or two, three months to the door (...), everything starts to change for you (...). So if you wait till that time and then educate people on it (...) as soon as they get home, that's still gonna be fresh in their mind and they might be willing to go get that [PrEP]."

DISCUSSION

- Post-release, participants prioritized housing and employment over health concerns like PrEP adoption.
- Participants faced limited access to HIV testing during and after incarceration, highlighting the need for greater PrEP utilization in this demographic.
- Participant views on their HIV risk varied; some perceived low susceptibility due to factors like having one sexual partner or engaging only in penile-vaginal intercourse.
- Post-release, inmates reported restricted HIV testing and PrEP access due to inadequate healthcare, including lack of health insurance, transportation barriers, and a limited number of physicians offering PrEP for former inmates.
- There is a need to educate this community about PrEP benefits post-release, while raising awareness about their potential vulnerability to acquiring HIV post-incarceration.

Community Health Worker Training

Amanda Eldridge, Cody Mullen, PhD, Yumary Ruiz, PhD, Natalia Rodriguez, PhD, Randy Hubach, PhD

Background

The Health Resources and Services Administration (HRSA) is working to expand the public health workforce through recruiting and training new Community Health Workers (CHWs) and providing upskilling of current CHWs on topics consisting of public health emergency response, increasing access to care, and addressing public health needs of underserved communities.

Methods

Recruit participants for the certification training through partnerships and social media posts.

Certified CHWs attend the Advanced/Upskilling training developed by Purdue

Students can either apply for an apprenticeship program, continue with their current employment, or apply to other CHW opportunities throughout the state.

CHW Certification Training

The Certified Training is completed by an Indiana Community Health Worker Association (INCHWA) approved training that is recognized by the State of Indiana.

Topics covered:

CCHW Core Competencies
Client-Centered Counseling
Introduction to Public Health and HIPPA
Motivational Interviewing
Cultural Humility

Advanced CHW Training

The Advanced Training focuses on upskilling already certified CHWs with topics required by the HRSA grant and topics relevant to Indiana's healthcare and public health.

Topics covered:

Vaccine Hesitancy
Emergency Response & Preparedness
Health Equities
10 Essentials of Public Health
Cancers & Infectious Diseases

Current totals for CHW Training

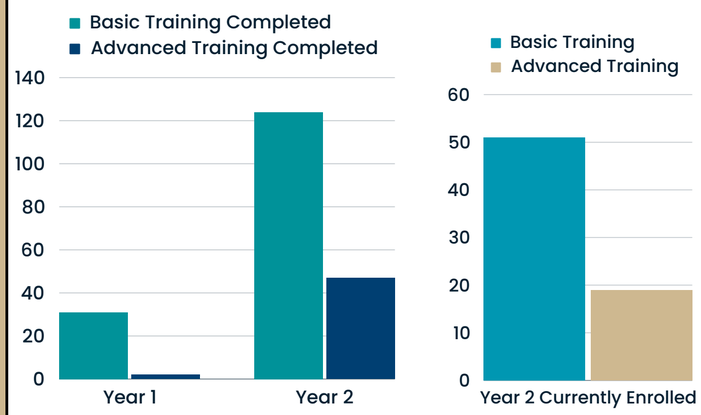

Current waitlist for New Trainees: 61*
Current waitlist for Advanced Training: 23*
*Current numbers as of 2/21/2024

Main Takeaways

The results show an interest in the Community Health Workers workforce in Indiana.

Limitations

The inability of grant funds to support certain populations.
The interest in the program was greater than expected causing a long wait list.

For more information, please contact:
Amanda Eldridge
chwtraining@purdue.edu

Partnership

Spanish-Language Resource Readability on Ophthalmology Websites

Devon Hori Harvey[1]; Qiancheng Wang[2]; Charline S. Boente[1]

[1]Indiana University School of Medicine, Department of Ophthalmology

[2]University of Wisconsin Madison School of Medicine and Public Health, Department of Ophthalmology and Visual Sciences

INTRODUCTION

Health literacy is essential for appropriate patient care.[1] Patient health literacy is impacted by limited English proficiency (LEP) which is associated with increased barriers to care for LEP patients, including Hispanic patients.[2] Institutional health literacy includes providing adequate materials for patient education and understanding.[3]

To better understand the current institutional health literacy of ophthalmology organizations in the US, this study analyzed the availability and readability of Spanish-language resources found on ophthalmology websites.

MATERIALS AND METHODS

Ophthalmology organization websites were identified through online searches of US state professional societies, university library searches, and the National Institute of Health Eye Care organization list. Websites were included if they had direct relation to ophthalmology and were categorized into 3 groups: patient-facing, physician-facing, or both patient/physician-facing. Websites were then reviewed for the presence of any Spanish-language resource.

For those with Spanish-language resources, readability analyses were conducted using Readability Studio Professional Edition Software v2020 (Oleander Software, Ltd, Vandalia, Ohio). Five different readability formulas were used for analysis:

- Crawford (CRAW)
- Gilliam-Peña-Mountain (GPM)
- Läsbarhetsindex (LIX)
- Rate index (RIX)
- SOL formula (SOL)

Websites were assigned a reading grade level which was compared to the recommended standard of a 6th grade reading level using a one-sample t-test or a one-sample Wilcoxon test. Statistical analysis was performed using Graphpad Prism v. 10.0.0 (Graphpad Software Inc., Boston, MA). Significance threshold was $p < 0.05$.

READABILITY ANALYSES

Patient-facing Websites	CRAW	GPM	LIX	RIX	SOL
Readability Score (mean ± SD)	5.72 ± 1.48	10.78 ± 2.91	11.36 ± 1.36	10.45 ± 2.34	11.57 ± 2.41
Significance	W = -5, p = 0.857	p = 0.001	p < 0.001	p < 0.001	p < 0.001

Physician-facing Websites	CRAW	GPM	LIX	RIX	SOL
Readability Score	6.5	15	13	11	13.3
Significance	N/A (*n* = 1)	N/A (*n* = 1)	N/A (*n* = 1)	N/A (*n* = 1)	N/A (*n* = 1)

Both patient/physician-facing Websites	CRAW	GPM	LIX	RIX	SOL
Readability Score (mean ± SD)	5.68 ± 0.70	9.75 ± 2.56	10.82 ± 1.38	9.58 ± 1.87	10.71 ± 1.85
Significance	p = 0.074	p < 0.001	p < 0.001	p < 0.001	p < 0.001

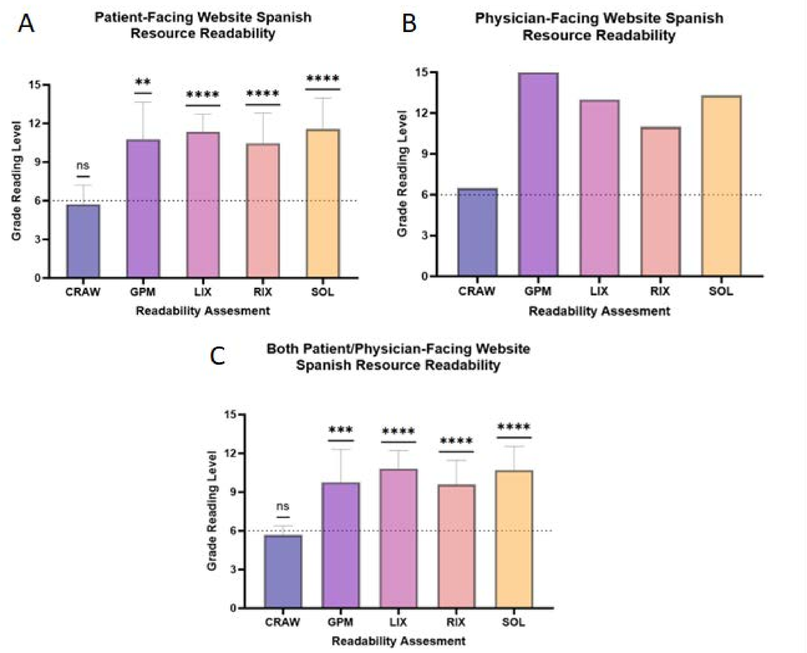

Physician-facing websites, and C) Both Patient/Physician-facing websites

The recommended grade reading level for patient education materials is 6, which is marked at the horizontal, dotted line. ** indicates $p < 0.01$, *** indicates $p < 0.001$, and **** indicates $p < 0.0001$.

SUMMARY

121 websites were included for analysis: 27% patient-facing, 25% physician-facing, and 48% both patient/physician-facing. **Only 26% (31) of all websites provided Spanish-language resources**. Of these, 39% were patient-facing, 3% physician-facing, and 58% both patient/physician-facing.

CONCLUSIONS

The institutional health literacy of ophthalmology organization websites in the US needs improvement. Given that approximately 40.7 million people in the US speak Spanish at home[4], ophthalmology organizations can partially improve their health literacy by increasing the availability of Spanish-language resources for Hispanic patients online. In addition, resources should be created by professional translators with an emphasis on a reading level of 6th grade or lower.

Increasing the availability of adequate Spanish-language ophthalmology resources will improve health literacy of Hispanic patients and address some of the ocular health disparities these patients face.

REFERENCES

1. Berkman ND, Sheridan SL, Donahue KE, et al. Health literacy interventions and outcomes: an updated systematic review. Evid ReportTechnology Assess. 2011;(199):1-941.
2. Sentell T, Braun K. Low Health Literacy, Limited English Proficiency, and Health Status in Asians, Latinos, and Other Racial/Ethnic Groups in California. J Health Commun. 2012;17(Suppl 3):82-99. doi:10.1080/10810730.2012.712621
3. Health Literacy in Healthy People 2030 - Healthy People 2030 | health.gov. Accessed August 10, 2023. https://health.gov/healthypeople/priority-areas/health-literacy-healthy-people-2030
4. S1601: LANGUAGE SPOKEN AT HOME - Census Bureau Table. Accessed August 10, 2023. https://data.census.gov/table?q=spanish+speakers+in+the+united+states&tid=ACSST1Y2021.S1601

Identifying the Genetic Basis of Mental Disorders in Individuals of African Ancestry

[1]Mary Kaka, [1]Apostolia Topaloudi, [2]Pritesh Jain, Guangxin Chen and [1]Peristera Paschou

[1]Department of Biological Sciences, Purdue University, West Lafayette, IN; [2]Department of Population and Global Health, LKC Medicine, Nanyang Technological University, Singapore

Introduction

- There are differences in genetic structure between European and African populations
- Missing diversity in genetics (African, Asian, Hispanic/Latino, etc., underrepresented in genomics)
- Need to fill in the gap for the future of personalized/precision medicine
- There is a high burden of mental disorders in non-white populations
- The mental health traits- like many complex traits- are multifactorial
- However, low sample size, hence the usage of proxy phenotypes such as **Neuroticism**
- Neuroticism: one of the Big-Five Personality traits and aggregated from 12 EPQ-RS measurement scales: **Mood swings, Miserableness, Irritability, Sensitivity, Fed-up feelings, Nervous feelings, Anxious feelings, Tense, Worry too long after embarrassment, Suffer from nerves, Loneliness, Guilty feelings**
- Has been found to be correlated with some major neuropsychiatric disorders (**Fig.1**)

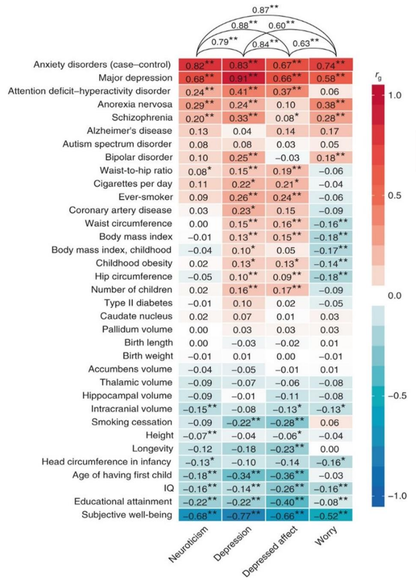

Figure 1: Heatmap showing genetic correlation between Neuroticism and other major psychiatric traits in individuals of European ancestry
Source: (Nagel et al., 2018b)

Objectives

- Conducting **genome-wide association studies (GWAS) for neuroticism** in individuals of African ancestry
- Exploring the **transferability** of African results to Europeans and vice-versa
- Assessing **trans-ethnic genetic architecture** for neuropsychiatric disorders

Methods

- Using standard procedures, we conduct GWAS on thirteen (13) phenotypes(Neuroticism and the twelve item-level questions) from the UK biobank genomic database.
- We repeat the same procedure for Africans, Europeans, East, and South Asians from the same database.

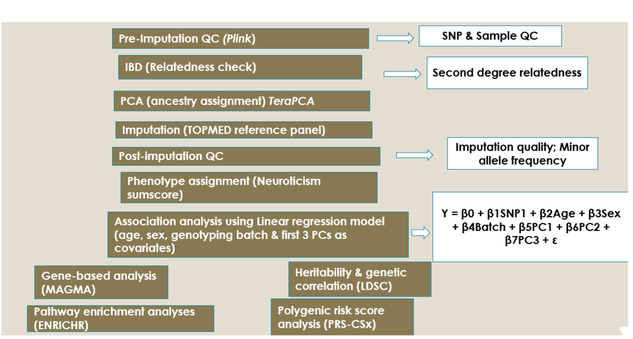

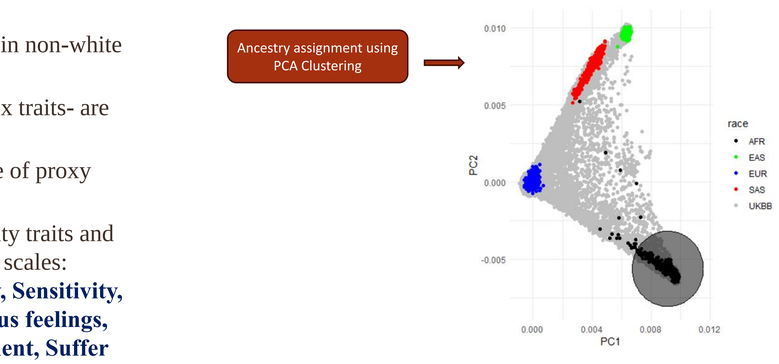

Figure 2: PCA plot showing ancestry clusters from UKBB

- **TeraPCA: UKBB + 1000 genomes (1kG) individuals**
- **Clustering all sample points (Individuals): 4PCs ± 3SD within mean**

Results

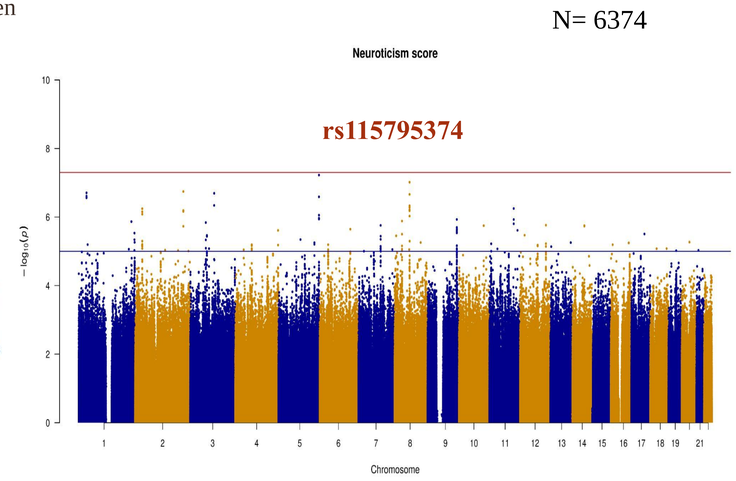

Figure 3: Manhattan plot showing the top SNP for Neuroticism in Africans (afr) in chromosome 5

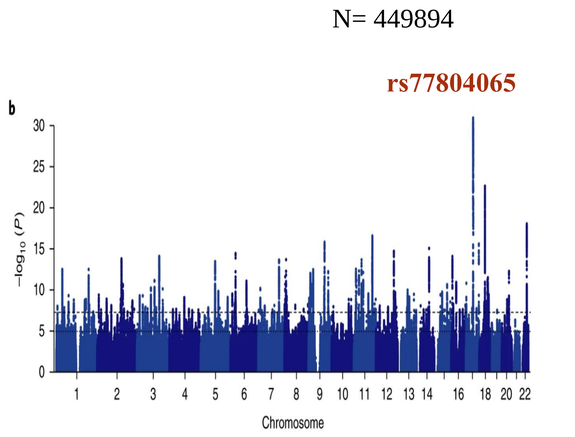

Figure 4: Manhattan plot showing the top SNP for Neuroticism in the largest European GWAS (Nagel et al., 2018b)

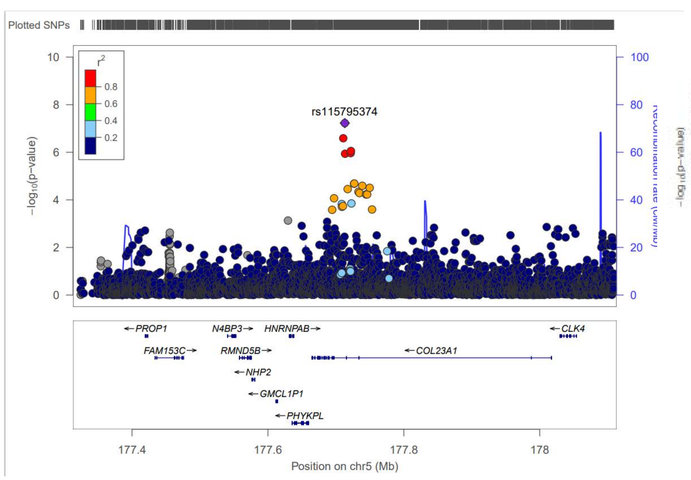

Figure 5: Regional plot of top hit from fig.3 using LocusZoom

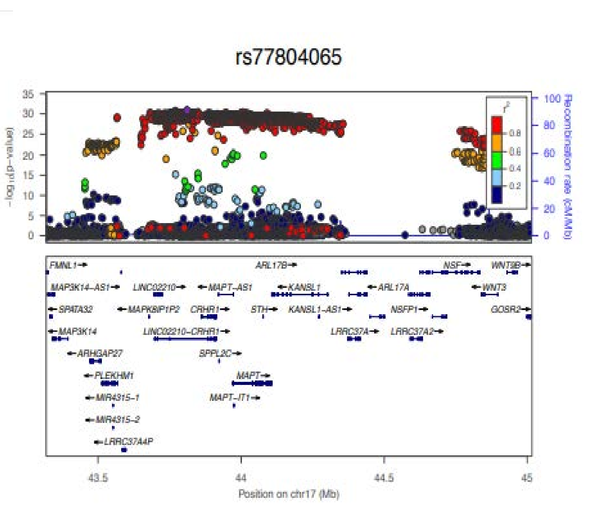

Figure 6: Regional plot of top hit from fig.4

Discussion

- Our top hit for Neuroticism score in Africans from the UKB is located on chromosome 5 with a p-value of 5.944e-08. The nearest gene to this from the DBSNP database is the COL23A1 gene. This gene has been reported in the GWAS Catalog for being significantly associated with Cannabis dependence, insomnia, and the rate of cognitive decline in Alzheimer's disease.
- However, more evidence-based search and annotation is needed to establish the gene's biological function. After FDR correction, no gene reaches significance in the gene-based analysis.
- LDSC currently estimates a relatively low heritability for neuroticism score in Africans with a value of -0.2139 as compared to the 0.100 in Europeans, this could be due to the low sample size as well the limitations in using an in-sample LD reference panel for the estimation.
- The GCTA-GREML analysis however gives an heritability estimate of 0.15 with a p-value of 6.44E-05 when no covariates were corrected for.
- We aim to boost power to reach genome-wide significance by incorporating additional datasets from Africans and other ancestries with similar phenotypes

Characteristics associated with access to kidney transplantation services in the Ohio River Valley

Catherine Kelty, PhD, MS;[1] Jade Buford, MPH;[2] Kelsey Drewry, PhD, MA;[2,3] Fisayo Adebiyi, MD;[1] Asif Sharfuddin, MD;[3] Jonathan Fridell, MD;[3] Jawad Sher, MD;[1] Anne Huml, MD;[4] Sharon Moe, MD;[1] Rachel Patzer, PhD, MPH[2,3]

[1]Division of Nephrology, IU School of Medicine, [2]Regenstrief Institute, [3]Department of Surgery, IU School of Medicine, [4]Department of Kidney Medicine, Cleveland Clinic

Background

For patients with end stage kidney disease (ESKD), demographic and socioeconomic characteristics affect access to kidney transplantation services. End stage renal disease Network 9, of the Ohio River Valley, is one of the 13 networks which had reduced waitlisting for Black patients compared to White non-Hispanic patients.[1] Additional research has shown that African American patients residing in Indiana, Kentucky, and Ohio had significantly longer time on the waitlist compared to white patients, and this time was significantly longer than the U.S. overall time on the waitlist.[2] Due to the known racial disparities in access, this study further investigated social disparities in access to kidney transplantation in this region. The objective of this study was to describe the medical and non-medical factors associated with referral, evaluation start, and waitlisting among patients with ESKD in the Ohio River Valley (Network 9).

Figure 1. Network 9 of the Ohio River Valley

Figure 2. Steps to Kidney Transplant

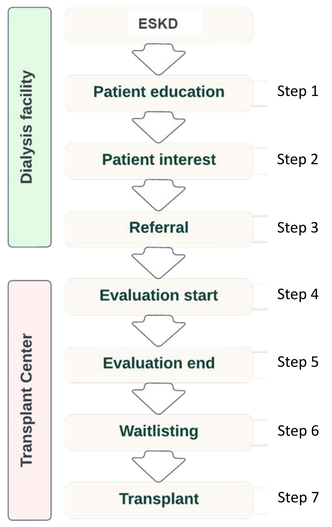

Materials & Methods

To identify patients with ESKD in Network 9, United States Renal Data System (USRDS) data were linked to referral and evaluation data from n=4 transplant centers contributing to the Early Steps to Transplant Access Registry (E-STAR), as well as neighborhood-level characteristics from the 2021 American Community Survey. Adult patients residing within Network 9 (Indiana, Kentucky, and Ohio; Figure 1) at dialysis start among n=680 dialysis facilities from January 2016-June 2020 (followed through June 2021) were assessed.

Outcomes assessed were: referral to a contributing transplant center among dialysis patients (Figure 2, step 3), transplant evaluation start among referred patients (Figure 2, step 4), and waitlisting among patients who started evaluation (Figure 2, step 6). Multivariable logistic regression models were utilized to examine the association between demographic, clinical, and socioeconomic factors and each outcome.

Table 1. Among patients in the USRDS dataset and on dialysis in Network 9, logistic regression modeling compared patient-, neighborhood-, and geographic-level characteristics with referral for kidney transplantation in Indiana (within 1 year of dialysis start), evaluation start within 6 months of referral (among all referred patients), and waitlisting within 6 months of evaluation (among all evaluated patients).

Variable	Referred within 1 year of dialysis start (n=4674) Odds ratios (95% CI)	Started evaluation within 6 months of referral, among all referred (n=3625) Odds ratios (95% CI))	Waitlisted within 6 months of evaluation, among all evaluated (n=688) Odds ratios (95% CI)
Patient Characteristics			
Age			
18-29	1 (Reference)	1 (Reference)	1 (Reference)
30-39	0.88(0.64,1.20)	0.84(0.61,1.16)	0.82(0.50,1.33)
40-49	0.84(0.62,1.13)	0.83(0.62,1.12)	0.86(0.55,1.35)
50-59	0.84(0.63,1.12)	0.81(0.60,1.08)	0.74(0.48,1.14)
60-69	0.79(0.59,1.05)	0.87(0.65,1.16)	0.75(0.48,1.16)
70-85	**0.53(0.39,0.73)**	**0.49(0.36,0.68)**	**0.45(0.25,0.80)**
Sex			
Male	1 (Reference)	1 (Reference)	1 (Reference)
Female	1.10(0.91,1.13)	0.97(0.87,1.08)	**0.74(0.60,0.92)**
Race			
White, non-Hispanic	1 (Reference)	1 (Reference)	1 (Reference)
Black, non-Hispanic	0.88(0.77,1.01)	**0.85(0.74,0.98)**	0.84(0.64,1.09)
Hispanic	**1.42(1.06,1.91)**	0.91(0.68,1.22)	0.97(0.57,1.65)
Asian	1.17(0.75,1.82)	1.12(0.73,1.74)	0.71(0.36,1.41)
Other(Unknown)	1.61(0.76,3.44)	1.84(0.87,3.86)	0.50(0.11,2.23)
Cause of ESKD			
Diabetes	1 (Reference)	1 (Reference)	1 (Reference)
Hypertension	1.16(0.99,1.36)	0.94(0.79,1.11)	1.35(0.98,1.87)
Glomerulonephritis	**1.26(1.03,1.55)**	**1.41(1.15,1.74)**	**1.52(10.6,2.18)**
Other / Unknown cause	1.17(0.98,1.40)	**1.26(1.05,1.51)**	1.18(0.83,1.67)
Comorbidities present			
Obesity (BMI ≥35 kg/m^2)	1.12(0.99,1.26)	**1.63(1.43,3.86)**	1.09(0.85,1.40)
Congestive heart failure	**1.16(1.02,1.32)**	**1.33(1.63,1.53)**	1.20(0.89,1.63)
Atherosclerotic heart disease	**1.21(1.06,1.50)**	0.90(0.75,1.08)	1.03(0.70,1.50)
Other cardiac disease	0.92(0.80,1.07)	1.08(0.93,1.25)	**1.44(1.04,1.98)**
Cerebrovascular disease (stroke)	0.92(0.75,1.13)	1.17(0.94,1.46)	1.70(0.98,2.95)
Peripheral vascular disease	0.96(0.78,1.18)	1.22(0.98,1.52)	1.42(0.83,2.41)
Hypertension	**0.77(0.65,0.92)**	0.85(0.80,1.14)	1.07(0.78,1.47)
Diabetes	**0.86(0.74,0.99)**	1.07(0.92,1.24)	**1.33(1.00,1.77)**
COPD	0.90(0.74,1.10)	**1.43(1.15,1.77)**	1.45(0.84,2.51)
Cancer	0.99(0.78,1.26)	1.11(0.86,1.43)	0.99(0.60,1.64)
Tobacco use	**1.26(1.06,1.51)**	**1.58(1.30,1.92)**	1.51(0.97,2.35)
Drug dependence	1.08(0.70,1.68)	1.52(0.92,2.48)	-
Alcohol dependence	0.83(0.57,1.21)	0.70(0.48,1.03)	1.51(0.62,3.67)
Neighborhood Characteristics (by ZIP code)			
≥20% population below poverty level	**1.25(1.00,1.57)**	1.06(0.84,1.33)	0.99(0.60,1.63)
Median household income (MHI)			
Low tertile	1.02(0.82,1.27)	0.85(0.68,1.06)	0.65(0.41,1.03)
Middle tertile	1.00(0.88,1.15)	**0.81(0.71,0.93)**	1.09(0.86,1.39)
High tertile	1 (Reference)	1 (Reference)	1 (Reference)
Geographic Characteristics			
Urban (≥50,000)	1 (Reference)	1 (Reference)	1 (Reference)
Large rural city(10,000-49,999)	0.92(0.78,1.09)	0.94(0.80,1.11)	1.19(0.87,1.62)
Small rural town (adjacent to town of 2,500-10,000)	1.25(0.93,1.68)	**1.41(1.15,1.74)**	0.66(0.36,1.23)
Isolated small rural town (not adjacent to town)	1.07(0.73,1.58)	**1.26(1.05,1.51)**	1.02(0.60,0.92)

Results

During the study period, there were 38,944 incident dialysis patients in Network 9, of which 8,824 were referred (4,674 [12%] referred within 1 year) to a contributing transplant center. Of the 8,824 referred patients, 3,955 started evaluation for transplant (3,265 [37%] within 6 months of referral). Of the 4,362 evaluated patients, 1,133 were waitlisted for transplant (688 [26%] waitlisted within 6 months of evaluation start).

Factors contributing to increased odds of <u>not</u> being referred by 1 year after dialysis start, in the adjusted analysis, included patient age >70 (OR=0.53, 95% CI 0.39-0.73) vs. younger age, and patients with unknown (OR=0.49, 95% CI 0.40-0.60) or no insurance (OR=0.28, 95% CI 0.19-0.41) vs. private insurance. **Factors contributing to increased odds of being referred by 1 year** were Hispanic ethnicity (OR=1.42, 95% CI 1.06-1.91) vs. white race and ZIP code-level poverty >20% (OR=1.25, 95% CI 1.00-1.57) vs. <20%.

Factors contributing to increased odds of <u>not</u> having a transplant evaluation within 6 months of referral were age >70 (OR=0.49, 95% CI 0.36-0.68) vs. younger age; Black race (OR=0.85, 95% CI 0.74-0.98) vs white race; Medicaid (OR=0.47, 95% CI 0.38-0.59), Medicare (OR=0.73, 95% CI 0.63-0.84), unknown insurance (OR=0.78, 95% CI 0.64-0.96), or no insurance (OR=0.30, 95% CI 0.20-0.46) vs. private; and middle MHI tercile (OR=0.81, 95% CI 0.71-0.93) vs. high MHI tercile. **Factors with increased odds of starting evaluation within 6 months were** residing in small rural (OR=1.41, 95% CI 1.15-1.74) or isolated rural towns (OR=1.26, 95% CI 1.05-1.51) vs. urban areas.

Factors contributing to lower odds of waitlisting 6 months after evaluation start included age >70 (OR=0.45, 95% CI 0.25-0.80) vs. younger age, female vs. male sex (OR=0.74, 95% CI 0.60-0.92), and Medicaid (OR=0.39, 95% CI 0.24-0.63) or Medicare (OR=0.61, 95% CI 0.49-0.77) vs. private insurance.

Discussion & Limitations

Among patients with incident ESKD referred to a transplant center in Network 9, increasing age, sex, race, insurance status, MHI, and rurality were associated with delayed access to kidney transplantation services. These findings will inform locally-tailored interventions to improve equity in kidney transplant access.

Limitations: Our analysis reflects transplant access at Network 9 centers that contribute to E-STAR (n=4 of 14). Reason for referral/no referral were not available; some patients may not have been referred due to medical ineligibility.

References

1. McPherson LJ, Di M, Adams AA, Plantinga L, Pastan SO, Patzer RE. Geographic Differences in Racial Disparities in Access to Kidney Transplantation. *Kidney International Reports. 2023/08/11/ 2023;doi:https://doi.org/10.1016/j.ekir.2023.08.002*
2. Saunders MR, Lee H, Alexander GC, Tak HJ, Thistlethwaite JR, Jr., Ross LF. Racial disparities in reaching the renal transplant waitlist: is geography as important as race? Clin Transplant. Jun 2015;29(6):531-8. doi:10.1111/ctr.12547

Acknowledgements:

The research was supported by CK's T32 postdoctoral fellowship in the IUSM Division of Nephrology and RP's RO1, The RaDIANT National Expansion Study (U01MD010611).

Conflicts of Interest: The authors have nothing to disclose.

PURDUE UNIVERSITY | Center for Health Equity and Innovation

PURDUE UNIVERSITY | Health Equity Initiatives

Redesigning Engagement with Communities at the Center

OVERVIEW

Since March 2022, through generous gifts from Jim and Jeannie Chaney, Dr. Jerome Adams, Executive Director of Health Equity Initiatives and the Purdue University Center for Health Equity (CHEqI) awarded 16 grants to Indianapolis community-based organizations (CBOs). The focus of the funding request was to develop innovative, sustainable models that address disparities in health affecting people who have been historically marginalized and underserved.

Taziyah's Open Art Studio

Funds support Taziyah's Open Art Studio offered to Arsenal Technical High School students both during and after school. Students engage in art therapy, where students utilize art as a tool for connections with themselves and others while working through struggles they experience in their day-to-day lives.

Gennesaret Free Clinics

Gennesaret provides quality and accessible patient-centered healthcare regardless of insurance coverage or ability to pay. CHEqI mini-grants contribute to the Health Recovery Homes initiative that offers respite housing for patients experiencing homelessness and funding to support medication access.

Indiana Community Health Worker Association

The Indiana Community Health Worker Association (INCHWA) created and implemented the GRITT (Growing Resilience in Trying Times) program to impact the mental health of frontline workers positively. After the first round of CHEqI Mini-Grant funding, INCHWA received a larger grant from the Indiana Department of Health to implement phase two of the GRITT program. After receiving a second round of funding from CHEqI Mini-Grants, INCHWA began implementing the third phase of GRIT: A GRITT Facilitator Certificate Program. INCHWA will provide specialized training to its CHW members to help them advance in their careers and become GRITT facilitators.

CONCLUSIONS

- **Communities must be at the center of health equity engagement activities.**
- **Community priorities, expertise, and needs should inform academic initiatives.**
- **Interdisciplinary faculty have significant opportunities to partner with communities to support meaningful change.**
- **Academic efforts to partner with communities will be difficult without dedicated time and effort to build bi-directional, mutually beneficial relationships.**

The Kheprw Institute

The Kheprw Institute builds community wealth and believes the most significant community resource is its people. Kheprw offers a variety of programs and initiatives for all adults and youth in the community. The CHEqI Mini-Grants help to fund Growing Good in the Hood, a community garden initiative.

Soul Food Project

As a nonprofit based in Indianapolis, Soul Food fosters wellness in the community by increasing access to local food through urban farms, offering education, and providing equitable employment. Soul Food partnered with Indy Parks and Recreation and a neighborhood association to launch a new community garden in Spring 2024.

Carlyn Kimiecik MSW[1,2], Jasmine D. Gonzalvo PharmD[1,3], Omolola Adeoye-Olatunde PharmD, MS[1,3] Jerome Adams MD, MPH[1,4], Steven R. Abel PharmD[5], Ephrem Abebe Bpharm, MS, PhD[3], Noll L. Campbell PharmD, MS[3], David R. Foster PharmD[3], Gicelle Garcia MPH[1], Sonak D. Pastakia PharmD, MPH, PhD[1,3]

[1]Center for Health Equity and Innovation, Purdue University
[2]College of Health and Human Sciences, Purdue University
[3]College of Pharmacy, Purdue University
[4]Office of the Provost, Purdue University
[5]Office Of Engagement (Emeritus), Purdue University

Pathways to Reduce COVID-19 Health Disparities with an Intermediate Evaluation Tool

Lily Darbishire, MPH, RDN, PhD; Casey Kinderman, BS
Regenstrief Center for Healthcare Engineering, Purdue University

ABSTRACT

Capacity building (CB) is necessary to induce community change that over time, can improve population health. Evaluation of capacity building activities are often missed due a lack of available tools and resources designed to capture outcomes that bridge the gap between inputs and impact.

Purdue University adapted an activity log system used to evaluate quantitatively and visually demonstrate intermediate impact within an Indiana initiative designed to reduce COVID-19 related health disparities Indiana Healthy Opportunities for People Everywhere (I-HOPE).

The activity log system described effectively demonstrated intermediate success. It also highlighted the relationship between upfront investment in intermediate community engagement activities and resulting change outcomes over time.

BACKGROUND

Purdue's Community Transformation Team (CTT) builds partnerships and capacity among communities to ultimately reduce health disparities across the state of Indiana. (Figure 1).

Funded initiatives, like I-HOPE, often encourage, if not require, impact results to be reported back to stakeholders, including funders, state health departments, academic institutions, and community participants, when long-term goals, such as changes in health status, may not be realized within one or two years. Also, the ability to maintain, sustain, or apply for new health-facing initiatives relies heavily on demonstrable success and community impact.

To fill this gap, Purdue's CTT created an activity log system, adapted from work by Chalmers et al., 2003, to track Purdue-led I-HOPE activities and associated intermediate impacts via change outcomes over a period of 3 years.

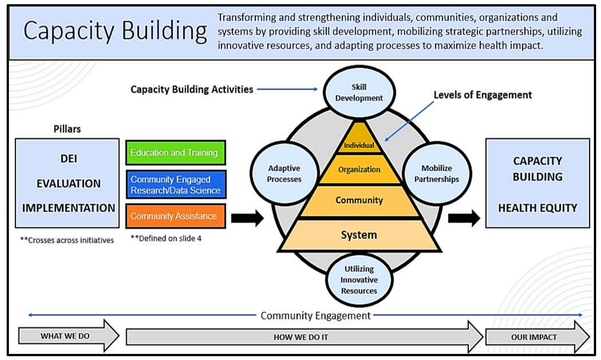

Figure 1. *Purdue Community Transformation Team's (CCT's) process map for capacity building. Community engagement is a core component for all CCT's capacity building activities.*

METHODS

Data were retrospectively collected by the CTT on Purdue-led I-HOPE activities and change outcome(s) from project management tools as well as team-member and partner interviews. The CTT created and defined categories for both activities and change outcomes that aligned with Figure 1.

Activities were recorded as education and training, community-engaged research, or community assistance. Change outcomes were categorized as an individual, organizational, community, or systems-level change. Activities were assigned unique identifiers that directly link each activity with the resulting change outcome(s). Cumulative totals were then calculated, recorded, and inputted into a line graph that overlays activities and associated change outcomes over time.

RESULTS

Analysis demonstrates that Purdue's CTT implemented a total of 687 capacity building and partnership activities that directly resulted in 1,313 changes in Indiana communities between 2021-2024, as part of the I-HOPE initiative (Figure 2).

Figure 3 demonstrates the categories in which change outcomes occurred. 182 individual changes; 101 organizational changes; 1,021 community changes; and 9 systems-level changes occurred.

Additionally, the results demonstrate achievement of intermediate goals set by the CTT.

- **Goal 1:** Increase knowledge, skills, and abilities of healthcare professionals and community members to address social drivers of health (individual changes).
- **Goal 2:** Improve organizational capacity of local health departments, non-profits, grass roots organizations, and critical care providers in underserved and rural areas (organizational changes).
- **Goal 3:** Expand community access to resources, events, healthcare, and education in underserved and rural areas (community changes).
- **Goal 4:** Strengthen systems of care and judicial systems to improve health equity among Indiana counties and communities (systems changes).

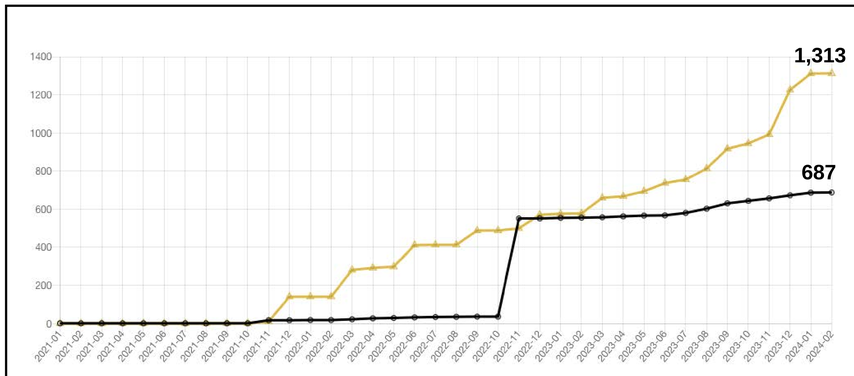

Figure 2. *Cumulative Activities and Change Outcomes Over Time*

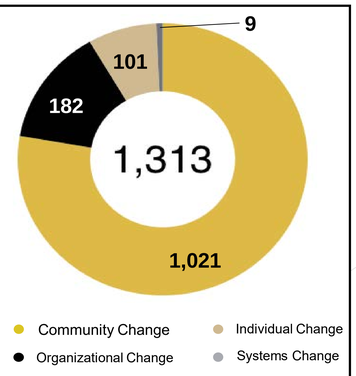

Figure 3. *Community Change Outcomes Categorized by Type*

DISCUSSION | CONCLUSION

Purdue's activity log system was effective in evaluating the intermediate success of partnership and capacity building activities within Purdue-led I-HOPE activities working to reduce health disparities in Indiana. The graph was used to demonstrate program fidelity without having to wait years or decades to see changes in health status. Using the graph, the CTT was able to secure funding to sustain the project for an additional 2 years.

While no change outcomes occurred during most of 2021, from 2022-2024 the number of outcomes doubled the number of activities, demonstrating the importance of upfront investment in listening, trust and relationship building, and tailored interventions to fit community needs. A logic model was used to guide the path between proposed CB activities and reduced health disparities in Indiana.

TRANSLATION

With the increased use of public health funding for community-based health promotion, it is important to understand the impact they have on their communities. It takes time to realize an outcome such as a change in health status. However, changes within communities may precede changes in health status. The activity log process is useful for observing the changes in a community's health promotion environment and providing an intermediate measure of an initiative's success.

REFERENCES

Chalmers, M. L., Housemann, R. A., Wiggs, I., Newcomb-Hagood, L., Malone, B., & Brownson, R. C. (2003). Process evaluation of a monitoring log system for community coalition activities: five-year results and lessons learned. *American Journal of Health Promotion*, 17(3), 190-196.

Acknowledgement of funding source: This poster was supported by funds made available from the Centers for Disease Control and Prevention, Center for State, Tribal, Local and Territorial Support, under NH75OT000073.

Disclaimer: The content of this presentation are those of the authors and do not necessarily represent the official position of or endorsement by the Centers for Disease Control and Prevention.

Collaborative Core for Cancer Bioinformatics – C3B

Sagar Utturkar, Nadia Lanman, Sheng Liu, Harish Kothandaraman, Jun Wan

PURDUE UNIVERSITY | Institute for Cancer Research

INDIANA UNIVERSITY MELVIN AND BREN SIMON CANCER CENTER

Abstract:

The Collaborative Core for Cancer Bioinformatics (C3B) is a joint bioinformatics core shared between the Indiana University Melvin and Bren Simon Comprehensive Cancer Center (IUCCC) and the Purdue University Institute for Cancer Research (PICR). The C3B performs services such as scientific consulting, training, and high-quality bioinformatics analyses. The core employs 6 full-time staff members and mentors 5 graduate research assistants and 1 undergraduate student. The core has performed numerous analyses including RNA-seq, scRNA-seq, ChIP-seq, CRISPR/Cas9, WGS, and spatial transcriptomics. Here, we highlight three projects completed by the C3B. In the first example, we performed single-cell RNA-sequencing (scRNA-seq) on canine muscle-invasive urothelial carcinoma primary tumors before and after treatment with the Cox inhibitor Piroxicam. Higher abundance and activity of tumor-infiltrating lymphocytes was found to be associated with favorable therapeutic response. These results can be extended to evaluate immunotherapies in canine clinical trials. Another example used bulk RNA-seq to investigate human cytokine-primed natural killer cell responses to adenosinergic signaling, which acts as a potent immunosuppressant in solid tumors. We found that adenosine induces upregulation of genes involved in immune responses while downregulating cellular metabolism and protein synthesis functions, thus leading to impaired anti-tumor immunity. Our results showed that adenosine acts on specific cellular pathways in NK cells rather than inducing broad inhibition of cellular functions. A third project integrated scRNA-seq, gene set enrichment analysis, and survival analysis with cutting-edge experimental methodologies in prostate cancer and found that cancer cell expression of the chromatin effector Pygo2 promotes immunotherapy resistance by restraining tumor T cell infiltration and cytotoxicity. A significant contribution of this study is the translational implications of targeting Pygo2. We synthesized JBC117 and JBC117ana as prototype Pygo2 inhibitors and showed that they largely phenocopied Pygo2 genetic deletion to generate single-agent and combinatorial efficacy with immune checkpoint blockade, including treating castration-resistant prostate cancer.

Personnel:

- Jun Wan, Ph.D (Core Director)
- Sheng Liu, Ph.D (IU Project Manager)
- Nadia Lanman, Ph.D (PU Project Manager)
- Sagar Utturkar, Ph.D.
- Harish Kothandraman, MS

Selected Services:

- Consulting
- Grant writing aid
- Manuscript preparation aid
- Data analysis
- Data integration
- Tool and method development
- Training
- Education

Equipment:

- 110 TB of storage on the Purdue Research Computing Data Depot
- 4 nodes on Bell (512GB and 32 CPU per node)
- 4 nodes on Negishi (128GB and 20 CPU per node)

Training Initiatives:

- The C3B supports and trains students through the awarding of graduate research assistantships funded through generous support by the Walther Cancer and the Hope Foundations
- The C3B works with undergraduate students and has also mentored high school students
- The C3B has hosted national and international workshops
- The C3B hosts workshops and trainings at Purdue, nationally, and internationally
- May 13-17, 2024 the C3B is hosting an RNA-seq workshop at Purdue University

Funding:

The C3B is supported by the Purdue Institute for Cancer Research (Grant P30CA023168), The Indiana University Melvin and Bren Comprehensive Cancer Center (Grant P30CA082709), the Hope Foundation, and The Walther Cancer Foundation.

Scientific Examples

Uncovering the effect of cyclooxygenase (COX) inhibitors in canine tumors through single-cell RNA sequencing (scRNA-seq) analysis (Dr. Deborah Knapp)

Dr. Deborah W. Knapp's (Purdue) research is aimed at improving the outlook for pet animals and people with cancer. Dr. Knapp's research focuses on muscle-invasive urothelial carcinoma (InvUC) and major research outcomes involve defining the molecular subtypes in canine InvUC and association with tumor immune signatures, and clinical trials in pet dogs underlining the value of canine model to study the human cancer and successful translation into humans.

In this study, we studied an effect of cyclooxygenase (COX) inhibitors in pet dogs with InvUC using scRNA-seq data before (pre) and after (post) treatment with COX inhibitor drugs. Our hypothesis is COX inhibitors enhance immune-stimulatory activity in various immune and stromal cells, thereby dampening tumor progression. Our analyses revealed a global map of tumor microenvironment (TME) in pet dogs with InvUC. Higher abundance and activity of immune cells was associated with favorable therapeutic response. Ongoing work is evaluating the correlation between TME and molecular subtypes. These results can be extended to evaluate the success and failure of immunotherapy in canine clinical trials in terms of TME.

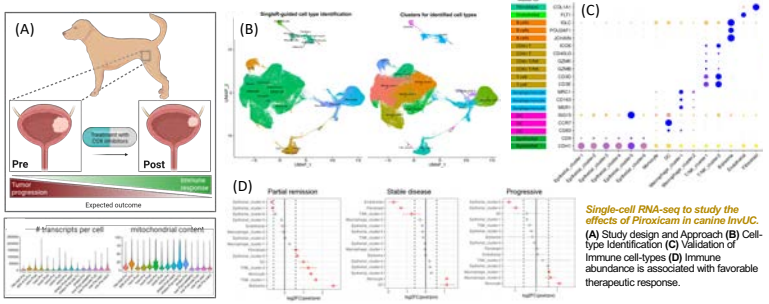

Single-cell RNA-seq to study the effects of Piroxicam in canine InvUC. **(A)** Study design and Approach **(B)** Cell-type Identification **(C)** Validation of Immune cell-types **(D)** Immune abundance is associated with favorable therapeutic response.

Paving the way for the Development of Novel Immunotherapies for Solid Tumors (Dr. Sandro Matosevic)

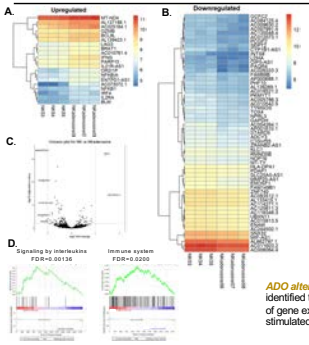

Dr. Sandro Matosevic's (Purdue) research program focuses on developing new immunotherapies for solid tumors using translational tools to reprogram the therapeutic behavior of natural killer (NK) cells and their interaction with the tumor microenvironment (TME). Many of the studies in his lab seek to identify ways to overcome immunometabolic suppression of natural killer cell function in the TME. We used RNA-seq to investigate human cytokine-primed natural killer cell responses to adenosinergic signaling, which acts as a potent immunosuppressant in solid tumors. We found that adenosine induces upregulation of genes involved in immune responses while downregulating cellular metabolism and protein synthesis functions, thus leading to impaired anti-tumor immunity. Interestingly, our results showed that adenosine acts on specific cellular pathways in NK cells rather than inducing broad inhibition of cellular functions. These results are paving the way to better designed immunotherapies which can reprogram natural killer immunometabolism, ultimately leading to improved targeting of solid tumors.

Associated Publication and Grants

1. Wang, J.; Toregrosa-Allen, S.; Elzey, B.D.; Utturkar, S.; Lanman, N.A.; Bernal-Crespo, V.; Behymer, M.M.; Knipp, G.T.; Yun, Y.; Veronesi, M.C.; et al. (2021). Multispecific targeting of glioblastoma with tumor microenvironment-responsive multifunctional engineered NK cells. Proc. Natl. Acad. Sci. USA, 118, e2107507118
2. Chambers AM, Wang J, Lupo KB, Yu H, Lanman NA, Matosevic S. (2018). Adenosinergic Signaling Alters Natural Killer Cell Functional Responses. Frontiers in Immunology. 9:2533.
3. V Foundation Funding

ADO alters transcriptional signatures of human NK cells. **(A)** Heatmap of upregulated genes in response to ADO treatment of IL-12/IL-15-activated human NK cells. Differentially-expressed genes were identified through DESeq2 and edgeR database analysis. **(B)** Downregulated genes in response to ADO treatment of IL-12/IL-15-activated human NK cells based on DEseq2 and edgeR analysis. (C) Volcano plot of gene expression changes in IL-12/IL-15 co-stimulated NK cells in response to ADO. **(D)** GSEA analysis of two most heavily enriched gene sets based on positive transcriptional associations for IL-12/IL-15 co-stimulated NK cells in the presence of ADO.

Targeting chromatin effector Pygo2 promotes cytotoxic T cell responses and overcomes immunotherapy resistance in prostate cancer (Dr. Xin Lu)

Dr. Xin Lu's (Indiana University) research investigates both cancer-cell-intrinsic and -extrinsic mechanisms of immune evasion and immunotherapy resistance. His research has revealed a number of targetable mechanisms on how the oncogenic signaling in neoplastic cells ("cancer-cell-intrinsic") exerts the cell non-autonomous functions to control the cancer-immune interactome in solid tumors. For example, a recent publication in Science Immunology (2023) found that cancer cell expression of the chromatin effector Pygo2 promotes immunotherapy resistance by restraining tumor T cell infiltration and cytotoxicity. Another publication on Cell Metabolism (2023) reveal how tumor-infiltrating neutrophils escape from ferroptosis (a newly identified iron-dependent non-apoptosis cell death) through the aconitate decarboxylase 1 (Acod1)-dependent immunometabolism switch and establish Acod1 as a target to offset immunosuppression and improve immunotherapy against metastasis. Diverse types of models and techniques, such as genetically engineered mice and cell models, functional genomics, experimental therapeutics, and cutting-edge experimental and computational methodologies (single cell RNA-seq, spatial transcriptomics, high-throughput drug and CRISPR/cas9 screen, molecular digital pathology, multi-omics integration, etc.) were employed.

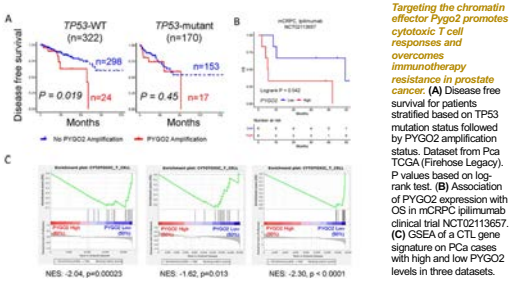

Targeting the chromatin effector Pygo2 promotes cytotoxic T cell responses and overcomes immunotherapy resistance in prostate cancer. **(A)** Disease free survival for patients stratified based on TP53 mutation status followed by PYGO2 amplification status. Dataset from Pca TCGA (Firehose Legacy). P values based on log-rank test. **(B)** Association of PYGO2 expression with OS in mCRPC ipilimumab clinical trial NCT02113657. **(C)** GSEA of a CTL gene signature on PCa cases with high and low PYGO2 levels in three datasets.

Associated Publication and Grants

1. Zhu Y, Zhao Y, Wen J, Liu S, Huang T,Hatial I, Peng X, Janabi HA, Huang G, Mittlesteadt J, Cheng M, Bhardwaj A, Ashfeld BL, Kao KR,Maeda DY, Dai X, Wiest O, Blagg BSJ, Lu X, Cheng L, Wan J, Lu X. (2023) Targeting the chromatin effector Pygo2 promotes cytotoxic T cell responses and overcomes immunotherapy resistance in prostate cancer. Science Immunology. 8(81): eade4656.
2. Zhao Y, Liu Z, Liu G, Zhang Y, Liu S, Gan D, Chang W, Peng X, Sung ES, Gilbert K, Zhu Y, Wang X, Zeng Z, Baldwin H, Ren G, Weaver J, Huron A, Mayberry T, Wang Q, Wang Y, Diaz-Rubio ME, Su X, Stack MS, Zhang S, Lu X, Sheldon RD, Li J, Zhang C, Wan J, Lu X. (2023) Neutrophils resist ferroptosis and promote breast cancer metastasis through aconitate decarboxylase 1,Cell Metabolism,35,10,1688-1703.e10.

“Wishing I had known more of what to expect”: Patient’s experiences of pregnancy loss in Indiana

Fatimah Lawal[1], Oluwapamimo J. Fafowora[1], Anayra Maldonado[2], & Kathryn J. LaRoche[1]
[1] Department of Public Health, Purdue University, [2] School of Communication, Purdue University

INTRODUCTION

- About 1 in 5 pregnancies end in miscarriage every year in the US.
- There is a dearth of research that documents patient’s miscarriage experiences.
- We explored women’s miscarriage experiences, including their experiences with the healthcare system.

METHODS

- Multi-modal community-based recruitment strategy
- 21 in-depth interviews with people living in Indiana who experienced a miscarriage within the last 5 years
- Recorded and transcribed interviews
- Content and thematic analysis

PARTICIPANT CHARACTERISTICS

- Participants age ranged from 27-40 years
- Majority of participants self identified as White (19), Black (1), Hispanic (1)
- Participants reported between one (n=19) and three (n=1) miscarriage experiences between 2018 and 2023
- The majority of participants (n=19) experienced one pregnancy loss

“... I feel like it's it's not talked about like, it wasn't until I had my miscarriage and opened up about it that I realized that, like two or three of my friends had had a miscarriage.”
Mikaila, miscarriage in 2018

“... And in the end the only test they could have done was a blood test. I know for a fact how quick and easy it was to get that [blood test]. And I didn't need an ER bill to get that test”
Nicole, miscarriage in 2020

*All names are pseudonyms

PRELIMINARY FINDINGS

- Participants did not have information about miscarriage (or consider it as something that could happen to them) until after they had experienced pregnancy loss.
- Consistently, participants reflected negatively on the care they received during their miscarriage encounter.
- Inconsistent with standards of care, most participants were not offered the complete range of options to manage their miscarriage.
- Participants expressed desire for providers to show **more empathy and sensitivity in communication** manner, in relation to the miscarriage encounter.
- Participants wanted additional information about pain and pain management, **the physical process of miscarriage**, and how to access emotional support and resources.

Lack of information means that many participants were sent to the emergency department when it was not necessary.

“... For me ... **if I hadn't gone to the ER it would not have been nearly this expensive or nearly this stressful.** So it's almost just like wishing I had known more of what to expect, so that I had a better idea of like when I really needed to go to the ER, or having access to that pain medication at home if I needed it, you know. So I could have stayed at home”.
Casidy, miscarriage in 2021

This has negative implications for people experiencing pregnancy loss and for the health care system.

DISCUSSION & RECOMMENDATIONS

- Identify options for miscarriage care outside the emergency department and/or train ED providers to offer specialized miscarriage care.
- Training providers on the use of empathy and patient-centered approaches can improve patients care experiences.
- People experiencing miscarriage should be offered all options for how to manage their miscarriage: watchful waiting, procedural evacuation, or medications.
- Normalizing conversations about pregnancy loss in health care settings could be helpful.

“I said, I'm 8 weeks, and they [health care providers] kind of just like laughed it off. And they were like, ***Well, unless you're 20 weeks, there's absolutely nothing we can do. So just stay home and wait it out***.”
Mallory, miscarriage in 2020

“They basically told me that I had to go to the ER [emergency room]. **There was no other options.** They wouldn’t see me, just wanted me to go to the ER.”
Amy, miscarriage in 2023

ACKNOWLEDGEMENTS

This project was funded with support from Dr. LaRoche’s research budget, the Purdue University Women’s Global Health Institute, the Indiana Clinical and Translational Sciences Institute, and by Award Number UL1TR002529 from the National Institutes of Health, National Center for Advancing Translational Sciences, Clinical and Translational Sciences Award. The content is solely the responsibility of the authors and does not necessarily represent the official views of the National Institutes of Health.

Questions, comments, collaboration interest? flawal@purdue.edu kjlaroch@purdue.edu

Glucose, glutamine, and fatty acids are utilized differently in breast cancer cells that preferentially metastasize to lung or liver

Marjorie Anne Layosa[1], Stephen Hursting[2], Dorothy Teegarden[1]

[1] Department of Nutrition Science, College of Health and Human Sciences, Purdue University
[2] Department of Nutrition, University of North Carolina at Chapel Hill

ABSTRACT

Metastasis is the primary cause of breast cancer-related deaths. We investigated whether utilization of different energy substrates supports metastasis to specific distant sites. Utilizing a breast cancer metastatic model that either preferentially metastasizes to the lung (metM-Wnt^{Lung} cells; MLg) or liver (metM-Wnt^{Liver} cells; MLr), we measured the uptake of radiolabeled substrates, ^{13}C-metabolic flux, and protein expression of metabolic enzymes to compare energy metabolism between cell lines. Results show that ^{14}C-glucose uptake is similar, but mRNA abundance of hexokinase, the initial rate-limiting step in glycolysis, was 22% higher in MLg. This is consistent with higher $^{13}C_6$-glucose flux into glycolytic metabolites pyruvate and lactate in MLg. Interestingly, high glucose (25 mM) exposure reduced viability of MLr by 39% suggesting MLg's better adaptability to glucose. Also, ^{14}C-glutamine uptake is 27% higher in MLg, consistent with increased mRNA abundance of glutamine catabolizing enzymes, glutamate synthase and dehydrogenase, and higher $^{13}C_5$-glutamine flux into the tricarboxylic acid cycle as α-ketoglutarate (18%) compared to MLr. However, high glutamine (4 mM) exposure increased cell growth of MLr by 20% suggesting MLr's adaptability to glutamine. Furthermore, ^{14}C-palmitate uptake is similar, but fatty acid synthesis utilizing both $^{13}C_6$-glucose and $^{13}C_5$-glutamine is higher in MLg. Inhibition of fatty acid synthesis and oxidation reduced cell growth of MLg by 11% and 21%, respectively, compared to MLr, suggesting MLg relies on increased fatty acid metabolism. Overall, we showed that breast cancer cells with preferential metastasis to lung and liver exhibit differential energy metabolism which may support their successful metastasis to these distant sites.

BACKGROUND

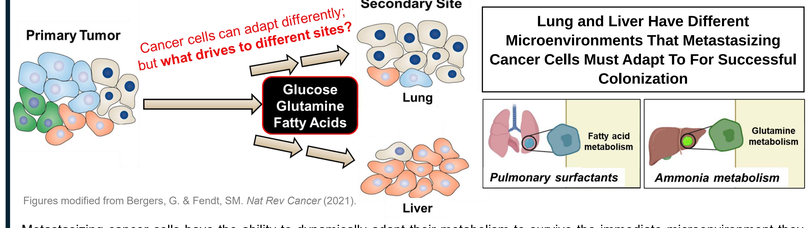

Figures modified from Bergers, G. & Fendt, SM. *Nat Rev Cancer* (2021).

Metastasizing cancer cells have the ability to dynamically adapt their metabolism to survive the immediate microenvironment they are exposed to throughout the metastatic cascade. However, breast cancer cells metastasize to distinct organ sites, including lung and liver[1]. Differential metabolic traits in specific metastatic cells may drive preferential colonization in specific, metabolically distinct metastatic sites.

METHODOLOGY

Wnt-Driven Metastatic Breast Cancer Model:

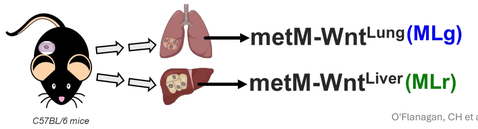

O'Flanagan, CH et al. *NPJ Breast Cancer* 3:26 (2017).

Cell Culture. Murine metM-Wnt^{Lung} and metM-Wnt^{Liver} mammary cancer cells [2] were cultured in Dulbecco's Modified Eagle's Medium (DMEM, Sigma, St. Louis, MO) with 5 mM glucose, 2 mM glutamine, no sodium pyruvate, with 10% final concentration fetal bovine serum and 1% final concentration penicillin-streptomycin.

^{14}C Radiolabeled Substrate Uptake. Cells were incubated for 10-15 mins with medium spiked with ^{14}C-Glucose (0.25 μCi/mL)), or ^{14}C-Glutamine (0.25 μCi/mL), or 1 mM of ^{14}C-Palmitic acid (0.23 μCi/mL) conjugated in fatty-acid free BSA. The cellular uptake of ^{14}C were quantified using a Tri-Carb 5110TR 110 V Liquid Scintillation Counter.

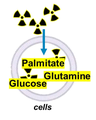

^{13}C Metabolic Flux. Cells were incubated for 2 hrs with $^{13}C_6$-glucose or $^{13}C_5$-glutamine. Methoxylamine hydrochloride in pyridine was used to derivatize metabolites. Following derivatization, metabolites were analyzed with gas chromatography-mass spectrometry (GC-MS) using a TG-5MS gas chromatography column and Thermo TSQ 8000 triple quadrupole mass spectrometer.

RT-qPCR. RNA was isolated from cells via TriReagent following the manufacturer's instructions. Reverse transcription of total RNA was conducted using MMLV reverse transcriptase and RT-qPCR was performed using Roche SYBR Green. mRNA expression was normalized to 18S.

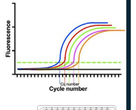

Viability Assay. Cells were seeded into 96 well plates overnight and then treated with 5 or 25 mM glucose, or 2 or 4 mM glutamine, or inhibitors. Cells were incubated with 1X (0.5 mg/mL) MTT in serum-free media for 2 hrs at 37°C. Crystals were dissolved in dimethyl sulfoxide (DMSO), and absorbance was determined at 570 nm with a spectrophotometer.

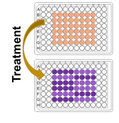

RESULTS

metM-Wnt^{Lung} Has Higher Glycolytic Activity and Adaptability to High Glucose Concentration

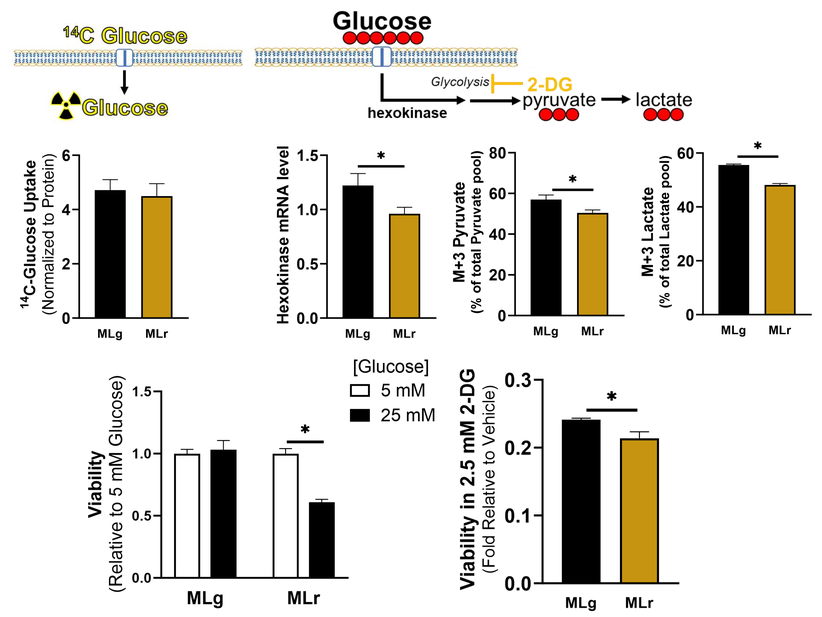

*Values are mean ± SEM. * represents p-value < 0.05 using t-test.*

metM-Wnt^{Liver} Has Lower Glutamine Flux, but Higher Adaptability to High Glutamine Concentration

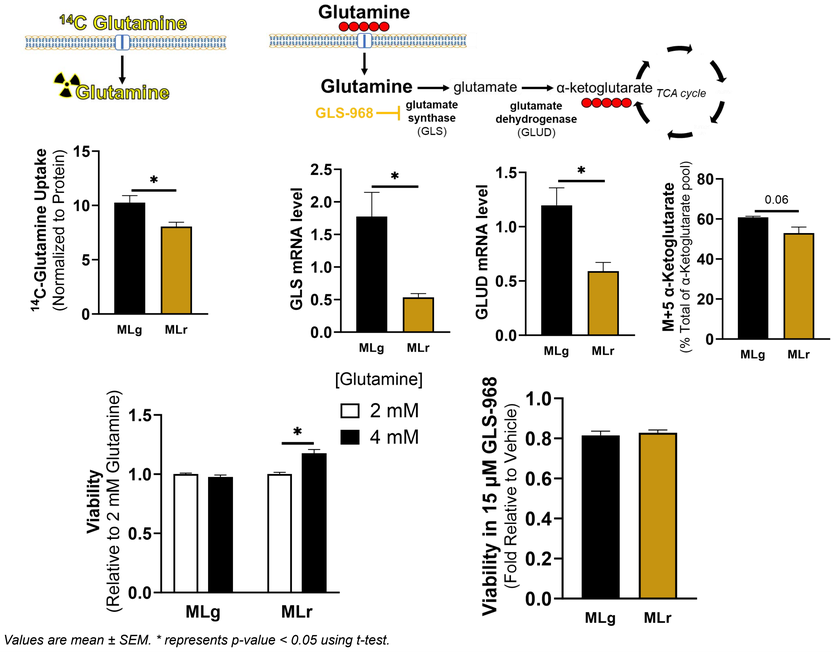

*Values are mean ± SEM. * represents p-value < 0.05 using t-test.*

RESULTS

metM-Wnt^{Lung} Has Higher Reliance on Fatty Acid Synthesis Oxidation

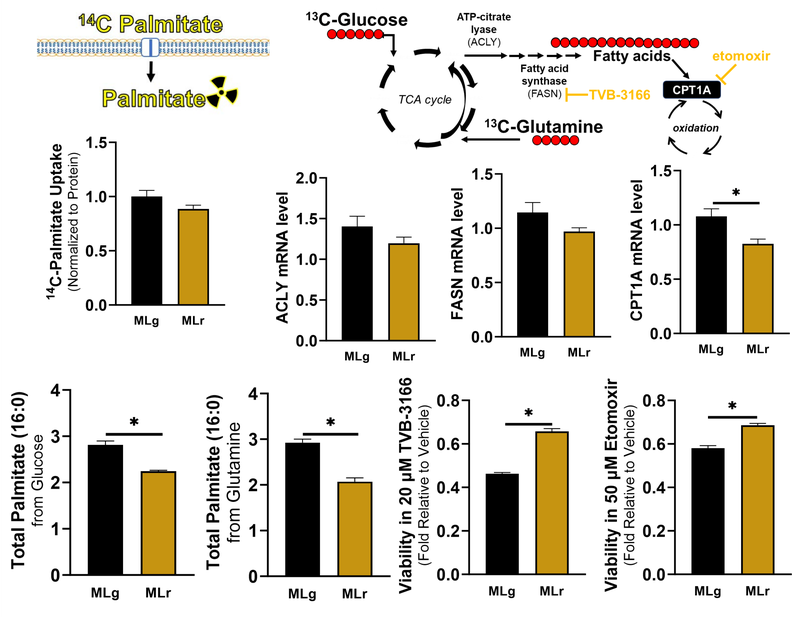

*Values are mean ± SEM. * represents p-value < 0.05 using t-test.*

CONCLUSION

Breast cancer cells with preferential metastasis to lung and liver exhibit differential energy metabolism which may support their successful metastasis to these distant sites.

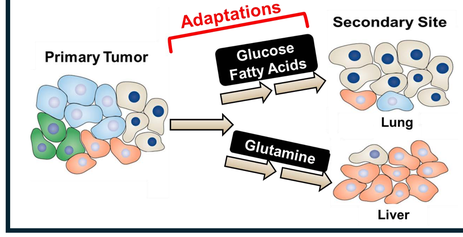

metM-Wnt^{Lung} cells have higher glycolytic and fatty acid metabolism while metM-Wnt^{Liver} has higher glutamine adaptation.

REFERENCES

1. Bergers, G., & Fendt, S. M. (2021). The metabolism of cancer cells during metastasis. Nature reviews. Cancer, 21(3), 162–180. https://doi.org/10.1038/s41568-020-00320-2
2. O'Flanagan, C. H., Rossi, E. L., McDonell, S. B., Chen, X., Tsai, Y. H., Parker, J. S., Usary, J., Perou, C. M., & Hursting, S. D. (2017). Metabolic reprogramming underlies metastatic potential in an obesity-responsive murine model of metastatic triple negative breast cancer. NPJ breast cancer, 3, 26. https://doi.org/10.1038/s41523-017-0027-5

ACKNOWLEDGMENTS

We acknowledge the support from Purdue University Institute for Cancer Research, Women's Global Health Institute and National Institutes of Health R01CA232589 and R01A271597.

Development of a novel diagnostic method, loop-mediated isothermal amplification (LAMP), for *Balamuthia mandrillaris*.

Chenyang Lu and Christopher A. Rice
Department of Comparative Pathobiology, Purdue University, West Lafayette, IN 47907

Introduction

- Commonly isolated from soil and dust: 27.32% solid matrices were *B. mandrillaris*-positive[2].
- Two life-cycle stages.
- Cause *Balamuthia* amoebic encephalitis (BAE) and cutaneous skin lesions.
- Mortality rate: ~ 92%[3].
- Epidemiology: 200-300 cases all over the world[4].

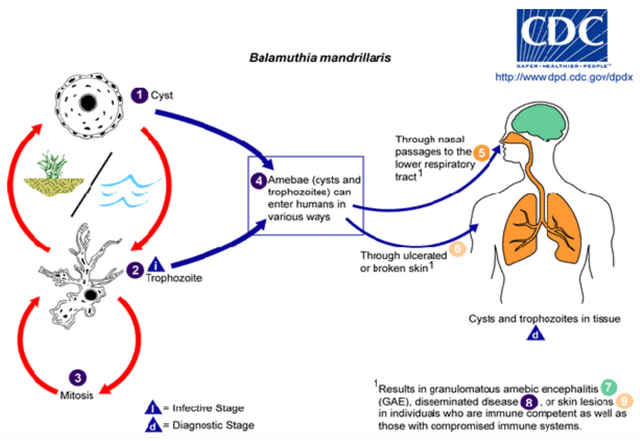

https://www.cdc.gov/parasites/balamuthia/pathogen.html[1]

Why do we need novel diagnostic method?

Neuroimaging methods: Nonspecific, same as tumor, bacterial or viral encephalitis

Microscopy methods: Morphology is same to histiocytes, requires expertise

Serological tests: Healthy individuals may have positive serology.

Immunodiagnostic test and molecular-based tests (gold standard): Only available in a few research centers, like the CDC.

Next-generation sequencing: Higher cost and specialized in few diagnostic and research centers.

Methods

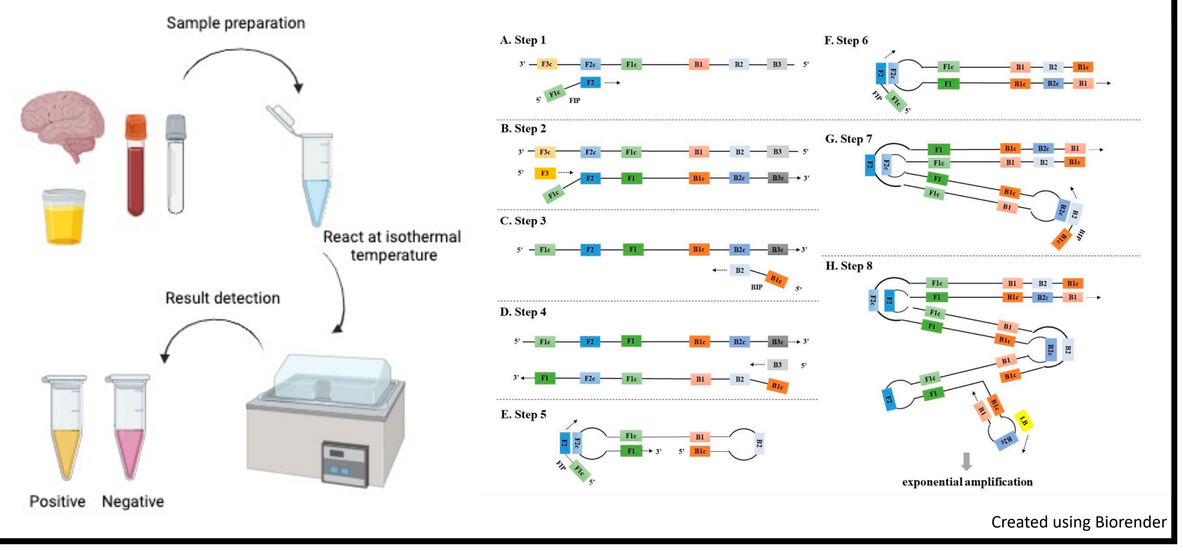

Created using Biorender

Conclusion

- Developed a novel diagnostic method, LAMP, for *B. mandrillaris*.
- Selected **18S rRNA** as the targeted gene.
- Optimized the LAMP condition: 1x primers (0.16 µM F3/B3, 1.28 µM FIP/BIP and 0.32 µM LF/LB) at **65°C for 30 min**.
- **Specificity**: detected 5 different *B. mandrillaris* strains, no cross-reactivity with the DNA of other free-living amoeba, selected protozoa or bacteria.
- **Sensitivity**: The lower limit of detection for a positive signal was 10 fg/µL of extracted DNA, 10 original trophozoites, or 1 heated trophozoite/100 µL of media, we show 10~100-fold greater sensitivity than traditional PCR method.

Future direction

- Quantify the copy number of the targeted gene per organism by using qPCR and dPCR.
- Test *B. mandrillaris* spiking in NI clinical samples, like CSF, blood, and urine.
- Test *B. mandrillaris* infected *in vivo* mouse clinical samples (study plan confirmed with CDC: N=30x NI and 30x I)
- Test *B. mandrillaris* clinical samples from the patients.

Results

Primer screening

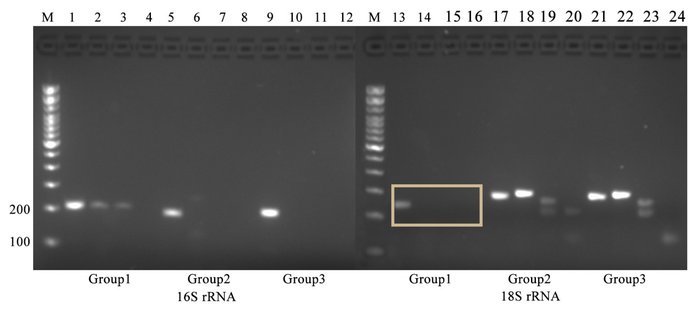

Primer	Sequence (5'-3')	Length (bp)
F3	TGGTGGAGTGATTTGTCTGG	20
B3	TCGGCTAATCACCGATTGTC	20
FIP	CGCTCACCCCCTGGTTTTGAATCGAACGAGACCTTAACCTGC	42
BIP	CGGTCGGCTCCAATCTTCGGACTTCTACCAATCCAACCGC	40
LF	AGCAGGATTGGCATGACT	18
LB	GTGCCCCTTGCCTTCTG	17

LAMP condition optimization

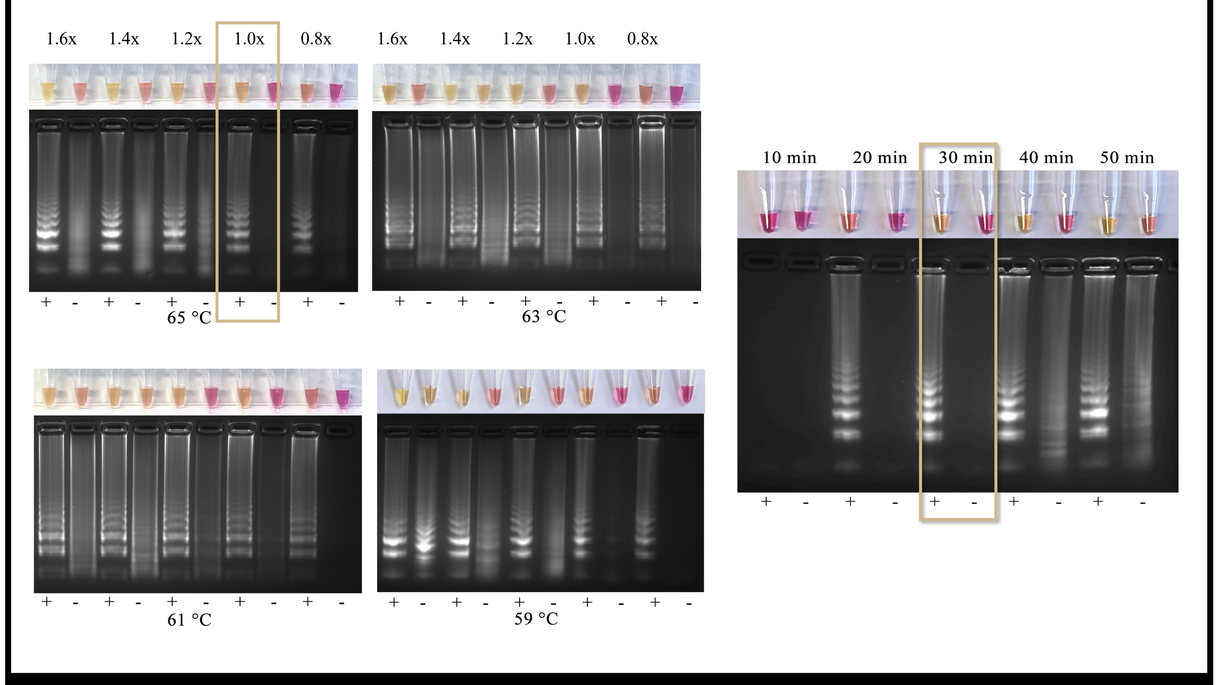

LAMP specificity

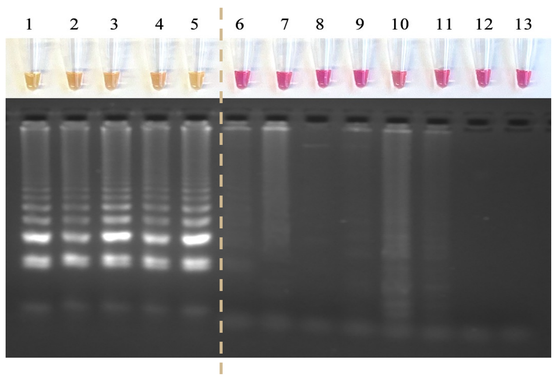

1. *B. mandrillaris*-V039; 2. *B. mandrillaris*-OK-1;
3. *B. mandrillaris*-SAM; 4. *B. mandrillaris*-RP5;
5. *B. mandrillaris*-N strain;
6. *A. castellanii*; 7. *N. fowleri* 8. *S. neurona;*
9. *T. gondii;* 10. *E. coli*; 11. *S. marcesens*;
12: *P. aeruginosa*;
13: Negative control

LAMP sensitivity

Cell number	DNA Concentration
10,000 (10^4)	~100 pg
1,000 (10^3)	~10 pg
100 (10^2)	~1 pg
10	~100 fg
1	~10 fg
0.1	~1 fg
0.01	~ 0.1 fg
0.001	~ 0.01 fg

Cell number (100 µL)	Cells per reaction (25 µL)
10,000 (10^4)	100 (10^2)
1,000 (10^3)	10
100 (10^2)	1
10	0.1
1	0.01
0.1	0.001
0.01	0.001
0.001	0.0001

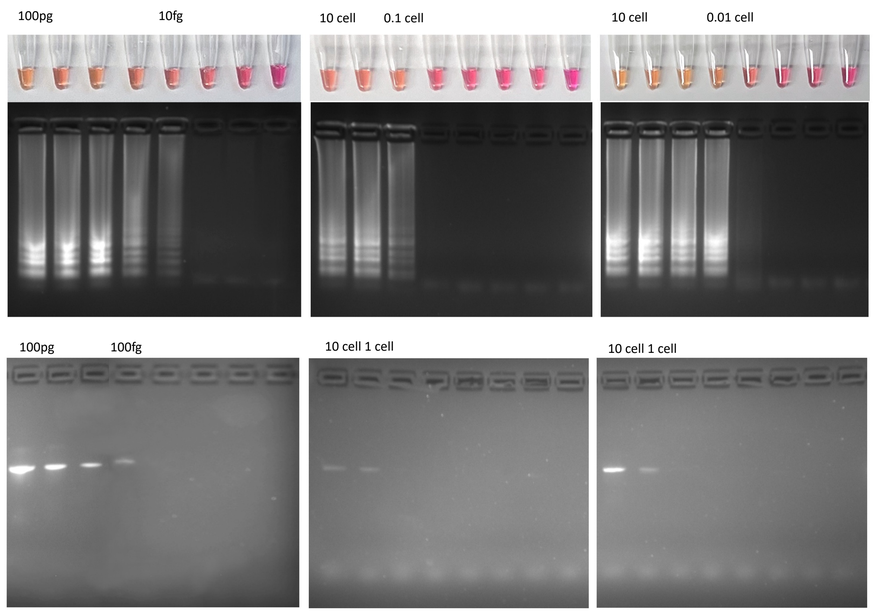

	DNA	Original cells	Heated cells
LAMP	10 fg/µL	0.1 trophozoite /reaction (10 cell/100µL)	0.01 trophozoite /reaction (1 cell/100µL)
PCR	100 fg/µL	1 trophozoite /reaction (100 cell/100µL)	1 trophozoite /reaction (100 cell/100µL)

Reference:
[1] Parasites - *Balamuthia mandrillaris* - Granulomatous Amebic Encephalitis (GAE): https://www.cdc.gov/parasites/balamuthia/pathogen.html
[2] Chaúque, B. J. M., da Silva, T. C. B., Dos Santos, D. L., et al. (2023). Global prevalence of free-living amoebae in solid matrices - A systematic review with meta-analysis. *Acta tropica, 247*, 107006.
[3] Visvesvara, G. S., Moura, H., & Schuster, F. L. (2007). Pathogenic and opportunistic free-living amoebae: Acanthamoeba spp., Balamuthia mandrillaris, Naegleria fowleri, and Sappinia diploidea. *FEMS immunology and medical microbiology*, *50*(1), 1–26.
[4] Cope, J. R., Landa, J., Nethercut, H., et al. (2019). The Epidemiology and Clinical Features of Balamuthia mandrillaris Disease in the United States, 1974-2016. Clinical infectious diseases : an official publication of the Infectious Diseases Society of America, 68(11), 1815–1822.

IN-UTERO DETECTION AND LONG-TERM MANAGEMENT OF CONGENITAL HEARTS DEFECTS – BRIDGING THE EXPERTISE GAP

PURDUE UNIVERSITY

BRETT A. MEYERS[1], STEVEN R. STEINHUBL[2], YUE-HIN LOKE[3], R. MARK PAYNE[4], PAVLOS P. VLACHOS[1,2]

[1] School of Mechanical Engineering, Purdue University, West Lafayette, IN, USA, [2] Weldon School of Biomedical Engineering, Purdue University, West Lafayette, IN, USA

[3] Division of Cardiology, Children's National Medical Center, Washington, DC, USA, [4] Indiana University School of Medicine, Pediatrics, Pediatric Cardiology, Indianapolis, IN, USA

Vlachos Research Group

BACKGROUND

Indiana: 8th highest infant mortality rate in the US

6.7 per 1,000 live births vs U.S. average of 5.4 per[1]

Congenital birth anomalies (CBAs) are the leading cause of infant mortality (21.9%)[2]

1 in 5 CBA deaths have an associated congenital heart defects (CHDs)[2,*]

Early detection of CHDs through prenatal ultrasound improves outcomes

Specialists detect 50%, while community hospitals detect ~13% of CHDs

Detection rates per state[3]

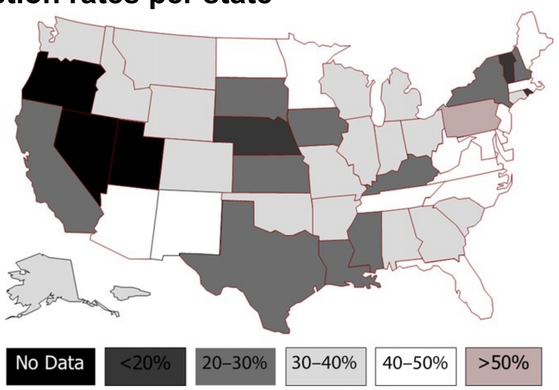

*Likely underreported since CHDs commonly missed during postmortem exams

Access barriers like income, education, insurance, and race affect CHD detection and management[4,5,6]

Diagnosis delays beyond 24 weeks gestational age are common, limiting available treatment options

Portable handheld ultrasound (PHUS) with smartphones can improve access, but lack of analysis tools limits use

We developed a novel fetal echocardiography analysis platform to assess and diagnosis of CHDs in utero[7,8,9]

Wide adoption of such tools can aid in population level screening for CHDs

Case A: Differences in heart hydrodynamics and morphology of single ventricle and normal hearts

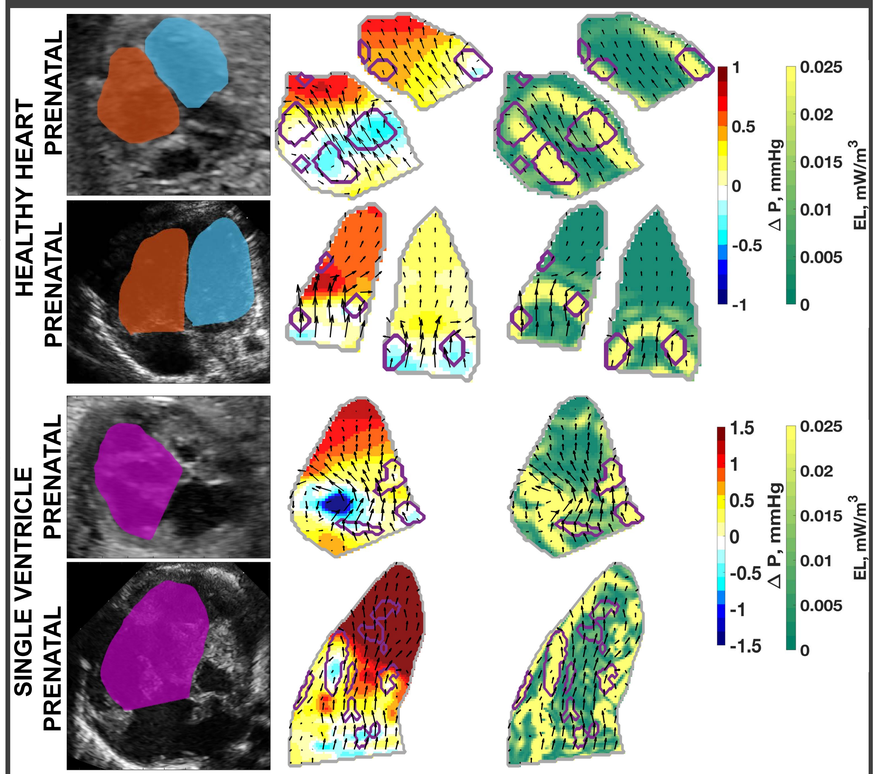

Case B: Altered flow patterns between Tetralogy of Fallot and normal hearts using echo and 4D flow MRI

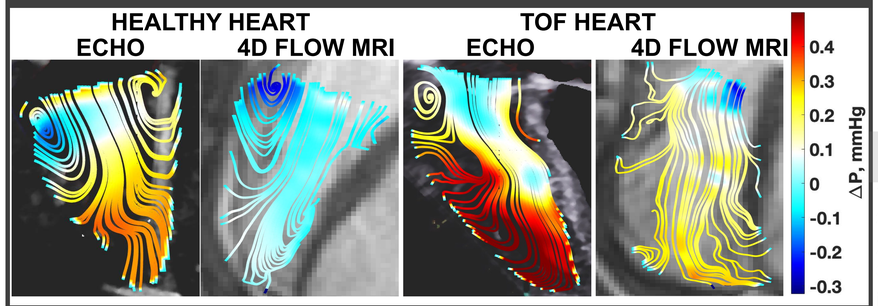

Early CHD detection by *in utero* fetal echo will inform *ex utero* surgical planning and management practices

vlachosresearch.org | Demo video | Ref 7 | Ref 8 | Ref 9

ANALYSIS PLATFORM

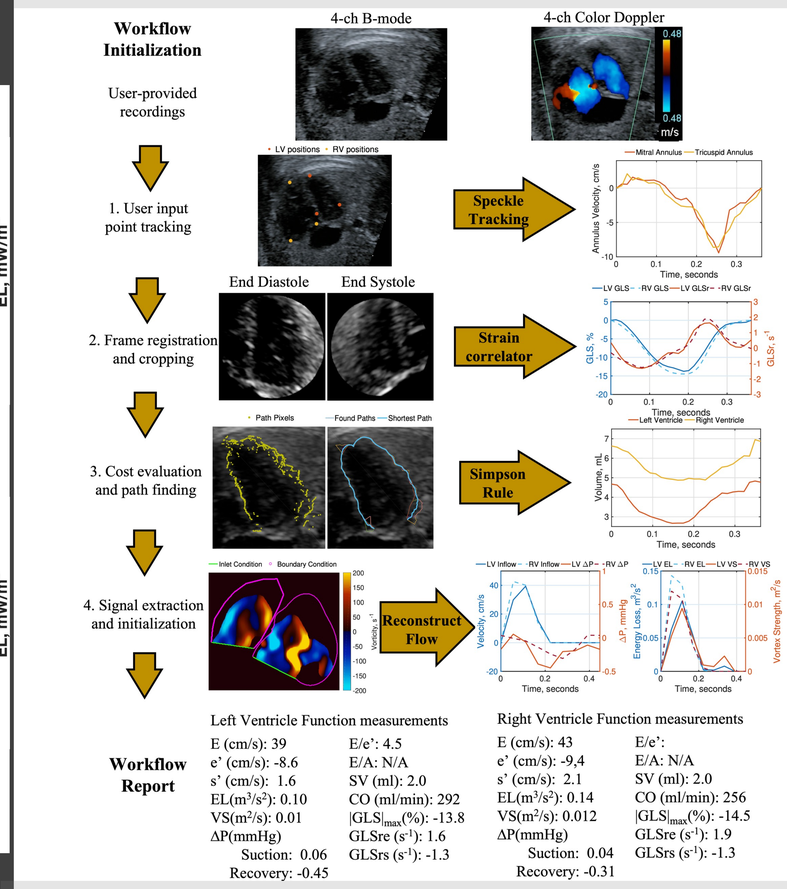

ONGOING COLLABORATIONS

INDIANA UNIVERSITY SCHOOL OF MEDICINE

- Quantifying hypoplastic left heart (HLHS) biomechanics
- Tracking longitudinal changes in heart function in sepsis

CHILDREN'S NATIONAL HOSPITAL

- Detecting heart function changes due to pulmonary insufficiency in repaired Tetralogy of Fallot (rTOF)

REFERENCES

[1]Center for Disease Control, National Center for Health Statistics

[2]Indiana Department of Health, Indiana Infant Mortality and Birth Outcomes, 2021. April 2023

[3]Quartermain, Michael D., et al. "Variation in prenatal diagnosis of congenital heart disease in infants." *Pediatrics* 136.2 (2015): e378-e385.

[4]Krishnan, Anita, et al. "Impact of socioeconomic status, race and ethnicity, and geography on prenatal detection of hypoplastic left heart syndrome and transposition of the great arteries." *Circulation* 143.21 (2021): 2049-2060

[5]Tillman, Alexandra R., et al. "Associations between socioeconomic context and congenital heart disease related outcomes in adolescents and adults." The American Journal of Cardiology 139 (2021): 105-115.

[6]Bucholz, Emily M., et al. "Socioeconomic status and long-term outcomes in single ventricle heart disease." Pediatrics 146.4 (2020).

[7]Meyers, Brett A., et al. "Colour-Doppler echocardiography flow field velocity reconstruction using a streamfunction–vorticity formulation." *Journal of the Royal Society Interface* 17.173 (2020): 20200741.

[8]Brindise, Melissa C., et al. "Automated Peak Prominence-Based Iterative Dijkstra's Algorithm for Segmentation of B-Mode Echocardiograms." *IEEE Transactions on Biomedical Engineering* 69.5 (2021): 1595-1607.

[9]Meyers, Brett A., et al. "A method for direct estimation of left ventricular global longitudinal strain rate from echocardiograms." *Scientific reports* 12.1 (2022): 1-11.

Novel Echocardiogram Analysis for Mortality Prediction in Pediatric Sepsis

Shailee Mitra[1], Brett Meyers[1], Daniel T Cater [2], Pavlos Vlachos[1]

[1]School of Mechanical Engineering, Purdue University, West Lafayette, IN, USA

[2] Department of Pediatrics, Indiana University School of Medicine, Division of Critical Care, Indianapolis, IN

BACKGROUND

❖ **Sepsis is a condition of inappropriate immune response to infection**. This is one of the leading causes of mortality and morbidity worldwide. In the United States, about **1.7 million** people get sepsis, and nearly **270,000** of them die from it.

OBJECTIVE: To determine if echocardiogram indices obtained using our algorithms are associated with mortality in pediatric sepsis.

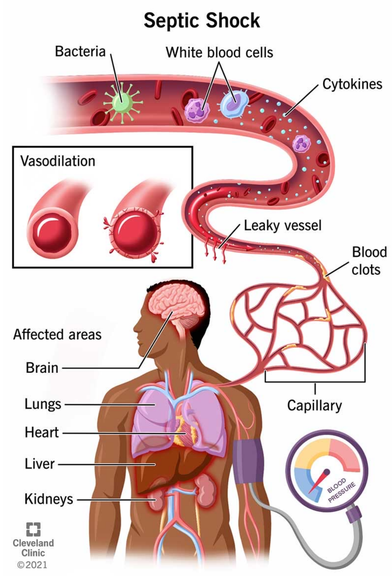

RESULTS: ECHOCARDIOGRAM INDICES OF LEFT AND RIGHT VENTRICLE

➢ Our cohort consists of **54** children (**45** recovered, **9** deceased) admitted to the pediatric intensive care unit (PICU). Our analysis include both left and right heart. Echocardiogram indices were compared in survivors versus non-survivors.

➢ Statistical analyses were performed using Kaplan Meier and Cox proportional hazard models.

Right Ventricle

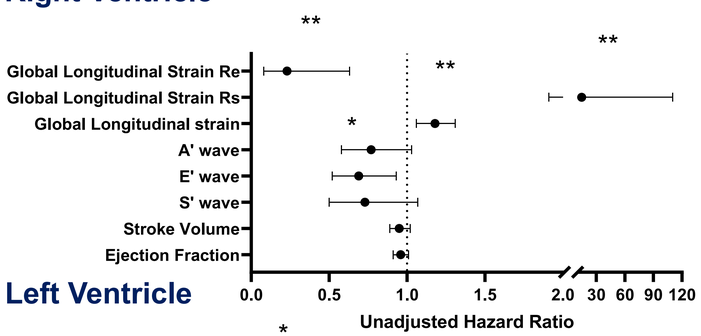

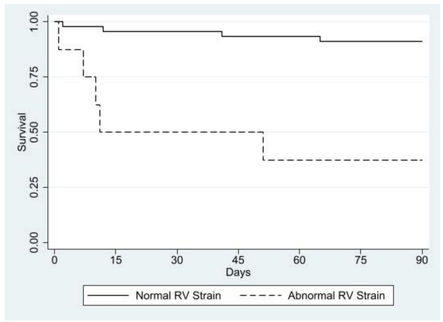

Left Ventricle

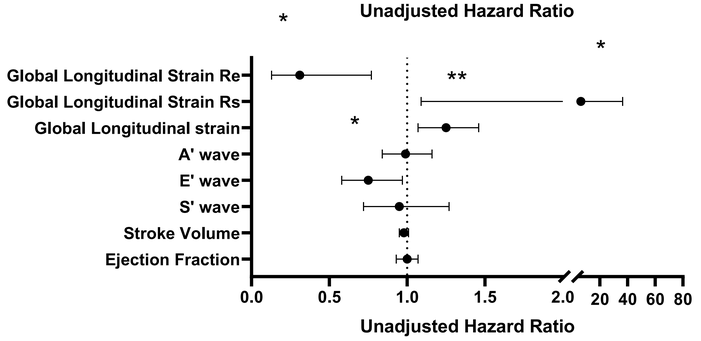

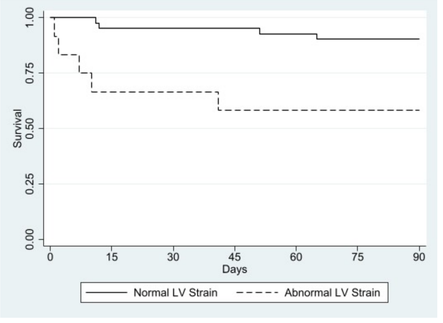

IN-HOUSE METHODOLOGY FOR QUANTIFYING BIOMARKERS

➢ We compute volume-based biomarkers using a semi-automated algorithm called **Prominence Iterative Dijkstra's (ProID).** This method creates a set of boundaries and quantifies the volumes based on boundary fit.

❑ Outputs: **Volume , Ejection Fraction .**

Our ProID method:

- **Requires only three user inputs**
- **Does not rely on any training**
- **This method applies to all age groups**

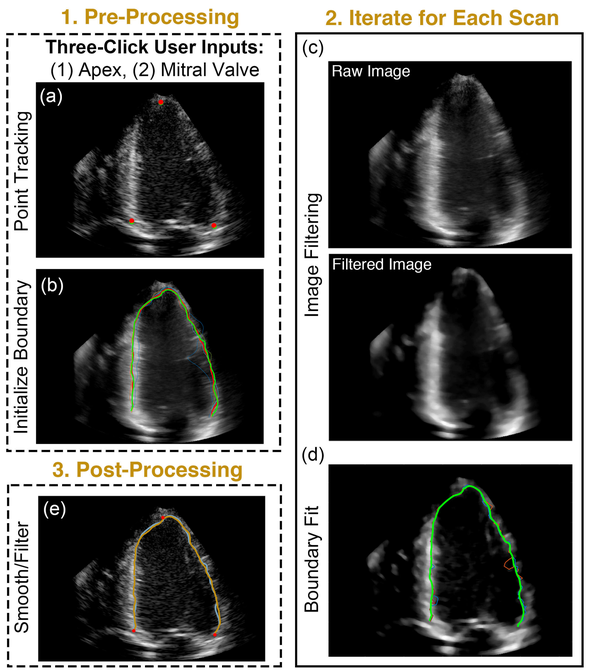

➢ **Direct Global Longitudinal Strain (GLS) method** estimates strain information from the full cardiac chamber image. A log scaled Fourier Magnitude Correlation quantifies scaling change of the heart chamber.

❑ Outputs **:Strain , Strain Rate**

Our Direct GLS method:

- **Removes almost all user variability**
- **Does not require additional smoothing, unlike commercial platforms**
- **Is vendor-agnostic**
- **Is inherently smooth and robust to noise**

(a) Point tracking **(b) Crop ROI & Align**

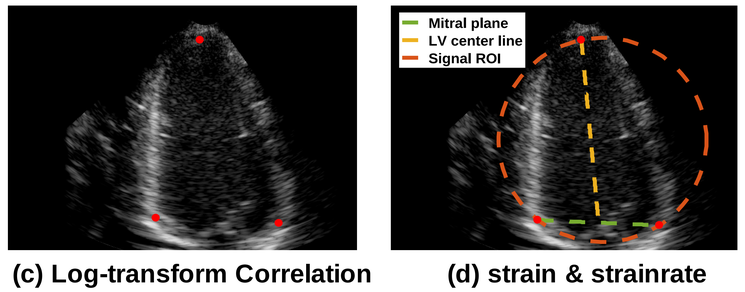

(c) Log-transform Correlation **(d) strain & strainrate**

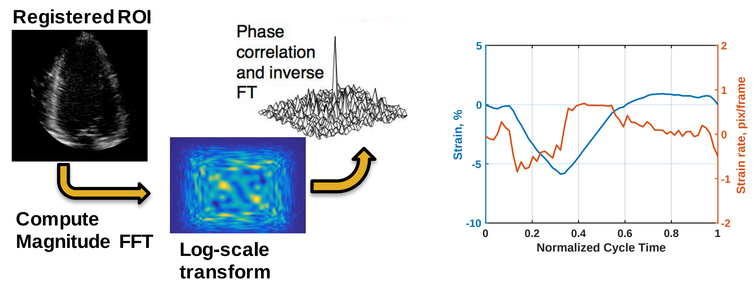

CONCLUSIONS

➢ Our novel algorithms show potential clinical utility in stratifying high-risk pediatric patients with sepsis .

➢ Abnormal strain biomarkers are associated with worse survival in pediatric patients with sepsis.

➢ The right ventricle showed a more robust association with mortality than the left ventricle.

FUTURE WORK

➢ Establish optimal determination of the echocardiogram biomarkers for normal versus sepsis subjects.

➢ Validate these findings in a larger cohort of patients.

REFERENCES

- https://my.clevelandclinic.org/-/scassets/images/org/health/articles/23255-septic-shock
- Brindise, M. C, Meyers, B. A, Kutty Shelby, & Vlachos, P. P Unsupervised Segmentation of B-mode Echocardiograms
- Brett A.Meyers , Melissa C. Brindise, Vivek Jani, Shelby Kutty, Pavlos P. Vlachos Direct estimation of global longitudinal strain from echocardiograms using a logarithm-scaled Fourier magnitude correlation

Prolyl Isomerase PIN1 Modulates Oncogene Induced Senescence by Regulating PML-Nuclear Body Dynamics

ARYAL LAB

Rodrigo Mohallem[1,2,*] & Uma K Aryal[1,2,#]

[1]Department of Comparative Pathobiology, Purdue University, USA; [2]Bindley Bioscience Center, Purdue University, USA.

Introduction & Abstract

Cellular senescence is induced by multiple factors

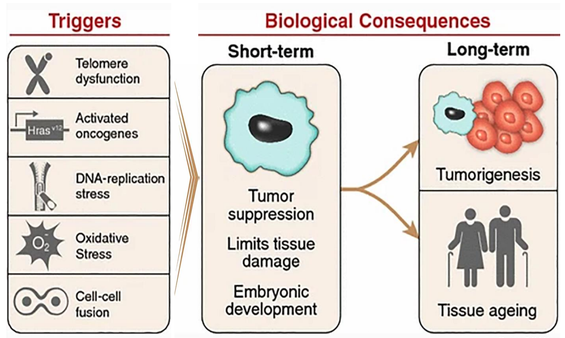

Somatic cells accumulate mutations during an organism's life span. Cells, however, have developed intrinsic mechanisms to prevent tumorigenesis in response to deleterious intrinsic and extrinsic factors, including telomere shortening, oxidative stress and proto-oncogene activation. Cellular senescence is a state of permanent cell cycle arrest, and it's the underlying cause of aging. When senescence is bypassed, cells begin to proliferate, and cancer ensues. This study reports changes in the nuclear proteomic and phosphoproteome of IMR90 human fibroblast cells during oncogene-induced senescence (OIS) by ER:RAS activation.

Our Work

Our analysis showed that one third of the quantified proteins were significantly regulated, several of which were hyperphosphorylated during OIS. Our results show that Pin1 is a key regulator of several PML-NB proteins, specifically regulating several proteins upon oncogene activation. We have found that the constitutive PML-NB protein SP100 is significantly downregulated when Pin1 is depleted. Reduced Sp100 protein levels have been correlated with cancer progression. Furthermore, we show that STAT3 is significantly upregulated in shPin1 during OIS, while senescence markers, such as p21, are significantly downregulated in response to Pin1 knock-down. Thus, our data provides preliminary evidence that PML-NB proteins are involved in regulating OIS via phosphorylation, and that the prolyl isomerase Pin1 acts as a tumor suppressor in response to oncogenic ras activation.

Experiment Workflow

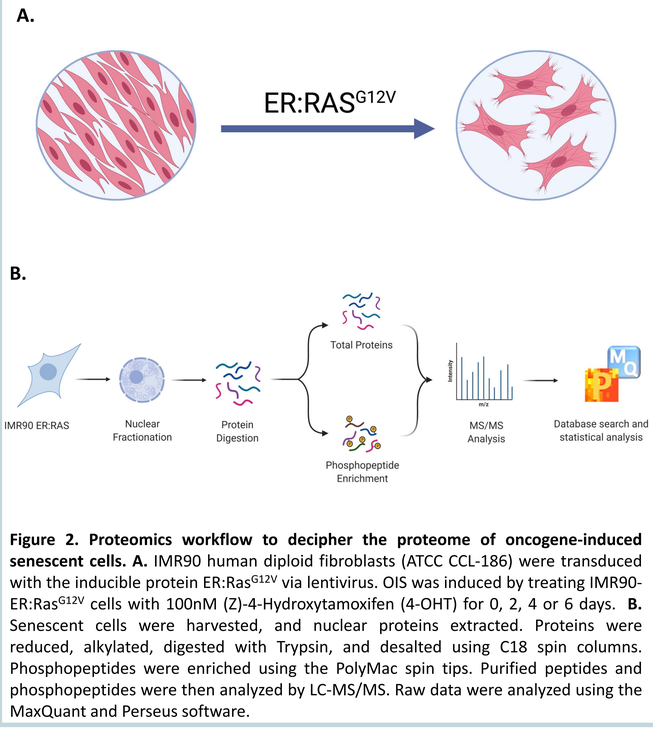

Figure 2. Proteomics workflow to decipher the proteome of oncogene-induced senescent cells. A. IMR90 human diploid fibroblasts (ATCC CCL-186) were transduced with the inducible protein ER:Ras^{G12V} via lentivirus. OIS was induced by treating IMR90-ER:Ras^{G12V} cells with 100nM (Z)-4-Hydroxytamoxifen (4-OHT) for 0, 2, 4 or 6 days. **B.** Senescent cells were harvested, and nuclear proteins extracted. Proteins were reduced, alkylated, digested with Trypsin, and desalted using C18 spin columns. Phosphopeptides were enriched using the PolyMac spin tips. Purified peptides and phosphopeptides were then analyzed by LC-MS/MS. Raw data were analyzed using the MaxQuant and Perseus software.

Results

OIS induces extensive phosphorylation of nuclear proteins, and regulates several signaling pathways

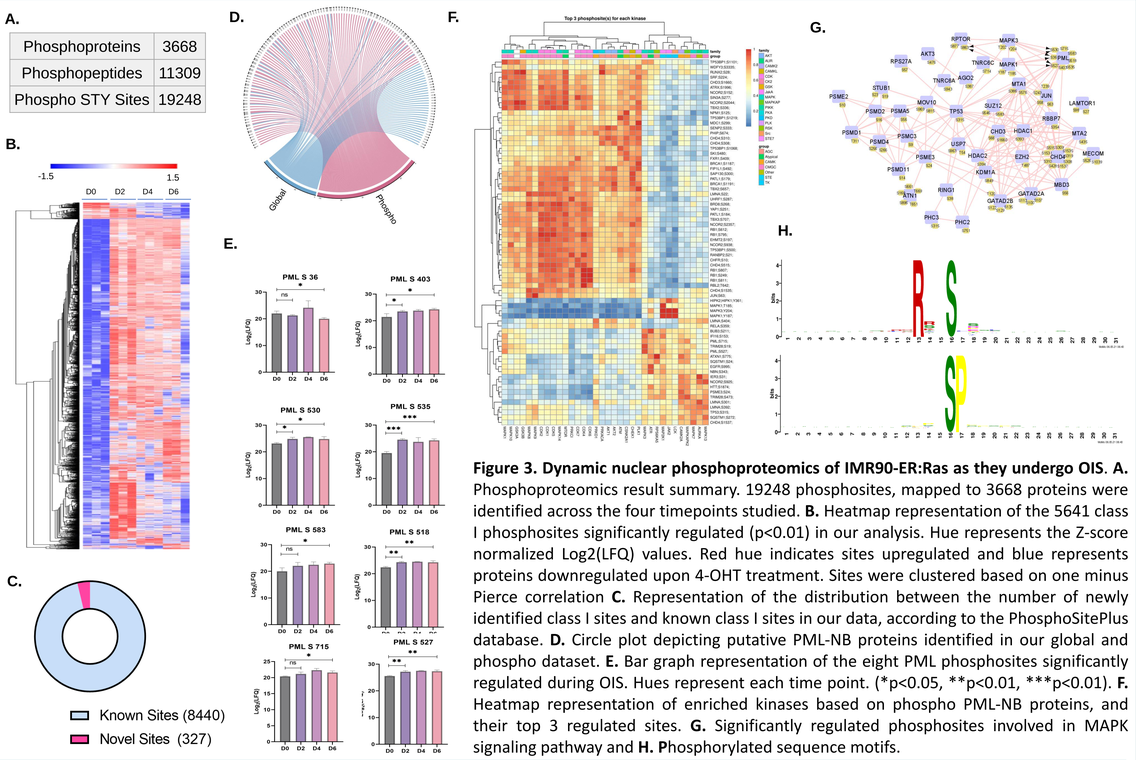

Figure 3. Dynamic nuclear phosphoproteomics of IMR90-ER:Ras as they undergo OIS. **A.** Phosphoproteomics result summary. 19248 phosphosites, mapped to 3668 proteins were identified across the four timepoints studied. **B.** Heatmap representation of the 5641 class I phosphosites significantly regulated ($p<0.01$) in our analysis. Hue represents the Z-score normalized Log2(LFQ) values. Red hue indicates sites upregulated and blue represents proteins downregulated upon 4-OHT treatment. Sites were clustered based on one minus Pierce correlation **C.** Representation of the distribution between the number of newly identified class I sites and known class I sites in our data, according to the PhosphoSitePlus database. **D.** Circle plot depicting putative PML-NB proteins identified in our global and phospho dataset. **E.** Bar graph representation of the eight PML phosphosites significantly regulated during OIS. Hues represent each time point. (*$p<0.05$, **$p<0.01$, ***$p<0.01$). **F.** Heatmap representation of enriched kinases based on phospho PML-NB proteins, and their top 3 regulated sites. **G.** Significantly regulated phosphosites involved in MAPK signaling pathway and **H.** Phosphorylated sequence motifs.

Pin1 knockdown induces cell proliferation and reduces the senescence phenotype

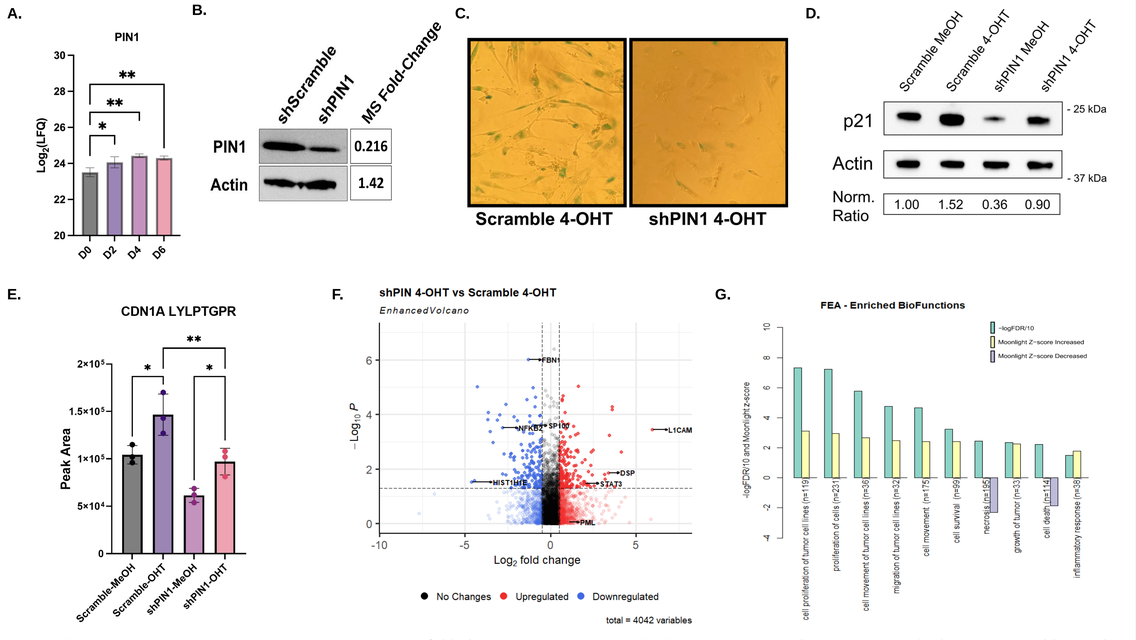

Figure 4. Pin1 acts as a tumor suppressor protein. **A.** Pin1 fold-change in response to 4-OHT treatment at each timepoint studied . **B.** Western blot analysis of Pin1 shRNA mediated knockdown, compared with the fold change calculated based of MS analysis. **C.** Senescence phenotype observed with SA-β-gal staining after 6 days of 4-OHT treatment. **D.** Western Blot analysis of p21 protein levels in response to 4-OHT treatment **E.** Bar graph representation of CDN1A Peak area measured by MRM. **F.** Volcano plot representations of protein levels in response to Pin1 knockdown at 6 days of 4-OHT treatment. **G.** Significantly regulated biofunctions predicted by the Moonlight R package.

Results

PIN1 regulates PML-NB formation during OIS

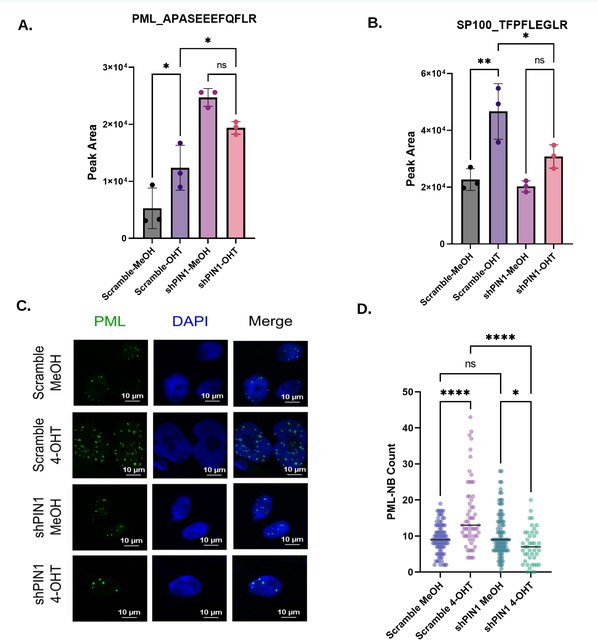

Figure 5. PML-NBs are regulated by Pin1. **A**. Pin1 regulates the levels of PML and **B.** SP100 during senescence. **C.** & **D.** PML nuclear body numbers are significantly decreased upon 4-OHT treatment in shPIN1 cells compared to the Scramble control. (*$p<0.05$, **$p<0.01$, ***$p<0.01$, ****$p<0.001$).

Conclusions & Future Directions

Concluding remarks

- Oncogenic Ras activation promotes reprograming of the cellular proteome and extensive phosphorylation events, and several protein are hyperphosphorylated, including PML
- PML-Nuclear Body proteins suffer extensive regulation during OIS. Phosphorylation of PML-NB proteins is likely necessary for their Ubiquitination and degradation, as 7 out of the 8 phosphosites identified in PML have been reported to promote its degradation
- PML-Nuclear proteins show site-specific regulations that are regulated by particular kinases during OIS, most of which are upregulated.
- Pin1 acts as a modulator of cellular senescence, and regulates the formation of PML-NBs during OIS.

Future work

- Specific roles of PML-NB in promoting OIS
- Identification of other PML PTMs

Acknowledgements

- All MS experiments were performed at the Purdue Proteomics Facility, in the Bindley Bioscience Center. This work was partially funded by Showalter Trust Fund.

Contact

*ferreir@purdue.edu; #uaryal@purdue.edu

Delayed working memory paradigm shows learning deficits in Fmr1 KO mice

Sanghamitra Nareddula[1], Violeta Saldarriaga[1], Paige A. Edens[2], Rachel Rudnicki [1,] Dr. Alexander A. Chubykin[1]

1. Department of Biological Sciences, Purdue University 2. Department of Biochemistry, Purdue University

Introduction

Autism spectrum disorder (ASD) is a neurodevelopmental disorder that widely affects information processing in the brain resulting in deficits in learning and memory. One of the most prevalent forms of ASD is Fragile X syndrome (FX). Previous studies have shown alterations in cell morphology, synaptic connections, and neural circuits pertaining to sensory perception in FX model systems. Consistent with this, our lab has identified significant differences in the visual response of FX mice to a passive visual perceptual experience paradigm. We hypothesized this affected visual working memory. We tested this hypothesis by developing a new working memory paradigm in mice based on a delayed visual discrimination task and discovered learning disabilities in Fmr1 KO mice.

Methods

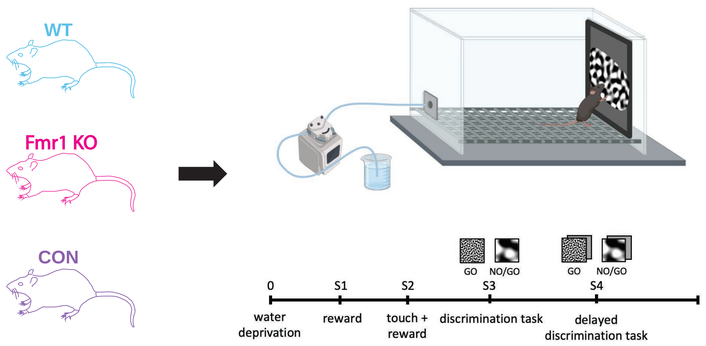

Fig1. Experimental setup showing freely moving behavior. Mice were subjected to an operant conditioning paradigm where they learnt to discriminate between two different stimuli. Following the discrimination stage, we subjected the mice to a unique delayed working memory task wherein they were required to decide whether or not to touch a grey screen shown after the Go or No-Go stimulus.

Results

Decreased performance in a visual discrimination task in FX

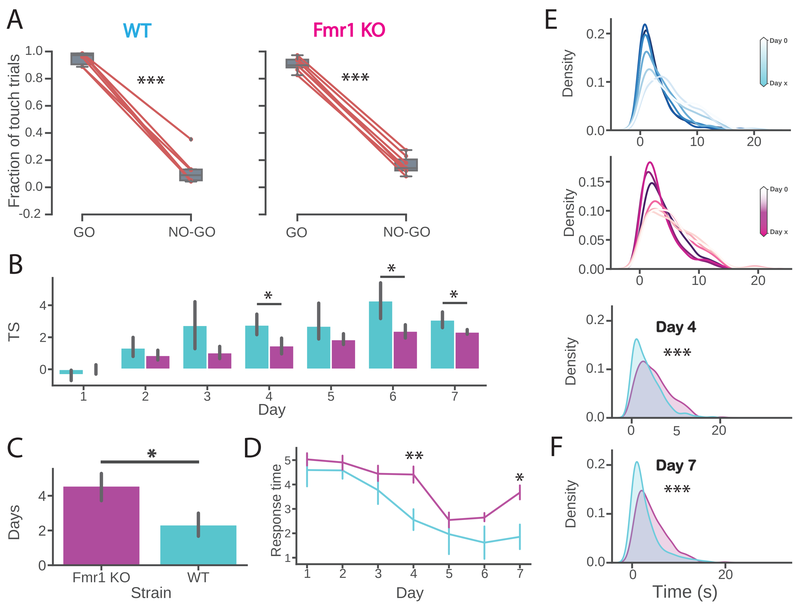

Fig2. A)Fraction of touch trials for the Go and No-Go stimulus on the final day of training B) Training scores (TS=(z(FA)-z(HR)) across days for WT and Fmr1 KO mice. C) Number of days taken to reach a training score of 2. D) Response time quantifying median time to first touch after stimulus is shown. E) Cumulative density plots showing first touch times for the Go stimulus across days of training in WT (Top) and Fmr1 KO (Bottom) mice. F) Cumulative density plot showing first touch times for the Go stimulus for day 4 and day 7 for WT and Fmr1 KO mice. (*p<0.05, **p<0.01, ***p<0.001).

Learning deficits in FX are increased in a delayed working memory task

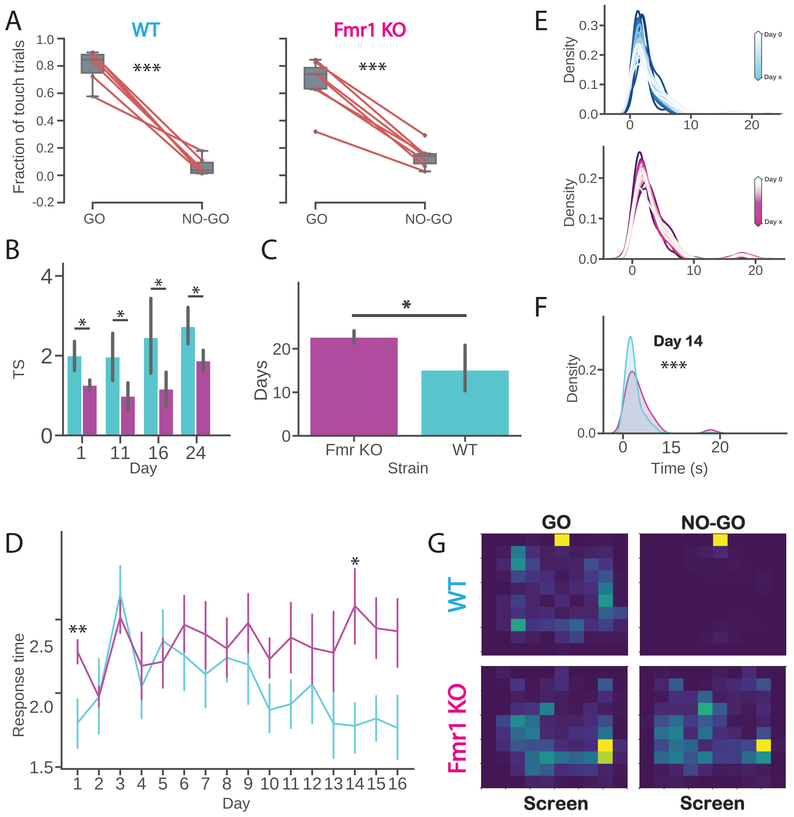

Fig3. A)Fraction of touch trials for the Go and No-Go stimulus on the final day of training. B) Training scores across days for different periods of training. C) Number of days taken to reach a training score of 2. D) Response time quantifying median time to first touch after stimulus is shown. E) Cumulative density plots showing first touch times for the Go stimulus across days of training in WT (Top) and Fmr1 KO (Bottom) mice. F) Cumulative density plot showing first touch times for the Go stimulus for day 14 for WT and Fmr1 KO mice. G) Representative heatmaps showing mice movement trajectories for the Go stimulus (Top) and for the No-Go stimulus (bottom). (*p<0.05, **p<0.01, ***p<0.001).

Conditional Expression of FMRP in V1 PV+ interneurons

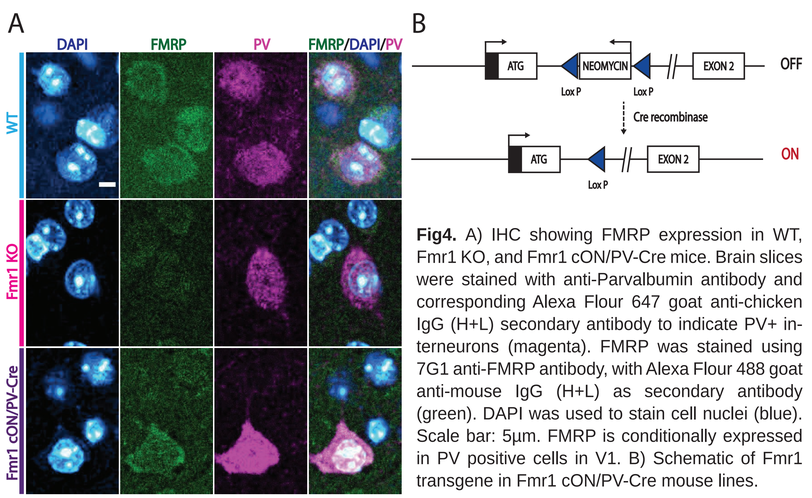

Fig4. A) IHC showing FMRP expression in WT, Fmr1 KO, and Fmr1 cON/PV-Cre mice. Brain slices were stained with anti-Parvalbumin antibody and corresponding Alexa Flour 647 goat anti-chicken IgG (H+L) secondary antibody to indicate PV+ interneurons (magenta). FMRP was stained using 7G1 anti-FMRP antibody, with Alexa Flour 488 goat anti-mouse IgG (H+L) as secondary antibody (green). DAPI was used to stain cell nuclei (blue). Scale bar: 5μm. FMRP is conditionally expressed in PV positive cells in V1. B) Schematic of Fmr1 transgene in Fmr1 cON/PV-Cre mouse lines.

Fmr1cON/PV-Cre shows improvements in learning

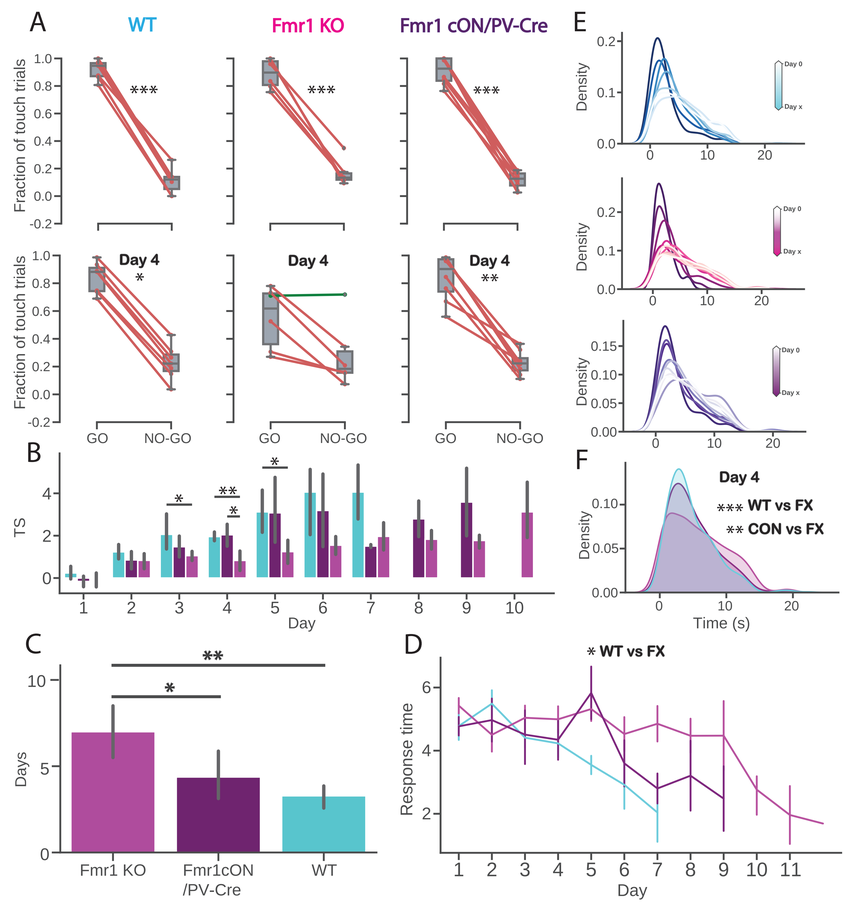

Figure 5. A)Fraction of touch trials for the Go and No-Go stimulus on the final day of training (Top) and day 4 of training (Bottom). B) Training scores across days for the different strains C) Number of days taken to reach a training score of 2. D) Response time quantifying median time to first touch after stimulus is shown. E) Cumulative density plots showing first touch times for the Go stimulus across days of training (Top: WT; Middle: Fmr1 KO; Bottom: Fmr1cON/PV-Cre). F) Cumulative density plot showing first touch times for the Go stimulus for day 4 for WT, Fmr1 KO, and Fmr1cON/PV-Cre mice. (*p<0.05, **p<0.01, ***p<0.001).

Discussion

Using an operant conditioning paradigm we were able to characterize behavioral differences across three different strains - WT, Fmr1 KO and our rescue strain, Fmr1cON/PV-Cre. We found that across the multiple behavior paradigms, both WT and Fmr1 KO mice were able to show proper discrimination of the visual stimuli. However, we found that the Fmr1 KO mice consistently required more training days and reached lower overall training scores compared to the WT. Additionally, using DeepLabCut software we discovered that Fmr1 KO mice demonstrated distinct movement patterns consistent with impaired memory during freely moving behavior. Our findings highlight the efficacy of this novel method for studying working memory in mice. By employing this approach, we can gain deeper insights into the specific impairments associated with Fmr1 KO mice, shedding light on the underlying mechanisms and potential therapeutic targets for addressing working memory deficits in this neurodevelopmental disorder. Further, our conditional rescue strain shows significant improvements in performance at the discrimination stage. Fmr1cON/PV-Cre mice were able to reach a TS value of 2 in lesser number of days compared to Fmr1 KO mice and similar to WT mice. They also showed similar response times to WT mice, quicker to react than Fmr1 KO mice. This shows that PV interneurons do indeed play an important role in the network responsible for visual working memory and rescuing FMRP in PV interneurons translates into behavioral phenotypes as well.

National Institute of Mental Health

Age-dependent changes in mouse brain and liver lipidomes

Punyatoya Panda[1], Christina R. Ferreira[2], Allison Schaser[3], Uma K. Aryal[1,2]

[1]Department of Comparative Pathobiology, Purdue University, West Lafayette, IN 47907, USA. [2]Bindley Bioscience Center, Purdue University, West Lafayette, IN 47907, USA.
[3]Department of Speech, Language, and Hearing Sciences, Purdue University

PURDUE UNIVERSITY College of Veterinary Medicine

ARYAL LAB

INTRODUCTION

Like genes and proteins, lipids play key structural, regulatory, and signaling roles. Thus, profiling lipids in different organs provides useful information for understanding the complex biological processes under various physiological or disease states. However, very little is known about the composition and age-dependent changes of lipids in the brain and liver, two most lipid-rich organs after adipose tissues. In this study, we performed exploratory lipidomic analysis of mice brain and liver at different ages via Multiple Reaction Monitoring Mass Spectrometry (MRM-MS) to determine changes in different classes of lipids and correlate the differences in lipid profiles with the age groups. The MRM-MS analysis was performed using ion transitions based on precursor (Prec) and neutral loss (NL) scans obtained from LIPID MAPS database for screening each sample independently for 24 different classes of lipids including different phospholipid classes such as phosphatidylcholines (PCs), phosphatidylethanolamines (PEs), ceramides, di- and tri-acylglycerols, and acylcarnitine.

EXPERIMENTAL WORKFLOW

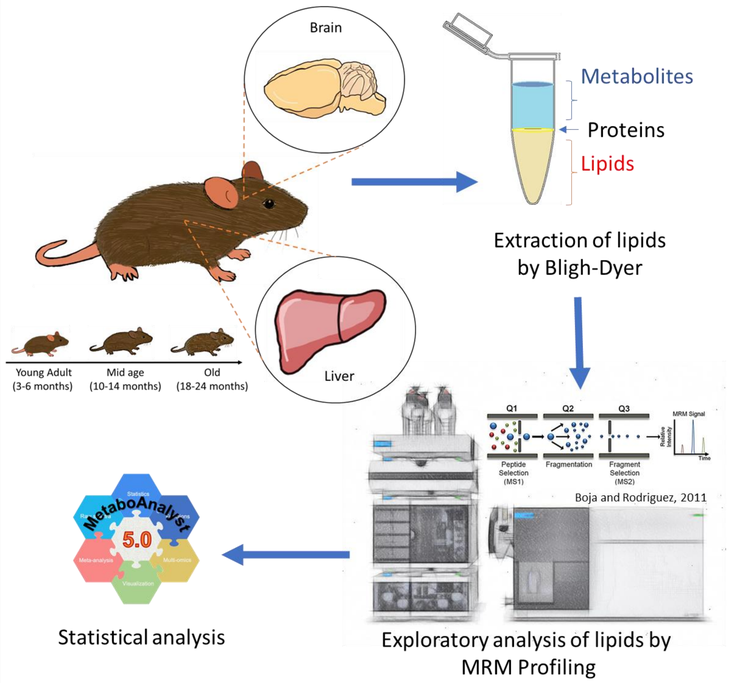

Figure 1: Experimental workflow. Mice from three different age groups were sacrificed. Their brain and liver were collected and homogenized, and the lipidome was extracted by Bligh-Dyer method. These were subjected to MRM spectroscopy, and statistical analysis and interpretation was done by Metaboanalyst.

RESULTS

SCREENING OF LIPIDS BY CLASS IN BRAIN AND LIVER

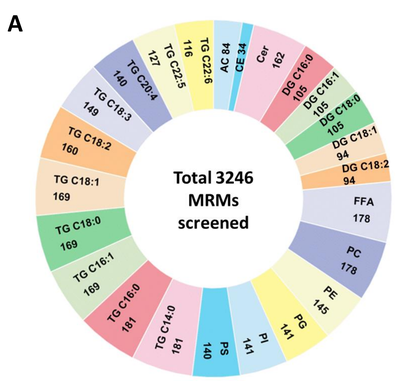

Abbreviation	Lipid
PC	Phosphatidylcholine
PE	Phosphatidylethanolamine
PG	Phosphatidylglycerol
PI	Phosphatidylinositol
PS	Phosphatidylserine
AC	Acylcarnitine
CE	Choline Esters
Cer	Ceramides
FFA	Free fatty acids
DG	Diacylglycerols
TG	Triacylglycerols

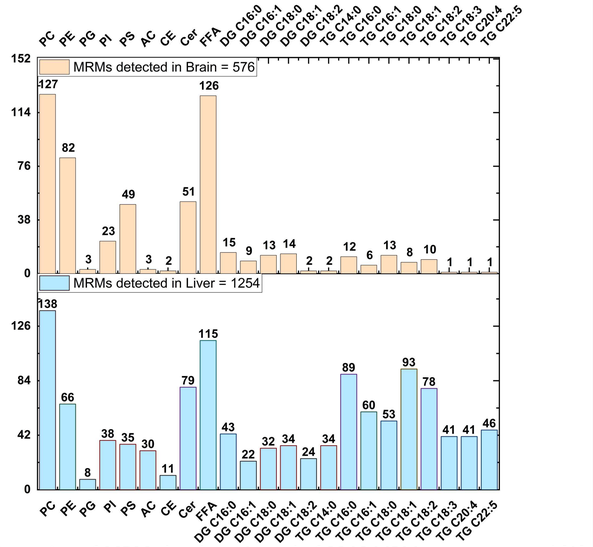

Figure 2: A. Screening of MRMs by class. A total of 3246 MRMs were screened [A] that included 24 classes of lipids. **B.** Distribution and coverage of MRMs across Brain and Liver. 576 were detected in the brain and 1254 were detected in the liver [B].

AGE INDUCED BRAIN AND LIVER PERTUBATIONS AND THEIR LIPIDOMIC COMPOSITION

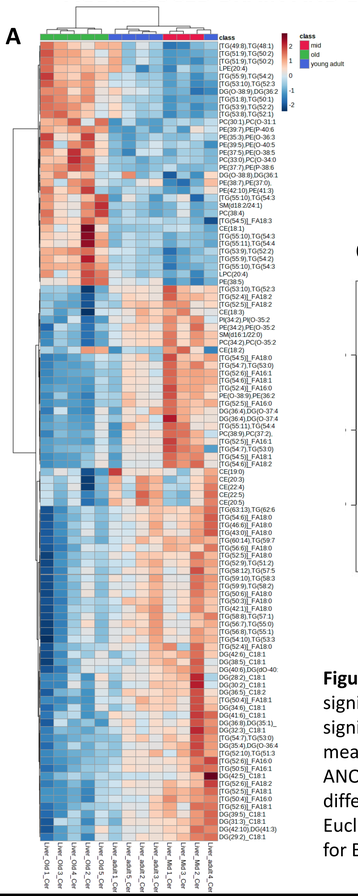

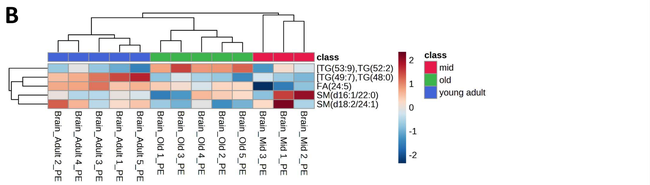

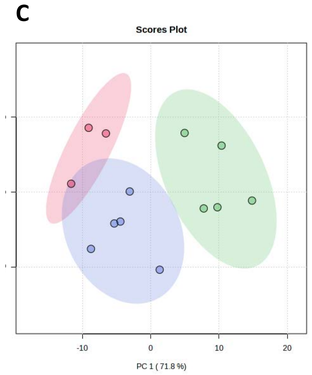

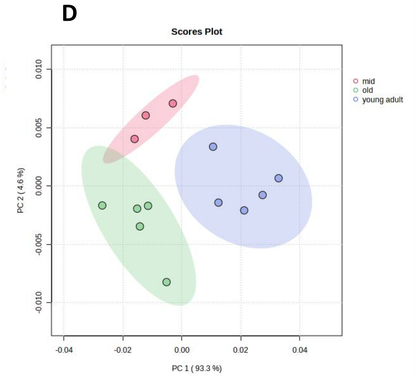

Figure 3: Changes of the brain and liver lipidome with age. A. Heatmap of ANOVA-significant Liver MRMs. ANOVA was performed with Tukey's HSD test. 105 ANOVA significant MRMs from different classes were plotted by Euclidean distance measurement and Ward clustering. **B**. Heatmap of ANOVA-significant Brain MRMs. ANOVA was performed with Tukey's HSD test and five ANOVA significant MRMs from different classes were plotted by average clustering and distance was measured by Euclidean method. **C,D**. PCA Plot. Principal Component Analysis of the significant MRMs for Brain [C] and Liver [D].

RESULTS

TOP LIPIDS CHANGING WITH AGE IN BRAIN AND LIVER

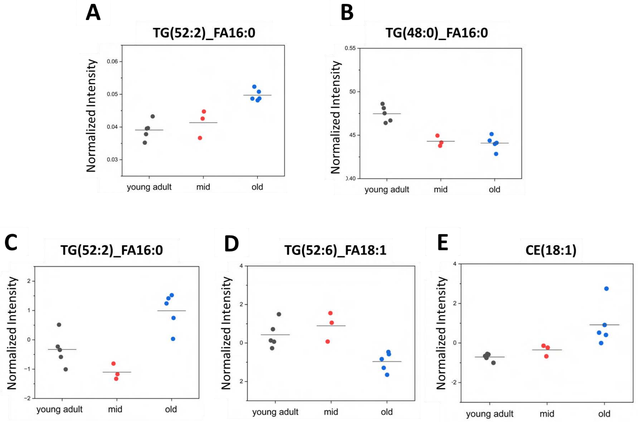

Figure 4:. Examples of lipids changing in the brain and liver. Scatter plots display top lipid MRMs that show increasing and decreasing pattern with age in the brain [**A,B**] and liver [**C,D,E**]. A and C depict how the same lipid is changing with age in both brain and liver.

SUMMARY

- We screened for a total of 3246 MRMs covering 24 lipid classes for both the liver and the brain.
- Of 576 MRMs detected in the brain, we found five significant lipid MRMs that varied across the different age groups.
- Of 1254 MRMs detected in the liver, we found 105 significant lipid MRMs that varied across the age groups.
- Liver is a metabolically a very active organ and is the site of oxidation of triacylglycerols (TG) for energy production. Our data suggests that the energy homeostasis is disrupted with age, as most of the TGs and DGs are changing in aging mice.
- Aging mice brain showed changing lipid profiles of free fatty acids, ceramides and phospholipids.
- Triacylglycerols, that lead to impairment of cognitive function are upregulated with age in brain.
- Increased ceramide concentrations have been reported in neurodegenerative diseases, which is also implicated by our results.

FUTURE DIRECTIONS

- Validation of MRM-MS data with targeted LC-MS/MS analysis using available lipid standards.
- Perform spatial lipidomics to profile brain-region resolved mouse brain lipidome.
- Perform brain-region resolved lipidome profiling using senescence and Alzheimer's disease mice models.
- Correlate lipidome data with the proteome and phosphoproteome data for mapping specific cellular pathways impacted by aging or age-related diseases.

ACKNOWLEDGEMENTS

This study was supported in part by Bindley Fellow program sponsored by the Bindley Bioscience Center to Uma K. Aryal. All the data were collected at the Metabolite Profiling Facility of Bindley Bioscience Center.
For more information, contact: uaryal@purdue.edu (Uma K. Aryal)

The Impact of Neochords Surgery on Hemodynamic Parameters in Mitigating Mitral Valve Regurgitation

Deerajkumar Parthipan[1], Brett Meyers[1], Pavlos Vlachos[1], Yannis Dimitroglou[2], Constantina Aggeli[3]
[1]School of Mechanical Engineering, Purdue University, West Lafayette, IN, USA
[2]Department of Cardiology, Onassis Cardiac Surgery Centre, 17674 Kallithea, Attica, Greece
[3]First Department of Cardiology, General Hospital of Athens Hippokration, University of Athens Medical School, 11527 Athens, Attica, Greece

BACKGROUND

2% of the U.S. population has primary MR.

- Mitral regurgitation (MR) leads to increased heart workload, left ventricle enlargement, pulmonary hypertension, atrial fibrillation, heart failure, reduced oxygenation, and risk of endocarditis.
- 1 out of 5 heart failure (HF) patients has moderate to severe or severe secondary MR

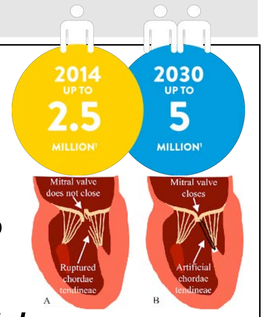

NeoChords is a device for MV repair, adding new chordae tendineae to help close the MV during systole.

Hypothesis:

- The hemodynamic parameters such as the Energy Loss, Kinetic Energy and Pressure within the heart are anticipated to have significant alterations following the Neochords surgery.
- Evaluate the effectiveness of Neochords surgery by measuring changes in intraoperative flow patterns.

METHOD

An in-house developed algorithm (DoVer) was used to reconstruct flow in the Left ventricle [1].

- The velocities are reconstructed using the vorticity-streamfunction relationship
- For the BC's the boundaries are segmented using an in-house developed peak - prominence based method

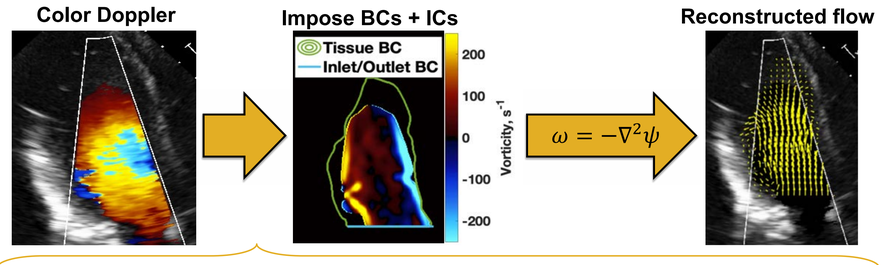

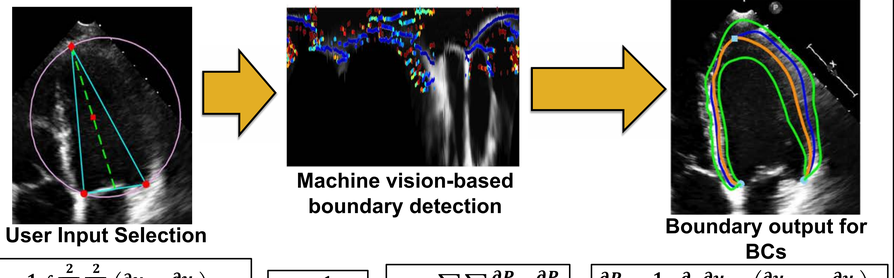

$$EL = \frac{1}{2}\int \sum_{i=1}^{2}\sum_{j=1}^{2}\left(\frac{\partial u_i}{\partial x_j} + \frac{\partial u_j}{\partial x_i}\right) dV \qquad KE = \frac{1}{2}v^2 \qquad \Delta P = \sum\sum \frac{\partial P}{\partial x} + \frac{\partial P}{\partial y} \qquad \frac{\partial P}{\partial x_i} = \frac{1}{Re}\frac{\partial}{\partial x_j}\frac{\partial u_i}{\partial x_j} - \left(\frac{\partial u_i}{\partial t} + u_j\frac{\partial u_i}{\partial x_j}\right)$$

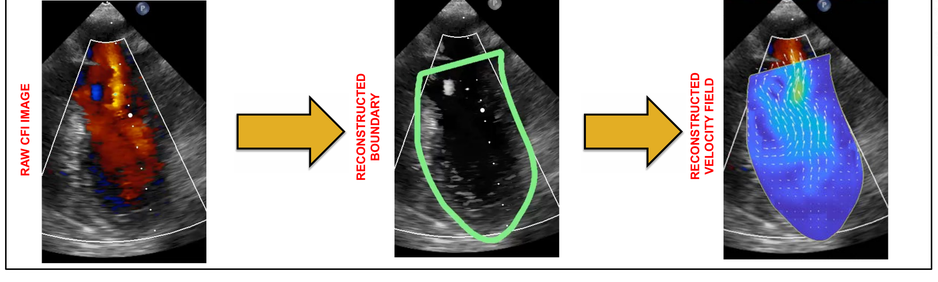

RESULTS

Hemodynamic parameters were evaluated in the left ventricle in a regurgitant heart and are compared pre and post surgery

- Cohort consisted of Echo images for 12 patients.

The peak systolic hemodynamic parameters were observed to be elevated in a regurgitant heart and lowered in a repaired heart post surgery.

Patient 1 – Hemodynamic Parameters are Elevated Post Surgery

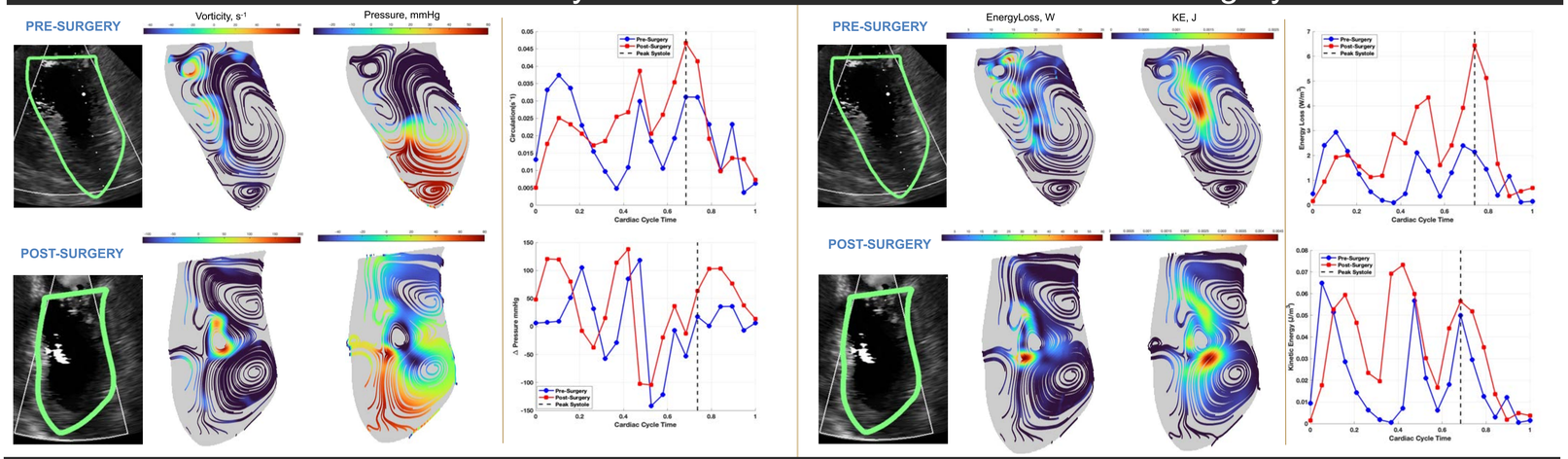

Patient 2 – Hemodynamic Parameters are Lowered Post Surgery

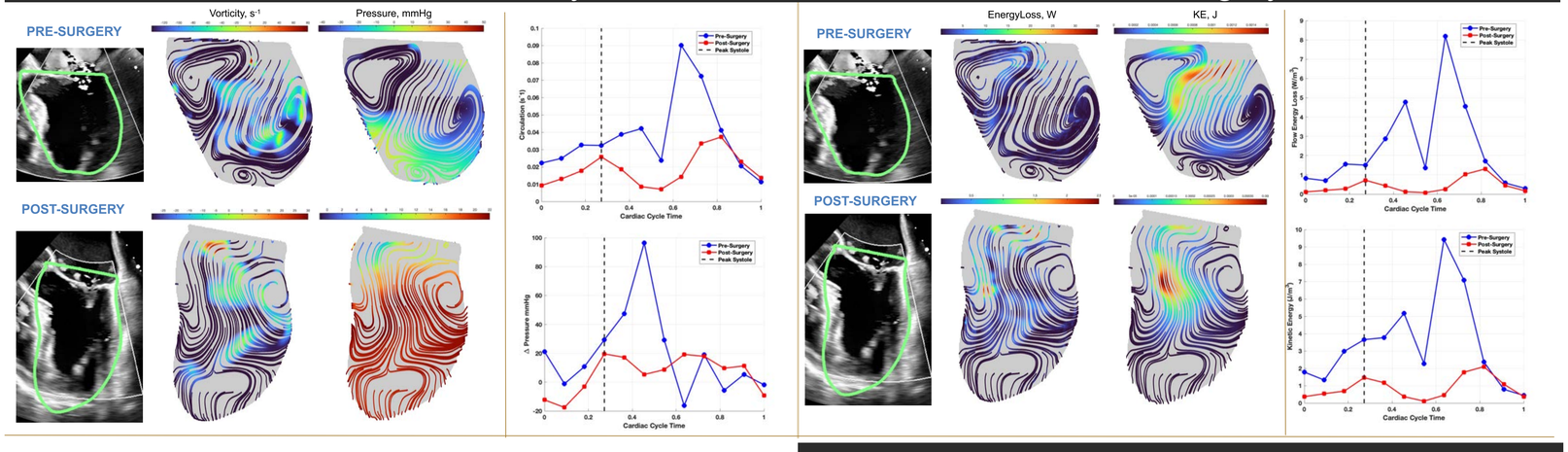

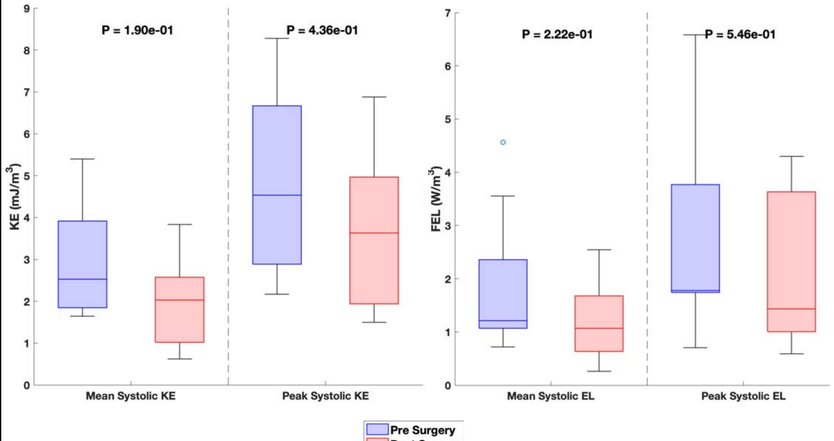

Altered Hydrodynamics were observed Pre and post corrective MV surgery.

The hemodynamic parameters can potentially be used as a marker of the *regurgitant severity.*

REFERENCES

[1] Meyers, Brett A., et al. "Colour-Doppler echocardiography flow field velocity reconstruction using a streamfunction–vorticity formulation." Journal of the Royal Society Interface 17.173 (2020): 20200741.
[2] Brindise, Melissa C., et al. "Automated Peak Prominence-Based Iterative Dijkstra's Algorithm for Segmentation of B-Mode Echocardiograms." IEEE Transactions on Biomedical Engineering 69.5 (2021): 1595-1607.
[3] Akins, C. W., Travis, B., & Yoganathan, A. P. (2008). Energy loss for evaluating heart valve performance. Journal of Thoracic and Cardiovascular Surgery, 136(4), 820–833.
[4] Zoghbi, W. A., et al. (2003). Recommendations for Evaluation of the Severity of Native Valvular Regurgitation with Two-dimensional and Doppler Echocardiography. Journal of the American Society of Echocardiography, 16(7), 777–802.

Investigating Gender-Based and Race-Based Inequalities in Death Causes

This project uses systematic statistical analysis to uncover evidence of inequalities in how various groups of people in the US are affected by various causes of death and investigate specific patterns to indicate especially vulnerable populations.

Abstract

There are many factors that are linked to how different parts of our national population are affected by mortality causes, many of which show disparities linked to gender and race. Exposing potential links and trends could help to provide targets for where underlying factors that lead to these inequalities are in order to assist in addressing them and improving overall health equity. Here, we have analyzed data from the CDC Wonder database and have utilized statistical analysis and visualization (such as with Chi-Square) in order to analyze trends in how various factors affect mortality due to specific popular causes of interest (including firearm related deaths, homicides, cancer, respiratory viruses, et cetera) and have focused on how these change with age. Interestingly, we find a number of causes that show racial impacts that change with age, such as deaths due to narcotics.

Detailed Methodology

First, the CDC Wonder database was used to gather data regarding deaths in the US from 2000 to 2020. From this, data was visualized using JavaScript Observable plots. After this, using Google Colab, data was analyzed by sorting into groups by year/age/gender/race. In addition, ICD-10 113 codes were organized by looking at causes of death of high interest, and were matched with data organization within the database. Then, Chi-Square independence tests were used to determine the scale of the effect of gender/race on numbers of deaths in various groups (with respect to the total populations of each group), providing a statistical measure of levels of disparity in this group. This data was then analyzed to find trends in disparity over age groups, time, and more in order to highlight where disparities are greatest.

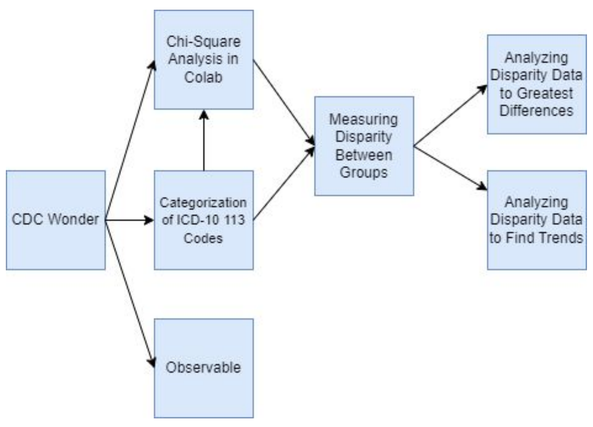

Changes in Differences by Race for Different Ages

One key finding made is as age groups vary, differences in how certain hazards affects different groups also can change. For example, in comparing African American narcotics-related deaths to those of White people, although younger White people have higher deaths rates relating to narcotics (as a proportion of the total population), later in life, more and more older African Americans die in deaths related to narcotics, which is almost a complete reversal in the trend. In addition, with causes like diabetes, disparities are almost inevident in comparison in younger age (in the teens and 20s) compared to later in life, with disparities only growing as the compared groups grow older.

Additional Details:

1. Although there are exhibited inequities in deaths between children, disparities are generally much more evident within adults, although the specific part of adulthood in which these disparities appear to be the strongest can vary.
2. In addition, natural causes seem to show the most disparities between races in older age, while other causes like causes like homicides are either more widely distributed or especially inequitable in younger populations.

Changes in Differences by Race for Different Genders

Another key finding is that gender-based disparities in affliction by certain death causes is also correlated to race. Across different racial groups, differences in how certain causes of death affect males and females can be greater or lesser depending on the group. In other words, there could be a suggested correlation/link between race and gender disparities. For example, throughout the 30-39 age range, there is no significant difference ($p < 0.05$) between male and female death rates related to firearms within the Asian/Pacific Islander population, while roughly 4 times as many men dying than women in the White population.

Works Referenced

CDC. (1997). CDC wonder. [Atlanta, Ga.] :CDC

ICD Coding: 113 Causes of Death. OK Share (n.d.) https://www.health.state.ok.us/stats/Vital_Statistics/Death/113_causes.shtml

Acknowledgement and Contacts

- Om Patel: pate1843@purdue.edu
- Prof. David Gleich: dgleich@purdue.edu

	3-7	8-12	13-17	18-22	23-27	28-32	33-37	38-42	43-47	48-52	53-57	58-62	63-67	68-72	73-77	78-82
Narcotics	37	17	-147	-1251	-1542	-830	-223	45	896	3870	9198	9241	8739	5557	1042	87
Falls	12	0	-20	-123	-88	-54	-16	-11	-5	0	64	6	-16	-53	-211	-752
Homicides	821	622	21986	97587	95117	67833	42162	27044	17673	12305	9684	4265	1553	1316	750	317
Drownings	210	863	889	291	84	88	44	20	1	11	47	7	5	5	1	10
Vehicles	210	47	-354	-378	93	505	413	217	246	426	423	172	147	32	-43	-12
Guns	246	3	91	270	219	149	28	0	0	0	-5	-4	-14	-2	0	0
Suicides	4	86	-623	-568	-573	-879	-1860	-2680	-3906	-4224	-3925	-3263	-2126	-1172	-959	-427
HIV	101	230	539	2915	10585	19067	28934	40127	49030	50884	47071	31963	18550	11174	4618	2540
Alzheimer's	0	0	0	1	0	2	0	0	-3	-16	-80	-48	-45	26	22	-6
Diabetes	2	51	200	360	1330	2115	2692	4017	5844	9531	17780	17703	16742	20090	20067	17744
Maternal	0	2	59	638	1185	1109	1141	1019	282	206	35	0	0	3	3	4
Cancer	0	-3	1	22	153	472	1018	3250	5867	13121	27816	23011	13420	13582	8625	6703
Heart	152	269	716	2391	4185	7798	11321	18988	26683	42047	68302	62824	49926	50299	28551	25736
R. Infection	64	19	62	117	203	350	502	548	575	560	598	3	-772	-2134	-4556	-6108
R. Disease	18	9	1	42	98	199	320	533	904	1590	1658	2420	3552	1794	2852	1
Other	1944	1343	1129	854	2381	4297	7960	15800	29279	52448	95710	74749	85895	72123	24359	57899

	3-7	8-12	13-17	18-22	23-27	28-32	33-37	38-42	43-47	48-52	53-57	58-62	63-67	68-72	73-77	78-82
Narcotics	37	17	-147	-1251	-1542	-830	-223	45	896	3870	9198	9241	8739	5557	1042	87
Falls	12	0	-20	-123	-88	-54	-16	-11	-5	0	64	6	-16	-53	-211	-752
Homicides	821	622	21986	97587	95117	67833	42162	27044	17673	12305	9684	4265	1553	1316	750	317
Drownings	210	863	889	291	84	88	44	20	1	11	47	7	5	5	1	10
Vehicles	210	47	-354	-378	93	505	413	217	246	426	423	172	147	32	-43	-12
Guns	246	3	91	270	219	149	28	0	0	0	-5	-4	-14	-2	0	0
Suicides	4	86	-623	-568	-573	-879	-1860	-2680	-3906	-4224	-3925	-3263	-2126	-1172	-959	-427
HIV	101	230	539	2915	10585	19067	28934	40127	49030	50884	47071	31963	18550	11174	4618	2540
Alzheimer's	0	0	0	1	0	2	0	0	-3	-16	-80	-48	-45	26	22	-6
Diabetes	2	51	200	360	1330	2115	2692	4017	5844	9531	17780	17703	16742	20090	20067	17744
Maternal	0	2	59	638	1185	1109	1141	1019	282	206	35	0	0	3	3	4
Cancer	0	-3	1	22	153	472	1018	3250	5867	13121	27816	23011	13420	13582	8625	6703
Heart	152	269	716	2391	4185	7798	11321	18988	26683	42047	68302	62824	49926	50299	28551	25736
R. Infection	64	19	62	117	203	350	502	548	575	560	598	3	-772	-2134	-4556	-6108
R. Disease	18	9	1	42	98	199	320	533	904	1590	1658	2420	3552	1794	2852	1
Other	1944	1343	1129	854	2381	4297	7960	15800	29279	52448	95710	74749	85895	72123	24359	57899

	3-7	8-12	13-17	18-22	23-27	28-32	33-37	38-42	43-47	48-52	53-57	58-62	63-67	63-67	73-77	78-82
Narcotics	2	0	383	4652	9250	10215	9329	7905	6736	5476	3944	2549	1325	319	43	6
Falls	20	25	164	1031	1194	1287	1393	1771	2438	2823	3085	2955	2921	2747	3413	4823
Homicides	3	10	2063	8665	7153	4862	3531	2482	1898	1596	1140	666	322	189	74	13
Drownings	569	87	1189	2588	1804	1288	1165	1274	1277	1194	1123	1016	847	790	726	650
Vehicles	105	219	1611	17118	18089	13023	10575	10411	10965	11911	11237	9468	6730	4651	4281	4384
Guns	76	126	516	800	571	297	294	309	348	342	402	315	300	205	272	223
Suicides	1	224	3909	19528	21575	18512	18171	18363	18517	19228	19600	18535	15419	16631	20610	22464
HIV	0	-1	-6	22	295	971	2868	5004	6757	6594	5522	3674	2437	1594	943	588
Alzheimer's	0	0	0	0	0	0	0	2	0	-9	-52	-83	-46	-154	-123	-320
Diabetes	0	0	1	43	85	130	392	977	2059	3763	5610	7129	8019	8727	9794	9895
Maternal	0	0	0	0	0	0	0	0	0	0	0	0	0	0	0	0
Cancer	40	42	115	602	263	-15	-814	-1612	-918	93	5178	19779	39424	64737	109666	164243
Heart	-3	1	156	628	1517	2931	6525	15521	35576	67083	103903	127555	137543	137423	159586	189698
R. Infection	6	0	0	23	13	11	1	0	-2	4	165	1104	2992	5869	13613	23642
R. Disease	0	0	1	50	84	66	179	235	490	1022	1802	2517	3447	5027	4688	5051
Other	219	225	1215	7758	10642	10794	11288	13524	19445	31691	41103	43633	38549	35567	49396	73202

	3-7	8-12	13-17	18-22	23-27	28-32	33-37	38-42	43-47	48-52	53-57	58-62	63-67	68-72	73-77	78-82
Narcotics	0	0	22	281	761	1045	1240	1385	1643	2257	2854	2860	2292	1272	299	63
Falls	7	2	11	64	119	123	118	207	313	499	705	689	557	472	362	399
Homicides	5	33	5222	26159	26035	18654	11449	7065	4423	3363	2333	1308	676	374	223	90
Drownings	146	185	901	1152	686	544	449	344	407	338	387	237	205	135	59	56
Vehicles	29	66	649	2773	4322	4130	3423	3122	2862	2767	2819	2369	1576	1082	778	615
Guns	60	38	224	408	319	217	116	71	43	58	45	34	17	4	0	0
Suicides	0	89	378	3289	3982	3378	2560	2038	1582	1471	1151	1020	791	747	775	631
HIV	0	0	-1	11	247	397	907	1495	2717	3542	3752	2963	1845	1092	594	311
Alzheimer's	0	0	0	0	0	0	0	0	0	0	1	2	8	5	1	-1
Diabetes	-3	-4	5	6	11	67	162	266	613	604	942	1205	1159	949	635	424
Maternal	0	0	0	0	0	0	0	0	0	0	0	0	0	0	0	0
Cancer	4	4	14	109	10	-58	-457	-787	-250	123	2797	8571	13585	18686	21958	24818
Heart	0	1	122	338	442	962	1834	3318	6005	10799	17883	22278	23040	20729	17182	14997
R. Infection	2	0	1	4	2	0	5	1	9	11	150	493	1421	2500	3581	3901
R. Disease	6	0	0	0	11	19	67	80	229	460	617	888	1346	1549	1562	1282
Other	88	74	251	1042	1399	1522	1487	1753	2716	6247	10454	12941	12989	11586	10262	11040

Would you like to contribute?

- Do you have any insights into any of these inequities that you would like to share?
- Are you interested in investigating any of these in further detail?
- Is there any other way that you would like to collaborate?
- If so, please contact us at the email addresses on the left!

Cancer Health Equity and Colorectal Cancer Awareness: A Community Health Educator Initiative

Michael A. Preston[1,2], PhD, MPH; Debbie Cadet[1], PhD, MSW; Rachel Hunley[1], BS, TTS; Reuben Retnam[1], BS; Sarah Arezo[1], BS; Vanessa B. Sheppard[1], PhD

[1]Purdue University, Pharmacy Practice, Center for Health Equity and Innovation

[2]Virginia Commonwealth University, Department of Health and Behavioral Policy

Massey Cancer Center Community Outreach & Engagement - Office of Health Equities & Disparities Research

Background

- Disparities in CRC incidence and mortality persist in rural and underserved communities
- National Outreach Network Community Health Educator (NON-CHE) project identified barriers to CRC screening and implemented the Screen 2 Save (S2S), a national initiative, to increase community knowledge, awareness, and engagement activities
- To assess the impact of this initiative in rural and underserved communities

Methods

- Descriptive and comparative analyses were used to examine the role of the NON-CHE on CRC knowledge and CRC screening intent
- 170 surveys were collected
- Data included demographics, participants' current CRC knowledge, awareness, and future CRC health plans
- A multivariate linear regression was fit to participants' survey scores for CRC knowledge
- Analyses were done in R 3.5.2

Results

- 441 participants in rural and underserved communities
- White participants had significantly higher CRC knowledge scores, correctly answering 1.94 (p=0.007) more questions on average
- After the NON-CHE intervention, this difference was not statistically significant
- The difference in participants' CRC knowledge had an overall mean of 0.92, with a standard deviation of 2.56
- Greater than 95% of participants agreed that S2S sessions impacted their intent to get screened for CRC

Table 1: Linear Model for Difference in Post- and Pre-Test Scores.

Predictors	*Estimates*	*95% CI*	*P*
Intercept	2.04	0.06 – 4.01	0.043
Female[1]	1.08	0.03 – 2.12	0.043
Unknown Gender[1]	2.84	-0.04 – 5.72	0.053
Age	-0.02	-0.04 – 0.00	0.023
Some High School[2]	1.01	-0.97 – 2.99	0.315
Some College[2]	-1.33	-2.67 – 0.00	0.051
College Graduate[2]	-0.21	-1.31 – 0.89	0.711
Unknown/Other Education[2]	0.21	-2.26 – 2.68	0.869
Black	-0.70	-2.15 – 0.75	0.341
White	-1.19	-2.71 – 0.34	0.126

[1]:Reference Category -- Male
[2]:Reference Category – High School Graduate

Conclusions

- NON-CHE facilitated community connections and increased awareness of CRC risk reduction, screening, treatment, and research
- Equity of access to health information and the health care system can be achieved with precision public health strategies
- NON-CHE combined with S2S is a powerful way to engage rural and underserved communities and impact participants' intent to "Get Screened"

Acknowledgements

- Supported by Cancer Disparities Research in Rural and Underserved Communities: RURaL [Reaching the Underserved, Rural, and Low-Income] Lab. Funding, Purdue University
- Supported by Institutional Research Grant IRG-18-159-43 from the American Cancer Society
- Supported by the Wright Center's Clinical and Translational Science Award (CTSA), CTSA grant number: KL2TR002648
- Supported by VCU Massey Cancer Center Office of Health Equity & Disparities Research, #P30CA016059

Reference

Preston, M, et al. J Cancer Educ, 2021.

Indiana CTSI Access Technology Program (ATP)

Facilitate the use of innovative technologies in investigator-initiated research

1. **Connect investigators to CTSI-designated service cores and resources**
   - ➢ https://indianactsi.org/servicecores/
2. **Technology Seminar Series - Zoom**
   - Fridays @ noon (biweekly)
   - Recordings are posted online
     - ➢ CTSI ATP web page:
       https://indianactsi.org/researchers/services-tools/tech-lab-resources/atp/
     - ➢ CTSI YouTube channel
3. **Grant Programs**
   - A. Core Pilot Grant Program
     - Up to $10,000 each
     - Over 25 grants awarded annually
   - B. Postdoc Challenge Grant Program
     - Up to $5,000 each
     - Four grants awarded annually
4. **OMICS Data Analysis Tools**
   - A. Ingenuity Pathway Analysis (IPA)

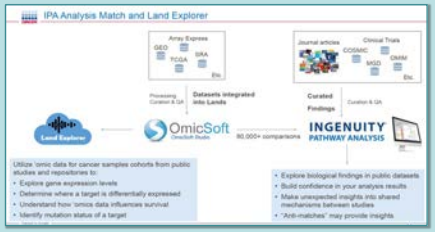

   - B. MetaCore Pathway Analysis Suite

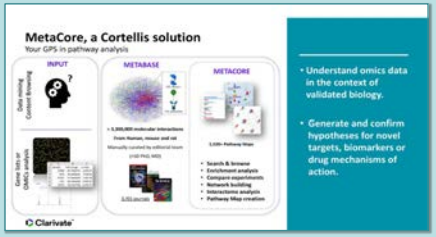

Mission

Improve the impact and competitiveness of CTSI investigator research by promoting access to innovative technologies available at Indiana CTSI-designated research cores.

Campus Liaisons		
Jill Reiter, Director	IU-Indianapolis	jireiter@iu.edu
Tammy Sajdyk	IU-Indianapolis	tsajdyk@iu.edu
Joel Ybe	IU-Bloomington	jybe@indiana.edu
Melanie DeFord	Notre Dame	mdeford@nd.edu
Natasha Nikoaidis	Purdue	nnikolai@purdue.edu
Tommy Sors	Purdue	tsors@purdue.edu
Coordinator		
Jenna York – jlyork@iu.edu		

Improve the quality of Indiana CTSI core services

1. **Core Oversight Program of CTSI-designated research cores**
   - Voluntary program to obtain CTSI-designated core status & eligibility for CTSI Core Pilot, Equipment, and Postdoc Challenge grants.
   - CTSI-designated cores are reviewed annually to promote best practices and ensure they have appropriate and clear operational policies, pricing structure, and user satisfaction.
2. **Business Management Assistance**
   - Partnership with IU Kelly School of Business to assist in improving project management, marketing, financial management, and resource efficiency management.

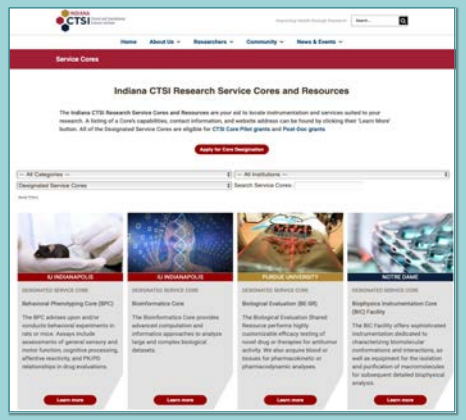

Manage key support cores that are vital to the Indiana CTSI mission.

Biospecimen Management Core

1. **Specimen Support Facility (SSF)**
   - Supports biorepository storage by providing and maintaining a secure and affordable solution for CTSI investigators and local and national biobanks.
   - Director: Rob Orr
   - Manager: Jenna York
   - ictsissf@iupui.edu

2. **Clinical Translational Support Laboratory (CTSL)**
   - Supports research by providing rapid sample processing, shipping, and storage for CTSI investigators and other collaborators.
   - Director: Jill Reiter
   - Manager: Rob Orr
   - ctslab@iupui.edu

SCAN ME

Going with the Flow in Neonatal Peritoneal Dialysis: Low-Cost, Clot Resistant PD Drainage Catheter Development

Sergio Ruiz Vega[a], Carl Russel III[ab], Siting Zhang[a], Mignon McCulloch[c], Aaron Lottes[a], Hyowon Lee[a], Danielle E. Soranno[d,a]

PURDUE UNIVERSITY
Weldon School of Biomedical Engineering

Background

- Pediatric patients in low- and middle-income countries (LMICs) with kidney disease rely on peritoneal dialysis (PD)
- Due to cost and availability, many patients receive treatment with off-label devices resulting in increased complications

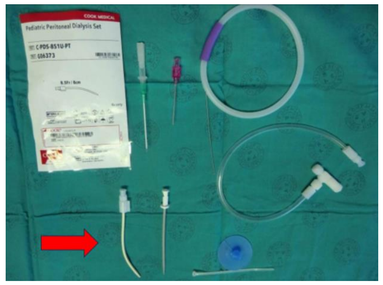

Figure 1. Previously available drainage catheter set

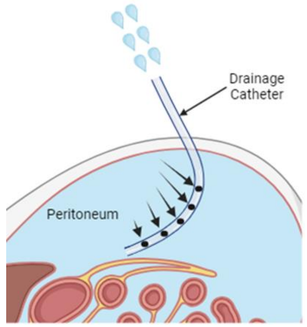

Figure 2. The use of drainage catheters in PD

Purpose

Develop a low-cost pediatric drainage catheter for PD

Evaluate and compare with an existing device under common failure methods

Manufacturing Methods

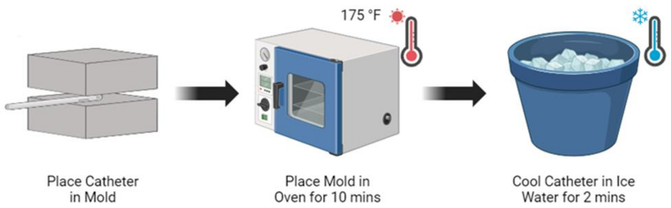

Figure 3. Flow chart of the catheter molding process

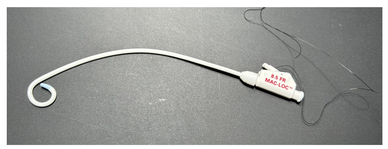

Figure 4. Control Catheter

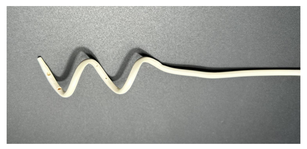

Figure 5. Helix Catheter

Occlusion Methods

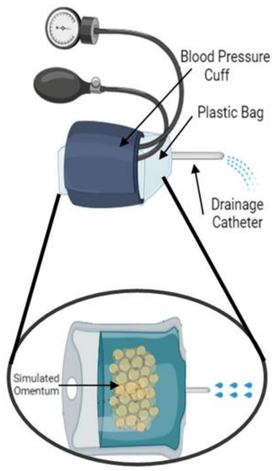

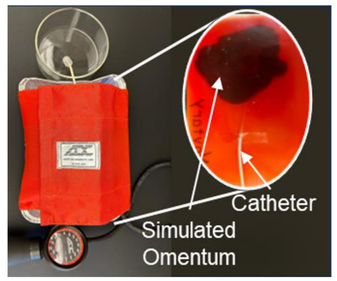

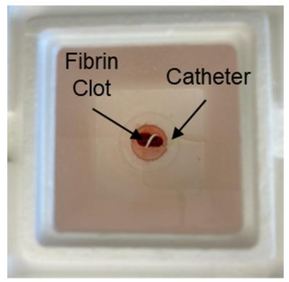

Figure 6. Left) Diagram of the simulated peritoneal cavity with a artificial omentum; Middle) Picture of the diagramed set up; Right) Picture of the fibrin clot simulation environment

Results

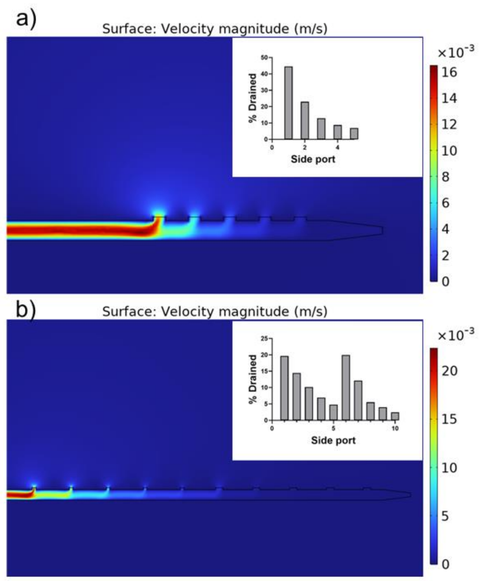

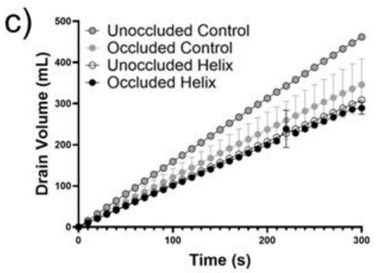

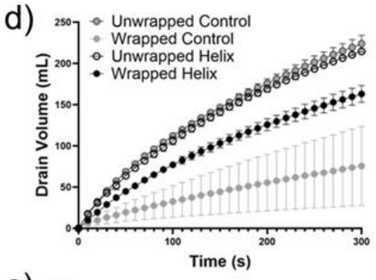

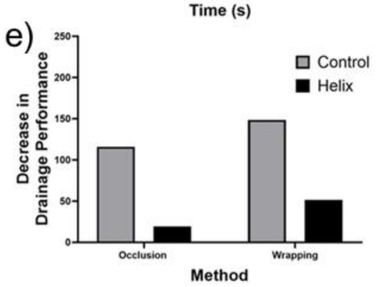

Figure 7. a,b) COMSOL simulations of fluid flow with inserts of the drainage distribution per side port c) Drainage volume of helical and control catheters with the presence or absence of a fibrin clot analog. d) Drainage volume of helical and control catheters with the presence or absence of omental wrapping. e) Difference in drainage in the presence of different occlusion methods

Discussion

- Varied side port diameters distribute flow evenly
- Varied side ports mitigate high pressure areas
- Helix design of catheter minimizes surface contact with side ports and omentum
- Helix catheter drainage is less affected by occlusion methods

Impact and Engagement

- This device has the potential of filling a needed gap in healthcare for LMICs and their pediatric populations
- Training and use of specific catheters for on label use may lead to less complications
- Collaboration with physicians like Dr. Mignon McCulloch, MD who train healthcare professionals in LMICs can lead to lives saved if they have access to the appropriate tools

Figure 8. Mignon McCulloch, MD (left) and Sergio Ruiz (right) attending the XIII Latin American Association of Pediatric Nephrology Congress

Figure 9. Testing the catheters on a simulated peritoneum similar to those that physicians use in their trainings

Acknowledgements

We would like to acknowledge Dyvia Patil for her support in providing knowledge of Cook Medical's products and arranging stock material to be provided for this project. Additionally, we would like to acknowledge Ty Morgan for sharing his concept of a helical-shaped catheter.

INDIANA UNIVERSITY SCHOOL OF MEDICINE
CROSSROADS Pediatric Device Consortium
COOK MEDICAL

[a] Weldon School of Biomedical Engineering, Purdue University, West Lafayette, IN, USA
[b] Indiana University School of Medicine, Indianapolis, IN, USA
[c] Red Cross War Memorial Children's Hospital, University of Cape Town, Cape Town, South Africa
[d] Department of Pediatrics, Indiana University School of Medicine, Indianapolis, IN, USA

Miniature Wireless LED-device for Photodynamic Therapy

Hailey Sanders [a], Sunghoon Rho [b], Prof. Thomas O'Sullivan [b]*, Prof. Bradley Smith [a]*

[a] Department of Chemistry and Biochemistry, 346 McCourtney Hall, University of Notre Dame, Notre Dame, Indiana 46556, USA
[b] Department of Electrical Engineering, University of Notre Dame, Notre Dame, IN, 46656, USA.

National Institutes of Health

Long Term Goal

The long term goal of this research is a new approach to neoadjuvant therapy of cancer that is based on photodynamic therapy. An implanted miniature wireless LED is used to irradiate a deep-seated primary tumor and induce an immunogenic response that will eradicate other tumors or sites of metastases. The implanted LED will be removed during the subsequent surgery. The technology can be used for cancers where neoadjuvant therapy is common, especially breast, esophageal, rectal, pancreatic, bladder, lung, and ovarian cancer.

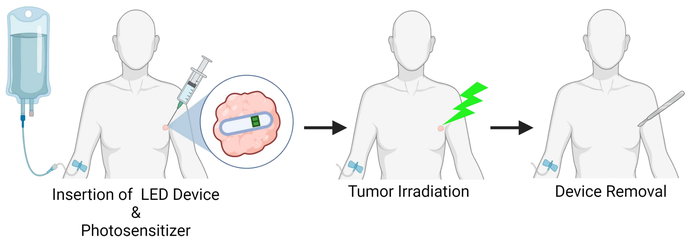

Introduction

Photodynamic therapy utilizes a two-step process for cancer treatment including the introduction of a photosensitizer (PS) and activation of the PS with specific wavelength of light to induce cell death.[1,2] Typically, this process involves molecular oxygen generating high amounts of singlet oxygen which is highly reactive and toxic to the cell.[3] However, the cytotoxic effect is restricted to areas accessible by visible wavelengths of light (**Figure 1a**). This is unfortunate as many visible dyes available are excellent photosensitizers.[4] To combat this obvious clinical limitation, recent research has focused on bringing visible light into deep tissue including the production of implantable light delivery systems.[5] This study focuses on the fabrication and use of a wirelessly powered light-emitting device (LED) to excite PS. Our device was designed with a volume of 23 mm^3, one of the smallest prototypes to date, and has the advantage of increased flexibility to employ it at relatively otherwise inaccessible locations. In addition, the device size allows for introduction with less invasive implantation methods. The device is wirelessly powered through radio frequency (RF) to produce light at the sight of disease. The device emits at 573 nm and we have tested its ability to excite Rose Bengal, an efficient PS, to produce singlet oxygen.[6] In addition, we tested the device with Rose Bengal Diacetate, a lipophilic derivative of the dye, in human colorectal cancer HT-29 cells and found it produced enough singlet oxygen to induce cell death. We report evidence of pyroptosis as the predominant pathway of HT-29 photoinduced cell death.

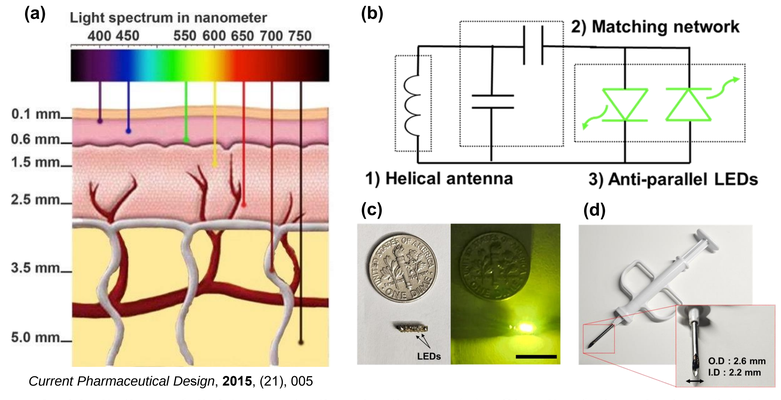

Current Pharmaceutical Design, **2015**, (21), 005

Figure 1: Limitation of light penetration in tissue (a). Circuit of the device (b) Image showing the wirelessly powered device emission of light (c), Scale bar = 10 mm. The device introduced in a 12 G needle with the zoomed-in image of the device inside the needle (d).

Wirelessly-powered Optical Emission

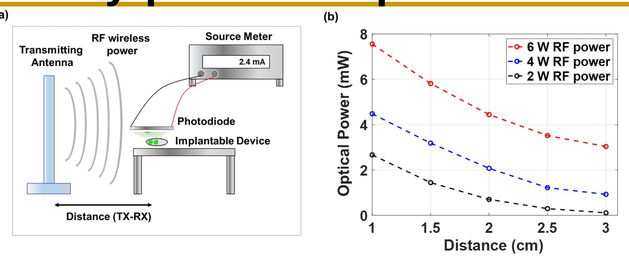

Figure 2: The measurement setup for the optical output of the device (a). The measured optical output of LEDs, as a function of distance from transmitting antenna at various transmitting powers (b).

Singlet Oxygen Cuvette Studies

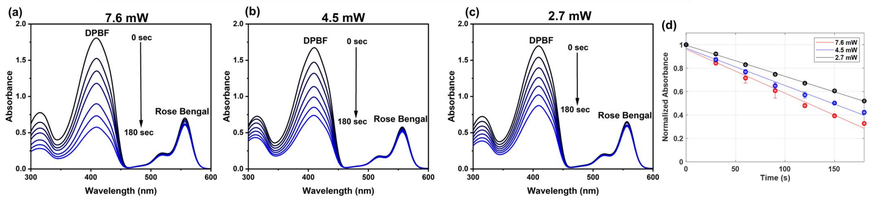

Figure 3: (a-c) Absorbance spectra of solutions containing 1,3-diphenylisobenzofuran (DPBF, 75 μM) and Rose Bengal (6 μM) in methanol and irradiated for 180 seconds with the wireless device at optical power of 7.6 mW, 4.5 mW, or 2.7 mW, respectively. (d) Normalized DPBF absorption at 415 nm (N=2) versus time.

In-Vitro Cell Photoinactivation

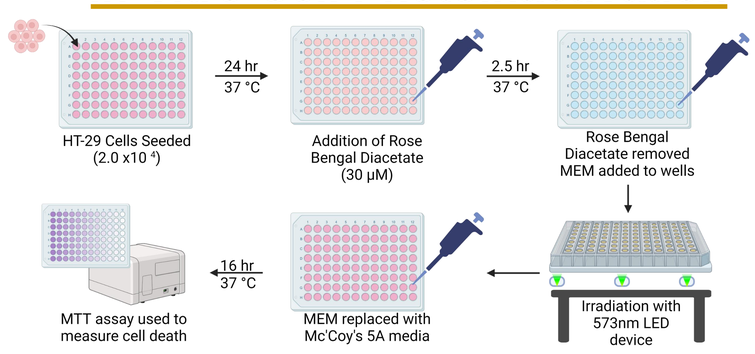

Scheme 1: Workflow of HT-29 photosensitization process.

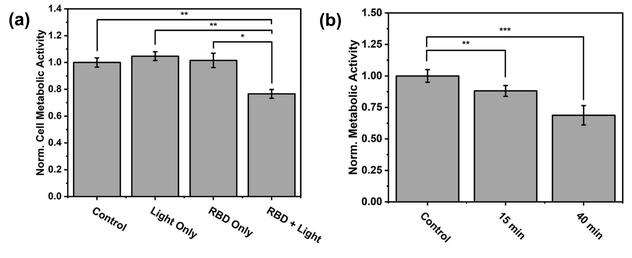

Figure 4: (a) Normalized cell metabolic activity of HT-29 cells treated with Rose Bengal Diacetate (RBD; 30 μM) only, light only (573 nm wireless device), or 30 μM RBD + light (40 minutes). Data is average of (N=3) experiments. (b) Normalized metabolic activity of HT-29 cell cultures measured by MTT assay. No treatment is the control condition. The other two conditions are 30 μM (RBD) + light for 15 minutes or 40 minutes. Data is average of (N=5) experiments with error bars indicating standard deviation. *** p=0.0003, ** p<0.01, *p<0.05.

In-Vitro Cell Microscopy Studies

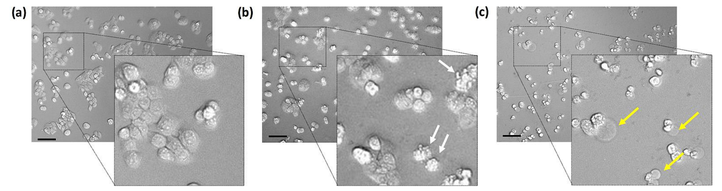

Figure 5: Brightfield microscopy images of HT-29 cells (20x). (a) Control cells, (b) Cells treated with Rose Bengal Diacetate (30 μM) and irradiated using the wireless device (30 minutes), imaged directly after irradiation, and (c) Cells imaged 16 hours after irradiation. White arrows indicate membrane ruffling. Yellow arrows indicate protruding bubbles. Scale bar = 50 μm.

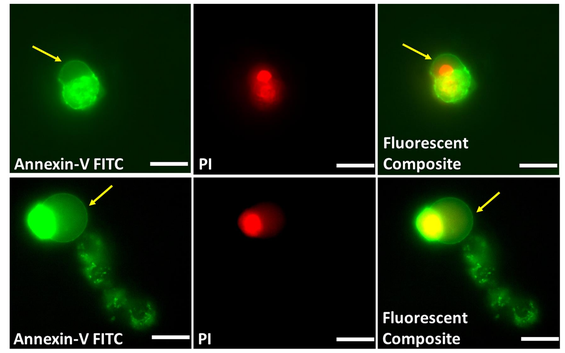

Figure 6: Two representative sets of dual-channel fluorescence microscopy images. Micrographs showing HT-29 cells treated with Rose Bengal Diacetate (30 μM), irradiated using the wireless device (30 minutes), allowed to incubate for 16 hours, then stained with Annexin-V FITC (Ex: 485/20 nm, Em: 524/24 nm) and Propidium Iodide (PI) (Ex: 562/40, Em 624/40). Yellow arrow indicates a protruding bubble (pyroptotic body) in each case. Scale bars = 30 μm.

Conclusions

This study tested the use of a miniature wireless LED device with a volume of 23 mm^3, one of the smallest prototypes to date. The device is wireless powered with RF and emits at 573 nm which can excite Rose Bengal as an effective PS to produce singlet oxygen. Use of the device with monolayer HT-29 cells, and Rose Bengal Diacetate revealed induced cell death with observed morphological changes observed as the formation of protruding membrane bubbles. Annexin V and Propidium Iodide stains in combination with formation of membrane bubbles suggest pyroptosis as major cell death pathway.

References

1. Kessel, D. Photodynamic Therapy: A Brief History. J Clin Med 2019, 8 (10). https://doi.org/10.3390/jcm8101581.
2. Sobhani, N.; Samadani, A. A. Implications of Photodynamic Cancer Therapy: An Overview of PDT Mechanisms Basically and Practically. J Egypt Natl Canc Inst 2021, 33 (1), 1–13. https://doi.org/10.1186/s43046-021-00093-1.
3. Sobhani, N.; Samadani, A. A. Implications of Photodynamic Cancer Therapy: An Overview of PDT Mechanisms Basically and Practically. J Egypt Natl Canc Inst 2021, 33 (1), 1–13. https://doi.org/10.1186/s43046-021-00093-1.
4. Fernandez, J. M.; Bilgin, M. D.; Grossweiner, L. I. Singlet Oxygen Generation by Photodynamic Agents. J Photochem Photobiol B 1997, 37 (997), 13–140.
5. Sun, B.; Bte Rahmat, J. N.; Zhang, Y. Advanced Techniques for Performing Photodynamic Therapy in Deep-Seated Tissues. Biomaterials 2022, 291 (July), 121875.
6. Panzarini, E.; Inguscio, V.; Dini, L. Timing the Multiple Cell Death Pathways Initiated by Rose Bengal Acetate Photodynamic Therapy. Cell Death Dis 2011, 2 (6). https://doi.org/10.1038/cddis.2011.51.

***Email: bsmith3@nd.edu (B. Smith)**
***Email: tosullivan@nd.edu (T. O'Sullivan)**
This work was supported by the NIH and STIR Grant

Genomic and proteomic profiling of *Acanthamoeba* isolates

Chayan Sharma[1], Sumeeta Khurana[1], Alka Bhatia[2], Amit Arora[3], Amit Gupta[4]

Department of Medical Parasitology, [2]Department of Experimental Medicine & Biotechnology, [3]Department of Medical Microbiology, [4]Advanced Eye Centre, Post Graduate Institute of Medical Education and Research, Chandigarh, India

Introduction

- *Acanthamoeba* are amphizoic amoeba majorly responsible for causing *Acanthamoeba* keratitis (AK) and Granulomatous amoebic encephalitis (GAE)
- Despite its ubiquitous nature, the frequency of infections is not high, probably due to existence of non-pathogenic isolates
- Whole-genome sequencing and an annotated genome assembly can unravel the biological functions
- Gene expression and proteomic analysis can provide information on biological processes and aid in the identification of potential genes involved in pathogenicity

Methods

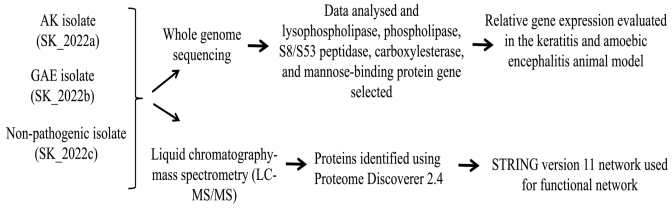

Results

- Hybrid genome of 51MB and 54MB assembled for SK_2022a and SK_2022b
- Illumina sequencing generated a genome of 22MB for SK_2022c
- Around 711 genes were exclusively present in the two pathogenic isolates and absent in the non-pathogenic isolate
- Genes including **phospholipase (A)**, **lysophospholipase (B), and mannose binding (E)** were significantly upregulated in the keratitis isolate during AK
- In the case of the amoebic encephalitis model, **phospholipase (A)**, **lysophospholipase (B)**, **S8/S53 peptidase (C), and carboxylesterase (D)** were significantly upregulated in the encephalitis isolate

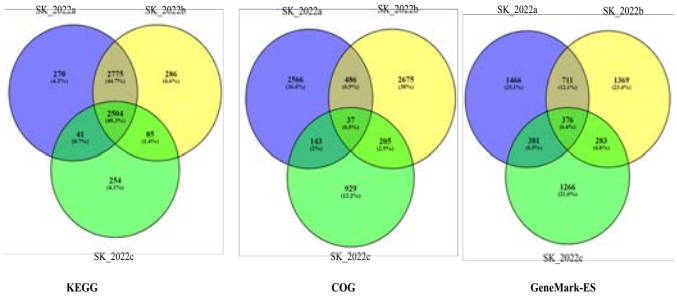

Fig 1: Venn diagram representing GeneMark-ES, Kyoto Encyclopedia of Genes and Genomes (KEGG), and clusters of orthologous genes (COG) data in the three *Acanthamoeba* sp. isolates

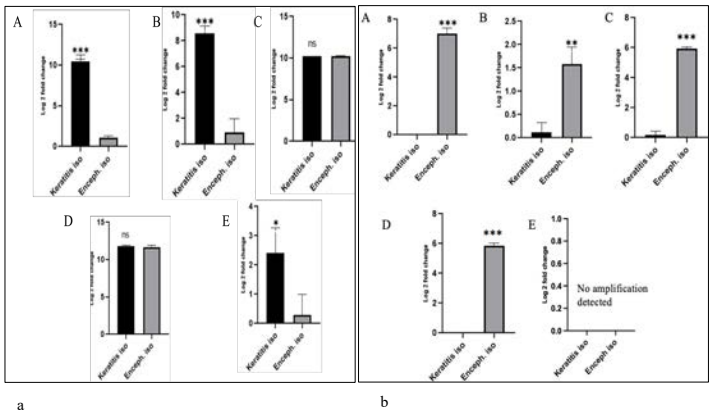

Fig 2: The expression of genes **(A)**, **(B)**, **(C)**, **(D)**, and **(E)** during (a) *Acanthamoeba* keratitis and (b) amoebic encephalitis in the mouse model

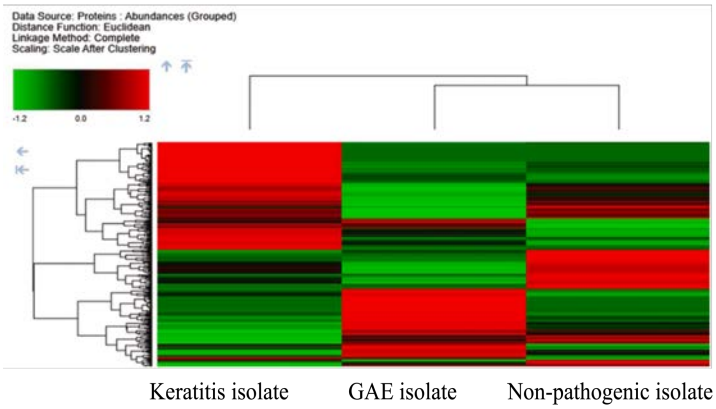

Fig 3: Heat map displaying color-coded differential protein expression

Discussion & conclusion

- Pathogenic isolates had proteins responsible for cellular functions, intracellular transport, and cell division
- Also, cysteine and serine proteases found upregulated in the two pathogenic isolates known for their role in the degradation of other proteins & peptides
- Gene knockout-out experiments of lysophospholipase, phospholipase, S8/S53 peptidase, carboxylesterase, and mannose-binding protein along with the transcriptome data could have provided a better insight into the proteases during the pathogenesis of *Acanthamoeba*

References

- Sharma C, Khurana S, Arora A, Bhatia A, Gupta A. An Insight into the Genome of Pathogenic and Non-Pathogenic Acanthamoeba. Pathogens. 2022 Dec 19;11(12):1558
- Sharma C, Thakur A, Bhatia A, Gupta A, Khurana S. Acanthamoeba keratitis in a mouse model using a novel approach. Indian journal of medical microbiology. 2021 Oct 1;39(4):523-7

LGBTQIA+ Affirming Practices: Evaluation of Knowledge, Attitudes, and Confidence in Future Practice of Intermediate Learners Participating in an Interprofessional Immersion Activity

*Lorraine V. Stigar, DrPH, Alexandra Marshall, PhD, Clare Brown, PhD, Kathryn Neill, PharmD
University of Arkansas Medical Sciences

Abstract

Lesbian, Gay, Bisexual, Transgender, Queer / Questioning, Intersex, Asexual, Plus (LGBTQIA+) individuals make up roughly 7% of the U.S. adult population. However, when compared to heterosexual cisgender individuals, LGBTQIA+ individuals experience greater health disparities across disciplines. A stratified convenience sample of students attending a graduate medical institution in the South was collected through the office of Interprofessional Education (IPE) to assess student Knowledge, Attitudes, and Perceived Future Practice when working with LGBTQIA+ patients or clients. Students were randomly assigned to either the intervention or the control group with the intervention group receiving a 15-minute educational module 1-week prior to an IPE Proposal Workshop. Pre-post-test were administered to both the intervention and the control group with the post-test including four open-ended questions. Students represented the college of medicine (n=29), college of nursing (n=39), college of pharmacy (n=11), college of health professions (n=41), and college of public health (n=13). Primary findings indicated a statistically significant difference occurred across all three domains indicating participation in the workshop, not the intervention, resulted in a difference in Knowledge, Attitudes, and Perceived Future Practice. College of medicine respondents showed differences in Attitudes (p=0.01) from pre- to post-survey, as well as Perceived Future Practice (p=0.03). Also, Perceived Future Practice (p=0.001) proved statistically significant overall indicating a correlation between the workshop and differences in Perceived Future Practice. Qualitative findings yielded three themes 1) Development of Knowledge Foundation and Information Sourcing, 2) Philosophy of Interpersonal Interactions, and 3) Integration of Knowledge and Attitudes to Applied Behaviors and Target Outcomes. The control group reported a desire for more education and changes to the IPE activity, while the intervention group reported more frequently increased comfort and respect for persons.

Methods

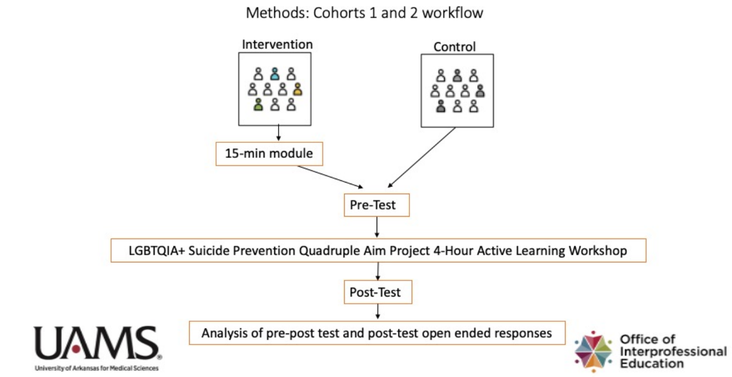

Quantitative Results

Pre_post*group
p-value = 0.54

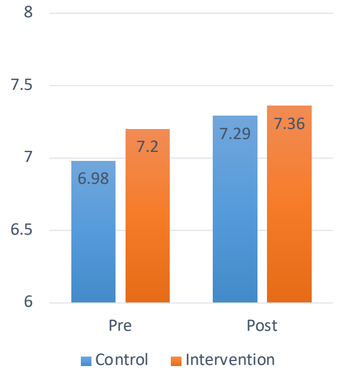

Pre_post*group
p-value = 0.57

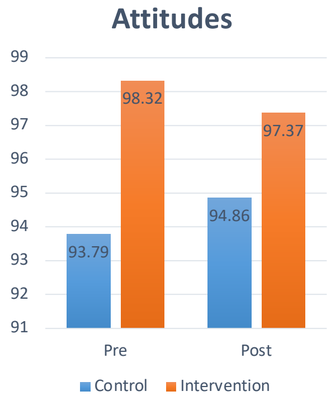

Pre_post*group
p-value = 0.43

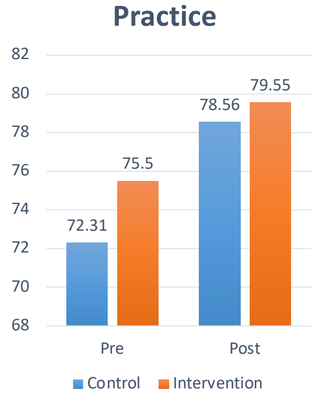

133 participants were included in the final quantitative sample and showed the interaction between the control and intervention group remained insignificant indicating no difference between the control and intervention group pre-post survey change and the 15-minute educational intervention. Despite this finding, significant correlations were found in pre-post overall indicating a correlation between the workshop itself and changes in Knowledge, Attitudes, and Perceived Future Practice.

Qualitative Results

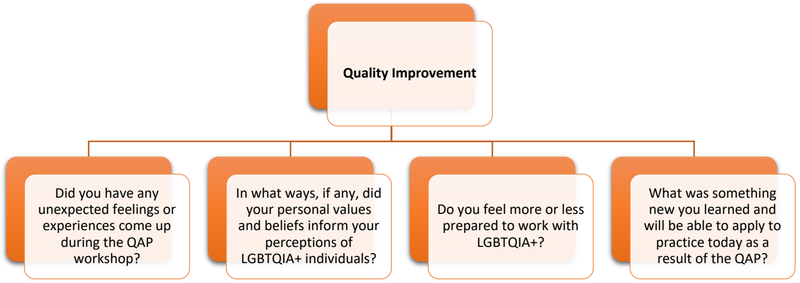

Control: Reported desire for more education and changes to IPE activity

Intervention: Reported increased comfort and respect for persons more frequently

Future Implications

- Formal evaluation of IPE activities
- Collection, evaluation, and dissemination of data collected by IPE team
- Adoption of supplemental educational content
- Future focus groups or surveys to garner insight of student needs

References

*Available Upon Request

Association between Health Insurance Coverage and Stage of Diagnosis for Cervical Cancer among Women in Indiana from 2011-2019

Mrithula Suresh Babu[1], Monica L. Kasting[1,2], Natalia M. Rodriguez [1,2]

[1] Department of Public Health, College of Health and Human Sciences, Purdue University, West Lafayette, IN, USA

[2] Cancer Prevention and Control Program, Indiana University Simon Comprehensive Cancer Center, Indianapolis, IN, USA

Introduction

- Cervical cancer is one of the most common types of cancer among women and it is caused by infection from the human papillomavirus (HPV).
- Screening for pre-invasive lesions reduces the likelihood of cancer progression and eventually leading to malignancy.
- The up-to-date cervical cancer screening rate among women between the ages of 21 to 65 years in Indiana was 76% in 2020, compared to the national average of 78%.
- Women diagnosed at earlier stages for cervical cancer have a better chance of survival than those diagnosed at later stages.
- Previous studies show that Hispanic and African American women are less likely to be diagnosed with cervical cancer at a localized stage when compared to Non-Hispanic White women.
- Cervical cancer screening prevalence declined by 11% during the COVID-19 pandemic.

The Healthy People screening data for cervical cancer in 2018 was 80.5%

(COMPARED TO 2020 TARGET OF 93%)

Methods

- Data source - Reported cases (N=2518) of cervical cancer from the Indiana State Department of Health (ISDH) registry from 2011-2019
- Analysis - Descriptive statistics, Chi-square tests and Multinomial logistic regression model
- Categorical outcome - stage of diagnosis of cervical cancer
- Covariates - race/ethnicity and insurance status (adjusted for age at diagnosis)

References

1. Arbyn, M.(2011). https://doi.org/10.1093/annonc/mdr015
2. Arbyn, M.(2020). https://doi.org/10.1016/S2214-109X(19)30482-6
3. CDC. (2023). https://gis.cdc.gov/cancer/USCS/#/CancerScreening/
4. Indiana Cancer Consortium. (2020). https://indianacancer.org/wp-content/uploads/2021/12/ICC_CevicalCancer_FF_2021.pdf
5. Wright, J. D.(2015). https://doi.org/10.1016/j.ajog.2015.07.012

Women with no insurance or public insurance are more likely to be diagnosed with cervical cancer at advanced stages

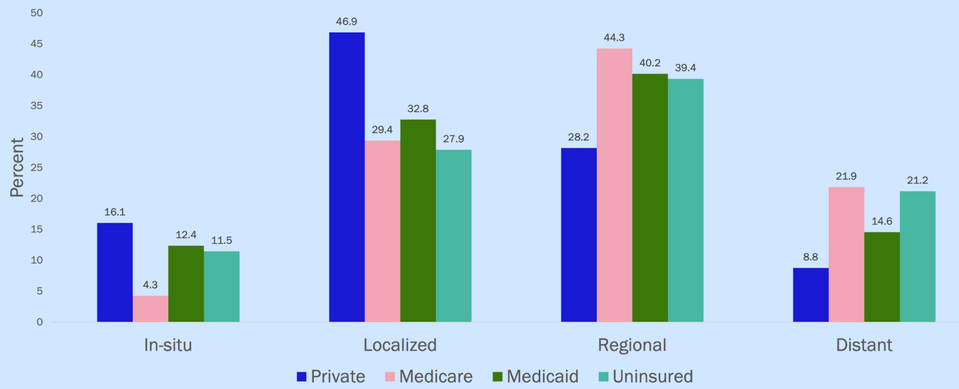

A higher proportion of Black and Hispanic women are uninsured or under public insurance

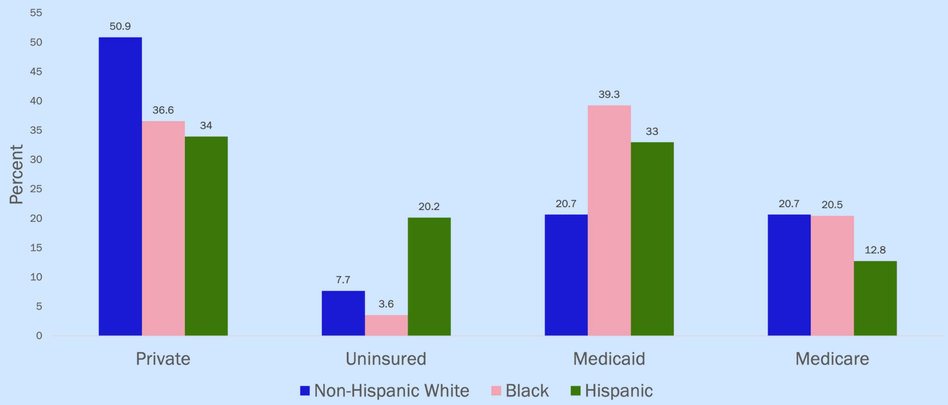

Results

- Average age at diagnosis was 48.98 years (SD = 14.98).
- The largest percentage of Non-Hispanic White patients had private insurance (50.9%), whereas the largest percentage of Black patients had Medicaid (39.3%). 20.2% of Hispanic patients were uninsured when compared to 7.7% Non-Hispanic White and 3.6% Black patients.

Stages of Cervical Cancer

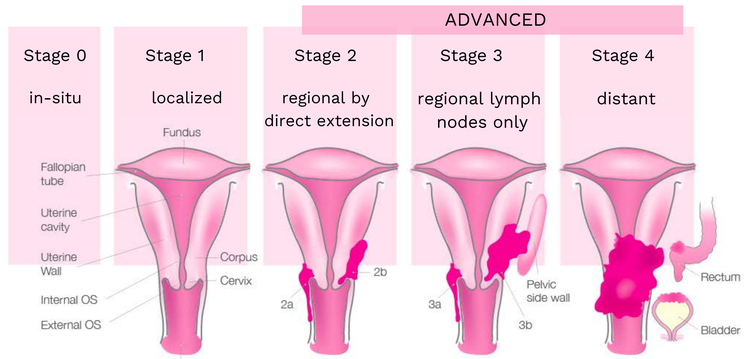

© Graphic adapted from Vag-Moose & Vai-Wave 2023

- Patients who are uninsured (OR = 2.475) and those who have Medicaid (OR = 2.321) were significantly more likely to be diagnosed at the regional stage than the in-situ stage, compared to patients with private insurance.
- Patients who are uninsured (OR = 4.432) and those who have Medicaid (OR = 3.007) were significantly more likely to be diagnosed at the distant stage than the in situ stage, compared to patients with private insurance.

Discussion

- This study highlights the imperative need for increased coverage for routine cervical cancer screening and preventive care services, especially for Black and Hispanic women who are disproportionately diagnosed at later stages of disease.
- It is also important to consider improving awareness of programs such as BCCP among uninsured women to increase screening and detection of cervical cancer cases at earlier stages.

Keep in Touch!

Perceptions on Antimicrobial Resistance by Health Professionals

PURDUE UNIVERSITY

Rachel Tonne, RVT, Nathalie Bencie, & Randolph D. Hubach, PhD, MPH

Department of Public Health

Introduction

In the US each year, more than 2.8 million antimicrobial resistant infections occur each year. AMR disproportionately affects those at higher risk of health inequity and disparity, including children, elderly, MSM, and people of color (1). It is vital that a One Health approach be considered to address AMR across several sectors in order to promote health for all groups of people. To the authors' knowledge, a comparison of the perceptions of veterinarians and human medical professionals in the United States in regards to antimicrobial resistance and its effects on their respective clinical practice has not been done. The purpose of this study was to understand the perceptions of allied health professionals towards antimicrobial resistance to alleviate barriers and encourage collaboration in order to combat antimicrobial resistance most effectively. This will allow for the development of the multisectoral approach that is necessary to combat antimicrobial resistance.

A qualitative interview-based approach allows for in-depth exploration of the perceptions of health professionals, including their respective concerns and barriers that affect their practices and their ability to combat antimicrobial resistance.

Methods

Screening survey of DVMs, NPs, MDs, and DOs

Participants engaged in semi-structured interview

2 Researchers independently developed codebook

2 Researchers independently coded interviews and performed periodic consistency checks

Overarching themes and appropriate subthemes developed from codes

Qualitative Themes

Theme 1: Shared Concerns

Subtheme 1: Development of "Superbugs"

Subtheme 2: Increased Difficulty in Treating

Theme 2: Clinical Discrepancies between Professions

"So I think a lot of people request them [antibiotics] and sometimes we have to decline that." - DVM

"I think that there's concerns, in terms of prescribing, patients finishing their antibiotics, and sort of choosing even to prescribe antibiotics to begin with, with infections that can clear on their own." - MD

Subtheme 1: Client Patient Satisfaction vs. Compliance

"I think not having like really, at least for me, not being able to have something like a carbon footprint, some sort of measurable thing, just makes it [AMR] less easy to evaluate." - DVM

"We do also have like antibiograms and like antibiotic therapy that are specific to each hospital that can kind of help guide if you're treating for a certain bug." - MD

Subtheme 2: Ability to Track/Test Trends

"I think I end up making an educated guess a lot of the time and hoping for the best, and I would say the majority of the time it works out okay. But you know, it definitely concerns me that there's no real way for me to measure my impact on antimicrobial resistance as a practitioner." - DVM

"I think it's one of the, like stewardship of antibiotics to prevent resistance, is one of the main principles that we use to make decisions about antibiotics when we prescribe them to patients." - MD

Subtheme 3: Stewardship vs. Empirical Therapy

Theme 3: One Health Implications

"I've seen examples indirectly that it [AMR] affects as well in terms of treating people's pets, but also through the use of antibiotics in agriculture and farm animals. I think especially outside of the United States and that's leading to antibiotic resistance in human medicine as well." - MD

Subtheme 1: Zoonotic Transmission

"Those are creating superbugs that are getting into people. And then those people travel to the US and they end up in the US. I mean, we don't want it in India either, but I mean, it's kind of like, well with everybody going everywhere around the world, it doesn't just matter what our behavior is here. It kind of matters what it is everywhere.... we're all connected." - DVM

Subtheme 2: Global Transmission

Demographics

Survey Responses: 40 total responses from DVMs, MDs, NPs

Interview Participants:

11 DVMS, 7 MDs/NPs

Age: 26 - 48 (mean of 35.28 years)

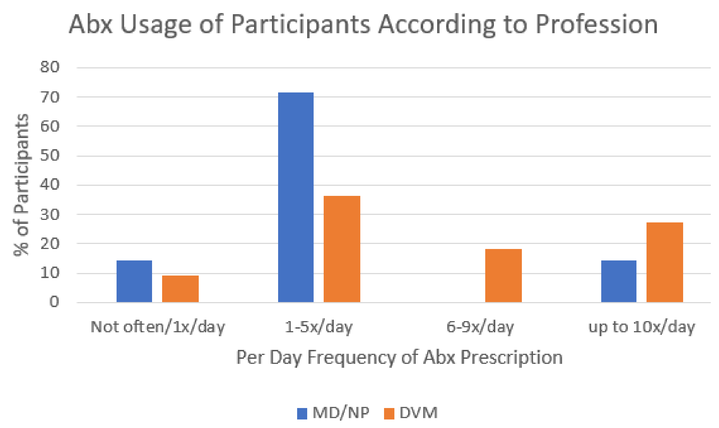

*one DVM unable to provide prescription frequency

Main Takeaways

This study found that while veterinarians and human health professionals share some common concerns with antimicrobial resistance, the professions have differing concerns for fulfillment of client needs, testing ability, and approach to therapy. There are also concerns regarding transmission, both zoonotic and in the global health sphere.

These results demonstrate the need for rapport with clients to promote compliance and satisfaction, as well as the need for increased availability of testing and trend tracking for DVMs. Meeting these needs will allow these health professionals to best serve their clients and patients across communities.

Limitations

One of the limitations of this study is that the responses were limited to those who were willing to participate in the study and the interviews. Another limitation is that a majority of the MD respondents were focused in internal medicine and may not represent the views of the wider profession.

Acknowledgements

This study was supported by a doctoral student research grant through the Department of Public Health at Purdue University.

References: 1. CDC. Addressing health equity across ar threats. Centers for Disease Control and Prevention. Published March 17, 2022. Accessed February 16, 2024. https://www.cdc.gov/drugresistance/solutions-initiative/stories/ar-health-equity.html

CDHu40: a novel marker gene set of neuroendocrine prostate cancer (NEPC)

Sheng Liu[1], Hye Seung Nam[2], Xuehong Deng[2], Elnaz Pashaei[1], Yong Zang[3], Lei Yang[4], Xin Lu[5,6], Chenglong Li[7], Jiaoti Huang[8], Michael K Wendt[2], Rong Huang[2], Jun Wan[1,6,9]

[1]Department of Medical and Molecular Genetics, Indiana University School of Medicine, Indianapolis, IN USA; [2]Department of Medicinal Chemistry and Molecular Pharmacology, Purdue University, West Lafayette, IN USA; [3]Department of Biostatistics & Health Data Science, Indiana University School of Medicine, Indianapolis, IN USA; [4]Department of Pediatrics, Herman B Wells Center for Pediatric Research, Indiana University School of Medicine, Indianapolis, IN 46202, USA; [5]Department of Biological Sciences, Boler-Parseghian Center for Rare and Neglected Diseases, Harper Cancer Research Institute, University of Notre Dame, Notre Dame, IN 46556, USA; [6]Indiana University Simon Comprehensive Cancer Center, Indiana University School of Medicine, Indianapolis, IN 46556, USA; [7]Deparment of Medicinal Chemistry, College of Pharmacy, University of Florida, Gainesville, FL USA ; [8]Deparment of Pathology, Duke University School of Medicine, Durham, NC 27710, USA; [9]Center for Computational Biology and Bioinformatics, Indiana University School of Medicine, Indianapolis, IN USA

INDIANA UNIVERSITY

Abstract

Prostate cancer (PCa) is the most prevalent cancer affecting American men. Castration-resistant prostate cancer (CRPC) can emerge during hormone therapy for PCa, manifesting with elevated serum prostate-specific antigen (PSA) levels, continued disease progression, and/or metastasis to the new sites, resulting in a poor prognosis. A subset of CRPC patients shows a neuroendocrine (NE) phenotype, signifying reduced or no reliance on androgen receptor (AR) signaling and a particularly unfavorable prognosis. NEPC is lack of appropriate unique identification markers. NEPC biopsy samples also often exhibit in mixed histology, further leading to diagnostic errors and inappropriate treatments.

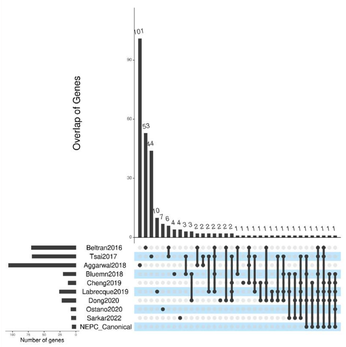

In this study, we employed computational approaches based on gene expression profiles and protein-protein interaction (PPI) networks. We identified 500 potential marker genes, which are significantly enriched in cell cycle and neuronal processes. The top 40 candidates, collectively named as CDHu40, demonstrated superior performance in distinguishing NE prostate cancer (NEPC) and non-NEPC samples based on gene expression profiles compared to other published marker sets.

Importantly, elevated CDHu40 scores derived from our predictive model showed a robust correlation with unfavorable survival outcomes in patients, indicating the potential of the CDHu40 score as a promising indicator for predicting the survival prognosis of those patients with the NE phenotype. We further highlighted markers indirectly linked to NEPC but related to neuroendocrine features, such as ALB, FGB, and FGG. Motif enrichment analysis on the top candidates suggests that REST and E2F6 may serve as key regulators in the NEPC progression.

Ultimately, our study leverages the genetic diversity present in individual NEPC studies and their protein-protein interaction network to construct a thorough understanding of the disease progression and underscores the prognostic significance of CDHu40.

Data sets used in this study

Data set	Data type	# of samples	# of NEPC samples	# of non-NEPC samples	Reference
WCM_NEPC_2016	Bulk RNA-seq	49	15	34	PMID: 26855148
PRAD_SU2C_2019	Bulk RNA-seq	232	22	210	PMID: 31061129
GSE32967	Microarray	22	14	8	PMID: 22156612
GSE149091	Bulk RNA-seq	4	1	3	PMID: 32531951 PMID: 32512818
GSE59984	Microarray	14	2	12	PMID: 29757368
PRAD_TCGA	Bulk RNA-seq	498	0	498	https://www.cancer.gov/tcga
Asberry2022	scRNA-seq	4	3	1	PMID: 36382181
Dong2020	scRNA-seq	5	4	1	PMID: 33328604

Flowchart of the study

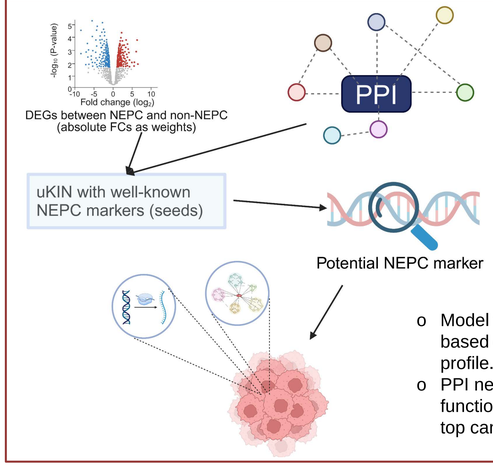

- Model to predict NEPC samples based on gene expression profile.
- PPI network and biological functions/pathways enriched in top candidate genes.

CDHu40 marker genes and their performance

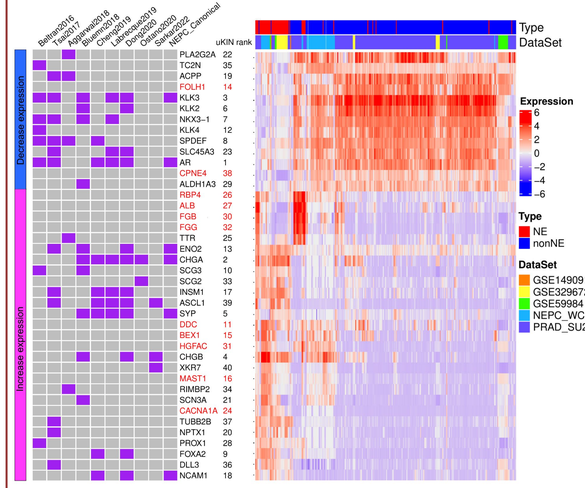

Dr. Chang-Deng Hu
Nov 29, 1961-Sep 1, 2022

- 1984 M.D. Bengbu Medical College, China
- 1997 Ph.D. Kobe University, Japan
- 2003 Assistant/Associate/Chaired Professor, Medicinal Chemistry, College of Pharmacy, Purdue University, USA

CDHu40 marker gens and their expression levels in different datasets. Left panel: overlap of CDHu40 genes and other marker gene sets published in the literature. The most left bar shows that marker genes were either down- (blue) or up- (purple) regulated in NEPC samples as we identified. Genes marked by red color were absent from all other published marker genes compared here. Right Panel: Expression profile of CDHu40 genes obtained by different data sets. Genes and samples were clustered by two-way clustering.

Performance of CDHu40 and other published gene sets for NEPC

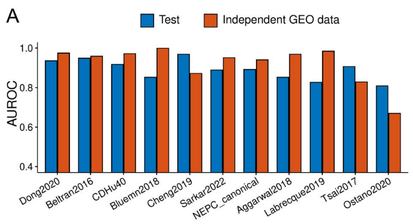

(A) Bar plot of area under receiving operating characteristics curve (AUROC) for each set. Gene sets were sorted by the average values of AUROC.

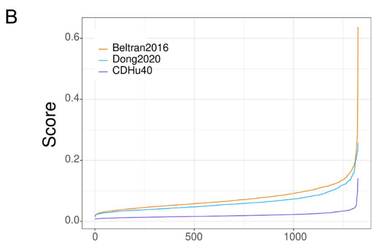

(B) NEPC scores of PRAD-TCGA samples estimated by Beltran2016, Dong2020, and CDHu40.

Cells with higher CDHu40 scores from scRNA-seq datasets.

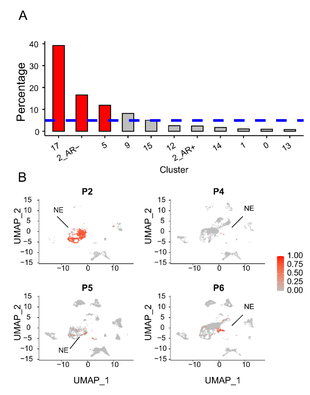

(A) Percentage of cells with higher CDHu40 scores in each cluster recognized by Asberry et al 2022 at Day 14 after neuroendocrine differentiation (NED). The red bars represent the significantly higher ratio, whereas the blue dashed line is the average percentage of high-CDHu40 score in all cells in the sample. (B) Cells with higher CDHu40 scores were marked in red given the patient samples with the scRNA-seq by Dong et al 2020.

CDHu40 score correlated with patient survival outcomes

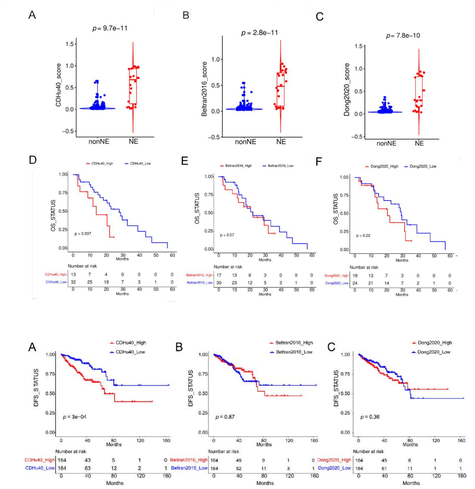

PRAD_SU2C_2019 samples. NEPC scores on clinical NE and non-NE samples evaluated by (A) CDHu40, (B) Beltran2016, and (C) Dong2020. Survival difference based on scores by (D) CDHu40, (E) Beltran2016, and (F) Dong2020, respectively.

Survival difference between higher and lower scores on PRAD-TCGA samples identified by (A) CDHu40, (B) Beltran2016, and (C) Dong2020.

Top 500 NEPC marker genes identified by our method

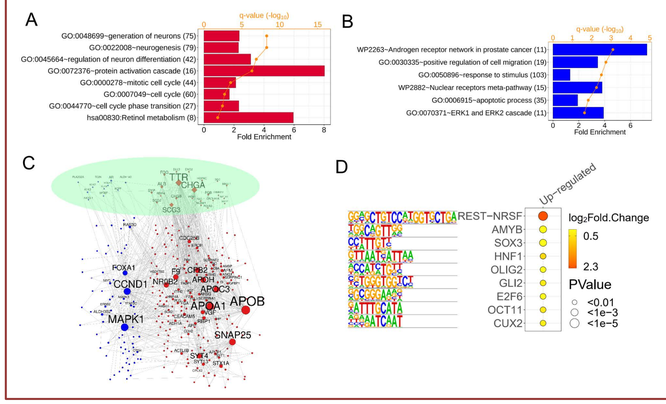

Gene ontology (GO) and KEGG pathway enriched in (A) up-regulated genes and (B) down-regulated genes. (C) PPI network of top 500 genes. Red and blue nodes are genes with elevated and lower expression levels, respectively, in NEPC samples. Yellow diamond nodes are CDHu40 genes . (D) Motifs enriched in the regions from upstream (2kb) to downstream (500bp) of 330 up-regulated candidate genes

Conclusions

- A novel integration method is proposed incorporating differential gene expression analysis between NEPC and non-NEPC samples as well as the uKIN algorithm based on the PPI network starting with several well-known NEPC biomarkers.
- CDHu40 score is a better diagnostic marker for NEPC and a reliable prognostic marker for NEPC patients.
- The top 500 candidates revealed enrichment in neural-related features and cell cycle process enriched in genes up-regulated in NEPC, along with repression in the AR network in NEPC. The PPI network for these top 500 genes identified hub genes associated with the cell cycle and progression of NED. Additionally, motifs of REST and E2F6 were enriched in promoter regions of these top candidates, suggesting their involvement in the generation of NE features and cell cycle regulation.
- Variations in CDHu40 gene expression profiles were observed across diverse datasets. Distinct subsets of non-NEPC samples were noted with elevated expressions of either RBP4, ALB, FGB, FGG, and TTR, or DDC, BEX1, HGFAC, and CHGB

Acknowledgement

NIH NATIONAL CANCER INSTITUTE
IUSCCC: P30CA082709
PUCCR: P30CA023168
WALTHER CANCER FOUNDATION
INDIANA UNIVERSITY MELVIN AND BREN SIMON CANCER CENTER
SCHOOL OF MEDICINE
The Ralph W. and Grace M. Showalter Trust

Cannabinoid Receptor Type II Agonist LY2828360 Reverses Sciatic Nerve Injury Hypersensitivity, Prevents Morphine Tolerance, and Blocks Morphine Reward

Jonah Wirt[1,2], Kelsey Guenther[1,2], Shahin Saberi[2], Andrea Hohmann[1,2,3]

[1]Program in Neuroscience, [2]Department of Psychological and Brain Sciences, [3]Gill Center for Biomolecular Science, Indiana University, Bloomington, IN

Introduction

◆Cannabinoids have many desirable therapeutic properties but can also produce unwanted side effects through activation of the CB_1 receptor (Lötsch et al. 2018; Howlett et al. 2002).

◆Activation of CB_2 receptors can reduce pain behavior without producing unwanted psychoactive effects (Deng et al. 2015).

◆The CB_2 receptor agonist LY2828360 suppresses persistent nociception in models of inflammatory pain and toxic neuropathy in mice (Guenther et al. 2023; Lin et al. 2018; Carey et al. 2023)

◆Whether LY2828360 is efficacious in other models of neuropathic pain or in other species is not known.

◆LY2828360 failed for efficacy in a clinical trial for knee pain due to osteoarthritis but was shown to be safe in humans.

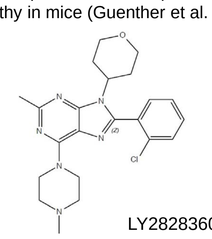

LY2828360

Aims

◆Determine whether the CB_2 receptor agonist LY2828360 is effective in reducing neuropathic nociception produced by spared nerve injury (SNI) in rats.

◆Examine the effects of chronic administration of LY2828360 in a sciatic nerve injury model to assess for potential analgesic tolerance.

◆Identify site of action of LY2828360 in suppressing sciatic-nerve injury induced neuropathic nociception using the CB_2 receptor antagonist AM630.

◆Determine whether co-administration of LY2828360 and morphine would prevent the development of morphine tolerance.

◆Investigate effects of LY2828360 in a conditioned place preference paradigm and its ability to interfere with morphine reward in a conditioned place preference paradigm

Methods

Pain measurement:

◆Spared nerve injury (SNI) pain model: ligation of the tibial and common peroneal branch of the sciatic nerve resulting in mechanical hypersensitivity in the paw ipsilateral to nerve injury.
Ipsilateral paw: SNI Contralateral paw: no injury

◆Assessment of mechanical paw withdrawal thresholds: electronic von Frey anesthesiometer (lower threshold reflects mechanical hypersensitivity)

Von Frey anesthesiometer Pain behavior

◆Acute studies: LY2828360 (3 or 10 mg/kg i.p.) injected 30 minutes prior to von Frey testing following baseline measurement

◆Chronic studies: Daily LY2828360 (3 or 10 mg/kg i.p.) for 10 days. Von Frey measurements on injection day 1, 4, 7 and 10. LY2828360 washout period also measured on day 11, 14, and 17.

◆Pharmacological Specificity Study: Pretreatment of CB2 antagonist AM630 (3 mg/kg i.p.) was administered 20 minutes before LY2828360 (10 mg/kg, i.p.) injection. Animals were then Von Frey tested 0.5, 1, 2, 4, and 6 hours post administration of LY2828360.

◆Morphine Tolerance Study: Daily LY2828360 (3 mg/kg i.p.) + morphine (6 mg/kg i.p.) for 10 days compared to morphine (6 mg/kg) alone. Von Frey measurements on injection day 1, 4, 7, and 10. Washout period also measured on day 11, 14, and 17.

Conditioned place preference:

◆Conditioned place preference was used to assess drug reward

◆Animals received VEH and drug (3 mg/kg LY2828360 i.p., 6 mg/kg morphine i.p. or LY2828360-morphine combination) on different days in distinct contexts

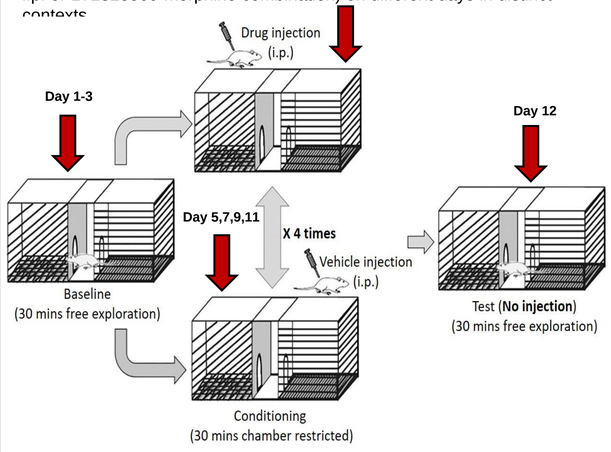

Adapted from (Amancio-Belmont et al., 2017)

Fig. 1. Acute administration of CB_2 agonist LY2828360 dose-dependently reduces mechanical allodynia produced by spared nerve injury (SNI)

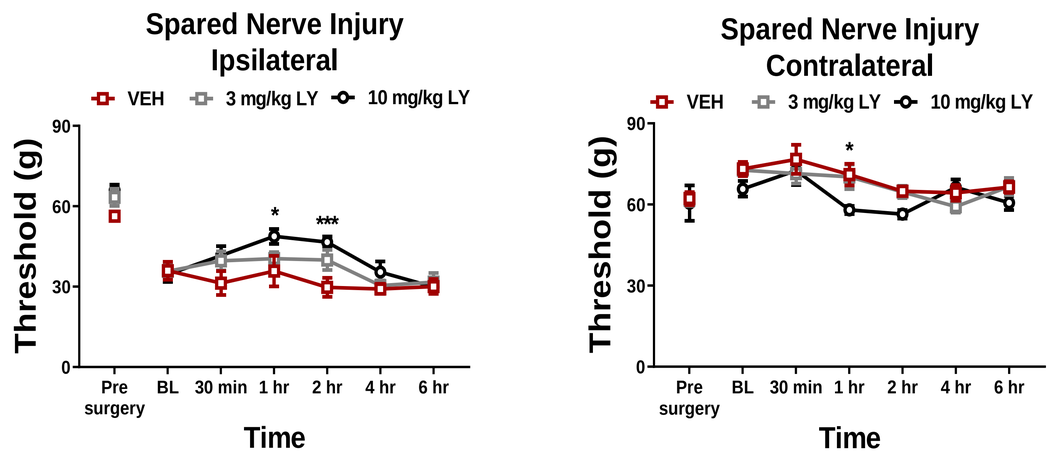

Mean (±SEM) von Frey threshold in the LY2828360 dose response experiment in SNI. Asterisks indicate group difference from VEH; *$p < 0.05$, ***$p < 0.001$.

Fig. 2. Acute co-administration of LY2828360 does not occlude analgesic efficacy of morphine

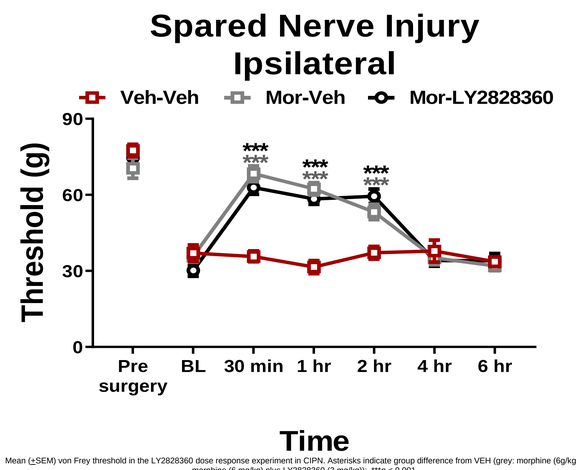

Mean (±SEM) von Frey threshold in the LY2828360 dose response experiment in CIPN. Asterisks indicate group difference from VEH (grey: morphine (6g/kg); black: morphine (6 mg/kg) plus LY2828360 (3 mg/kg)).; ***$p < 0.001$.

Fig. 3. Chronic administration of LY2828360 reduces mechanical allodynia produced by spared nerve injury (SNI)

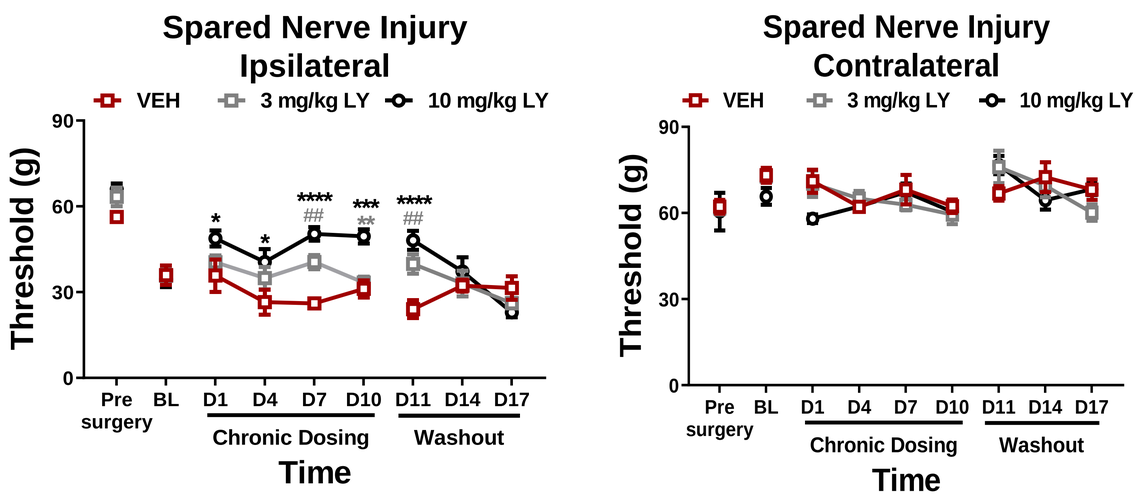

Mean (±SEM) von Frey threshold in the chronic LY2828360 experiment in SNI. Asterisks indicate group difference from VEH (black: 10 mg/kg; grey: 3 mg/kg), hashtag indicate difference between 3 and 10 mg/kg; *$p < 0.05$, **$p < 0.01$, ***$p < 0.001$, ****$p < 0.0001$.

Fig. 4. Chronic co-administration of LY2828360 prevents the development of morphine analgesic tolerance

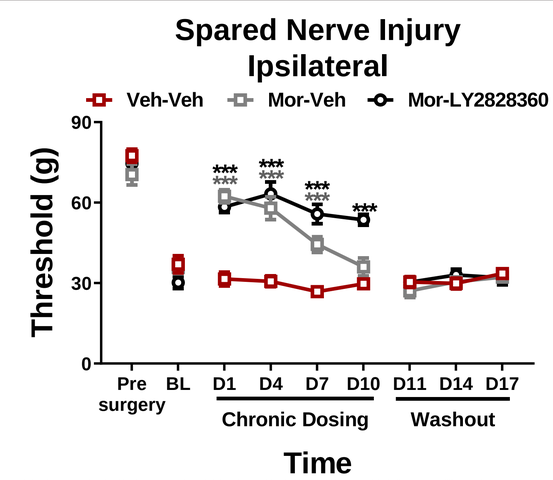

Mean (±SEM) von Frey threshold in chronic morphine administration combined with LY2828360. Asterisks indicate group difference from VEH (grey: morphine (6g/kg); black: morphine (6 mg/kg) plus LY2828360 (3 mg/kg)).; ***$p < 0.001$.

Fig. 5. Anti-allodynic effect of LY2828360 is blocked by CB_2 antagonist AM630

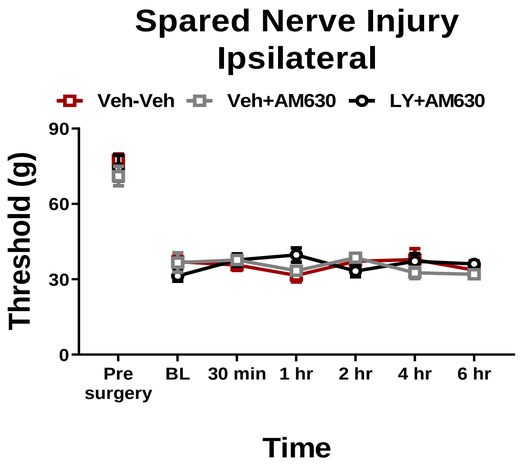

Mean (±SEM) von Frey threshold in rats receiving AM630 and/or LY2828360 in sciatic nerve injury.

Fig. 6. LY2828360 does not produce reward but blocks morphine reward in the conditioned place preference paradigm

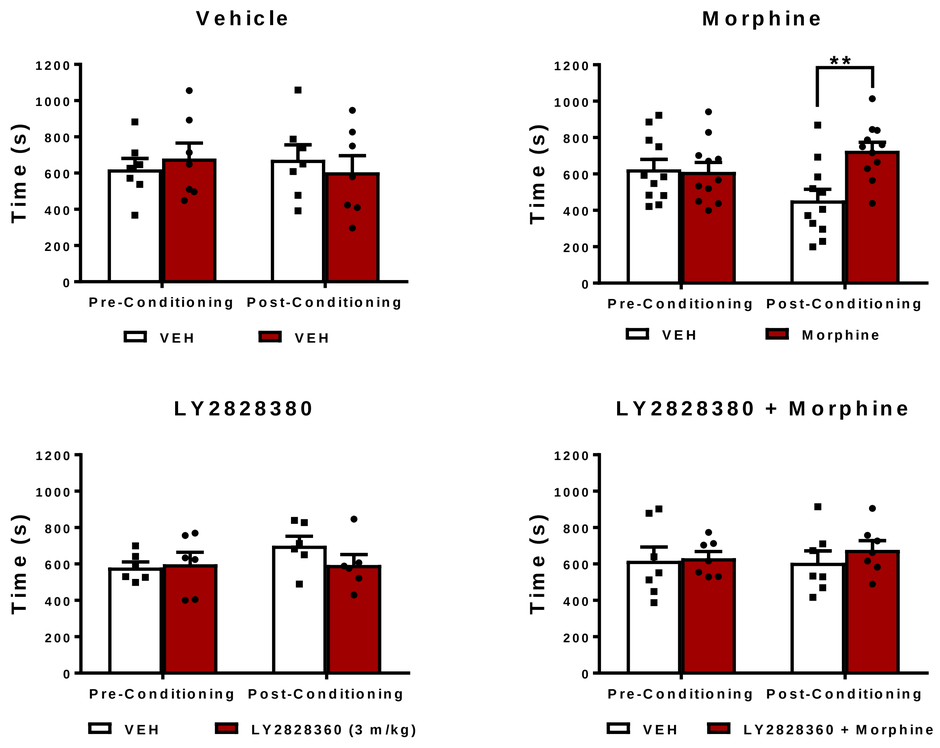

Mean (±SEM) time in CPP chambers paired with VEH, morphine, LY2828360 or LY2828360 + morphine. Asterisks indicate group difference from VEH chamber **$p < 0.01$.

Conclusions

◆LY2828360 reduced established neuropathic nociception produced by sciatic nerve injury in rats. No loss of efficacy was observed with repeated dosing, consistent with the lack of development of tolerance.

◆Pre-treatment with the CB_2 receptor antagonist AM630 blocked the anti-allodynic effect of LY28282360 in the sciatic nerve injury model, confirming a CB_2 receptor mediated mechanism in this model.

◆Co-administration of LY2828360 and morphine prevented morphine tolerance from developing in the scatic nerve injury model. This indicates potential cross talk between CB2 receptors and opioid receptors in the development of opioid tolerance.

◆LY2828360 prevents the rewarding effect of morphine in the conditioned place preference test and does not have rewarding effects on its own in this paradigm.

References

Carey LM, Xu Z, Rajic G, Makriyannis A, Romero J, Hillard C, Mackie K, Hohmann AG (2023) Peripheral sensory neuron CB2 cannabinoid receptors are necessary for both CB2-mediated antinociceptive efficacy and sparing of morphine tolerance in a mouse model of anti-retroviral toxic neuropathy. Pharmacological research 187: 106560

Deng L, Guindon J, Cornett BL, Makriyannis A, Mackie K, Hohmann AG (2015) Chronic cannabinoid receptor 2 activation reverses paclitaxel neuropathy without producing tolerance or cannabinoid receptor 1-dependent withdrawal. Biological Psychiatry 77: 475-487

Guenther KG, Xu Z, Romero J, Hillard CJ, Mackie K, Hohmann AG (2023) Conditional deletion of CB2 cannabinoid receptors from peripheral sensory neurons eliminated CB2-mediated antinociceptive efficacy in a mouse model of carrageenan-induced inflammatory pain. Neuropharmacology 237: 109601

Lin X, Dhopeshwarkar AS, Huibregtse M, Mackie K, Hohmann AG (2018) Slowly signaling G-protein biased CB_2 cannabinoid receptor agonist LY2828360 supresses neuropathic pain with sustained efficacy and attenuates morphine tolerance and dependence. Mol Pharmacol 93: 49-62

Lötsch J, Weyer-Menkhoff I, Tegeder I (2018) Current evidence of cannabinoid-based analgesia obtained in preclinical and human experimental settings. European Journal of Pain 22:471-484

Acknowledgments

SUPPORT: DA047858, DA041229 (to AGH), and T32 DA042584 (JW, AGH). JW is a Harlan Research Scholar.

DISCLAIMER: This project was funded with support from the Indiana Clinical and Translational Sciences Institute which is funded in part by Award Number UL1TR002529 from the National Institutes of Health, National Center for Advancing Translational Sciences, Clinical and Translational Sciences Award. The content is solely the responsibility of the authors and does not necessarily represent the official views of the National Institutes of Health.